Universitat Autònoma de Barcelona
Facultat de Biociències
Departament de Genètica i de Microbiologia

Ph.D Thesis

Relationship between the SOS system and the chemoreceptors clustering in *Salmonella enterica* sv. Typhimurium

Albert Mayola Coromina

Directors:
Prof. Jordi Barbé Ph.D and Prof. Susana Campoy Ph.D

September 2013

Universitat Autònoma de Barcelona
Departament de Genètica i de Microbiologia

Relationship between the SOS system and the chemoreceptors clustering in *Salmonella enterica* sv. Typhimurium

Thesis submitted by Albert Mayola Coromina to aim for the degree of Doctor in Microbiology by the Universitat Autònoma de Barcelona,

Albert Mayola Coromina

With the approval of the Thesis directors,

Prof. Jordi Barbé Garcia, Ph.D Prof. Susana Campoy Sánchez, Ph.D

Bellaterra, September 2013

This work was supported by grant BFU2011-23478 of the Ministerio de Economía y Competitividad de España. Albert Mayola Coromina was recipient of a predoctoral fellowship from Universitat Autònoma de Barcelona.

Abstract

The RecA protein is known to be the main bacterial recombinase and the activator of the SOS system. RecA is associated not only with DNA recombination and repair but also with several other functions such as the control of integron dynamics, prophage induction and the transfer of antibiotic resistances and virulence factors. Furthermore, in the last years a novel role of the RecA protein as a modulator of the swarming motility in *Escherichia coli* and *Salmonella enterica* serovar Typhimurium has been revealed. Up to date, it is known that the lack or the excess of RecA causes a dramatic depletion of the swarming motility in the aforementioned bacterial species. Also, the ability to swarm of an *S.* Typhimurium strain overexpressing the *recA* gene can be recovered by concomitantly overexpressing the *cheW* gene. Moreover, there are experimental evidences of the interaction between RecA and CheW proteins.

The *cheW* gene is one of the chemotaxis system core genes. Its product, the CheW protein, is known to serve in the cell as the coupling protein between the CheA histidine kinase and the chemoreceptors trimers of dimers to form the basic chemotaxis signaling unit. Several chemotaxis signaling units are known to aggregate at the cell poles forming a macromolecular structure known as chemoreceptor signaling arrays that, apart from their

role in signal transduction during chemotaxis, are known to be required for swarming motility. *E. coli* mutants that either overexpress or lack the *cheW* gene are known to have severe impairments in the formation of this chemoreceptor clusters. This have been linked with the depletion of the swarming and chemotactic abilities displayed by those mutants.

The molecular mechanism by which the SOS system modulates the swarming motility through RecA still remains unknown. There are sufficient evidences pointing towards a link between the chemotaxis and the SOS systems through a RecA-CheW interaction. Thus, the main aim of this work has been to elucidate the role of the SOS system, through the RecA protein, in the swarming motility of *S.* Typhimurium.

Results presented here demonstrate that RecA and CheW proteins of *S.* Typhimurium are able to interact both *in vivo* and *in vitro,* thus establishing a link between the SOS system and the bacterial motility. Also, the importance of a concrete stoichiometric relationship between both proteins have been established as a key factor for swarming motility. The molecular mechanism that exactly allows the SOS system to control the swarming motility still remains poorly understood but in this work it has been demonstrated that strains that either overexpress or lack the *recA* gene present a severe impairment to successfully structuring the chemoreceptor clusters arrays at its cell poles.

In conclusion, the present work clarifies the relationship between the SOS and chemotaxis systems of *S.* Typhimurium through the interaction between the RecA and CheW proteins. The molecular mechanism behind the RecA modulation of the swarming motility still needs to be further investigated, but in this work the affectation of the ability to form chemoreceptor signaling arrays in cells with an excess or lack of RecA is reported. Thus, it is hypothesized that RecA affects the clustering process in *S.* Ty-

phimurium and that the inability to successfully form this clusters is at the core of the swarming impairment shown by the *recA* mutants of this specie.

Acknowledgments

First and foremost I would like to thank my Thesis directors, professors J.Barbé, Ph.D and S.Campoy, Ph.D for the confidence they have demonstrated towards me since the beginning of my research project. I appreciate all their contributions of time, ideas, and funding to make my Ph.D. experience productive and stimulating.

I also would like to thank professors M. Llagostera, Ph.D and P. Cortés, Ph.D for their advice, help and collaboration during all these years.

I would like to specially thank all the laboratory colleagues, now friends, I have had during all this time:

L. Medina for teaching me at the beginning and at the end, and to put up with me and my sense of humor,

A. Lissidini for being an important professional and personal support despite our political differences,

S. Escribano for her help in printing PDF documents,

C. Bardina for showing always the optimistic face of our job,

D. Spricigo for being the steadiness behind the hyperactivity,

L. Teixidó for transmitting me some of her organization skills and for other small summer things,

J. Colom for the fun chicken-killing moments,

J. Aranda for discovering me another dimension of the word sarcasm,

O. Irazoki for her help in the last moments of my research,

M. Tort for her help in the difficult second year,

F. Madarena, for being always as clear as water,

E. Roig for her help in everything I needed,

and to many others I have been with and have contributed, even with a comma, to this work or to my day-to-day life: Bete, Enoy, Noe, Raúl, Jennifer...

I want to thank my friends, specially those from "Cata de Maltas" for morally support me several times: Arnau Der Kaiser Ph.D, Anthony, Roger The Negretista, and Penisé, Eloy Qué Ruta and Guillem The Pitón from The Gordaco Team.

I am deeply grateful to Tsan for everything she gave and gives me.

And lastly, I want to thank my family for their encouragement and support and for allowing me to reach this objective through their hard work.

Contents

List of Figures

List of Tables

Nomenclature

A_X	Absorbance at a given X wavelenght
AHLs	N-acyl-homoserine lactones
APS	Ammonium persulfate
ATP	Adenosine-5'-triphosphate
ATR	Acid tolerance response
BCIP	5-Bromo-4-chloro-3-indolyl phosphate
BSA	Bovine serum albumin
CCW	Counter clock wise
CW	Clock wise
ECA	Enterobacterial common antigen
ECM	Extra cellular matrix
EDTA	Ethylenediaminetetraacetic acid
GST	Glutathione S-transferase

HAA β-hydroxydecanoyl-β-hydroxydecanoate

HBB Hook-basal body

IMAC Immobilized metal affinity chromatography

indels Insertions and deletions

IPTG Isopropyl β-D-1-thiogalactopyranoside

LPS Lipopolysaccharide

MCPs Methyl-accepting chemotaxis proteins

MOI Multiplicity of infection

MQ-water Milli-Q water

NBT Nitro blue tetrazolium chloride

OD_X Optical density at a given X wavelenght

PBS Phosphate buffered saline

PCR Polymerase chain reaction

PVDF Polyvinylidene fluoride

rpm Revolutions per minute

SCV Salmonella-containing vacuole

SDS Sodium dodecyl sulfate

SNPs Single Nucleotide Polymorphisms

SOB Super optimal broth

SPI-1 Salmonella pathogenicity island 1

TBS Tris buffered saline

TEMED Tetramethylethylenediamine

U Enzyme unit

Chapter 1

Introduction

1.1 *Salmonella enterica* serovar Typhimurium

1.1.1 Classification and general characteristics

The *Salmonella* genus is classified inside the γ-proteobacteria class and belongs to the *Enterobacteriaceae* family. It is composed by Gram negative, non-spore-forming, rod-shaped bacteria which are facultative anaerobes and mainly show peritrichous motility (Fàbrega and Vila, 2013).

Table 1.1 shows the currently accepted classification of the species belonging to the *Salmonella* genus according to the Wold Health Organization (WHO, 2007). Subspecies II to VI are mainly environmental or found in fish, amphibians or reptiles. Subspecies I (*enterica*) is the main one found in mammals and birds being the main cause of disease within these organisms (Fàbrega and Vila, 2013).

Table 1.1. *Salmonella* serotypes classification.

Species	Subspecies code	Subspecies name	Serotypes
Salmonella enterica	I	*enterica*	1531
	II	*salamae*	505
	IIIa	*arizonae*	99
	IIIb	*diarizonae*	336
	IV	*houtenae*	73
	VI	*indica*	13
Salmonella bongori	V		22
Total			2579

Reference:WHO (2007)

Each subspecies group is composed by the so called serotypes or serovars. Serovars classification is accomplished on the basis of the distinct types of antigens found in the cell wall of different *Salmonella* strains. The O antigen (also somatic, surface or cell wall antigen) consists on a first filter that differentiates serovars according to the composition of the lipopolysaccharide (LPS) O-antigen exposed at the cell surface. Then, serovars are further filtered using the basis of the H antigen (also flagellar antigen). The H antigen classification is based on the existence of two types of flagellin in the *Salmonella* species encoded by the *fliC* (phase 1 H antigen) and *fljB* (phase 2 H antigen) genes (WHO, 2007; McQuiston *et al.*, 2011).

For the purpose of this work, a summary of the prevalence of the motility behavior found in the *Salmonella* genus is presented. Kim and Surette (2005) published a systematic and wide analysis of the swimming and swarming ability of different *Salmonella* strains from the SARB and SARC collections (Salmonella reference collections B and C). Concretely,

Table 1.2. *S. enterica* and *bongori* from SARC collections motility behavior.

Species	Subspecies code	Strains tested	% strains swimming	% strains swarming
S. enterica	I	11	91	91
	II	22	95	95
	IIIa	4	100	100
	IIIb	5	100	100
	IV	32	100	100
	VI	11	100	100
S. bongori	V	9	100	100

Reference:Boyd *et al.* (1996); Kim and Surette (2005)

SARB represents 37 distinct serovars from group I and SARC is composed of 96 strains representing the seven *Salmonella* subspecies (Boyd *et al.*, 1993, 1996).

The conclusions of this study pointed that swarming phenotype is a conserved trait among *Salmonella* genus as 97 to 100 % (depending on the carbon source) of the tested strains are reported to be swarming-proficient. The non-swarmer strains found are reported to have defects either on flagellar function or in LPS structure; both defects could severely impair the swarming motility as it is discussed in subsequent sections. The authors pointed that the conservation of the swarming ability among the *Salmonella* genus is indicative of its important role in survival and persistence of this bacterial genus (Kim and Surette, 2005).

1.1.2 Pathogeny

In the case of humans and other mammalians, host infection by *Salmonella enterica* spp. usually occurs first by ingestion of contaminated food or water and, second by the capacity of the bacteria to pass the stomach and colonize the gastrointestinal tract, primarily the terminal ileum and colon (Schleker *et al.*, 2012; Thiennimitr *et al.*, 2012; Velge *et al.*, 2012). The first host defense line that *Salmonella* must cross is the acidic conditions in the stomach. To overcome this, *Salmonella* triggers the acid tolerance response (ATR), an adaptative mechanism that enhances the cell survival at lethal pH conditions such as the ones present in the stomach (Alvarez-Ordóñez *et al.*, 2011). Once in the small intestine, *Salmonella* possesses several mechanisms to survive to the harsh conditions presents in the gut, such as bile salts presence, osmotic-adverse conditions, anaerobiosis, and the interaction with other microorganisms, which allow the bacteria to efficiently traverse the intestinal mucous layer and contact with intestinal epithelial cells (Alvarez-Ordóñez *et al.*, 2011; Schleker *et al.*, 2012). Then, *Salmonella* adheres to and invades nonphagocytic enterocytes by a mechanism known as bacterial-mediated endocytosis, or adhere to and enter through endocytosis mediated by the M cells of the Peyer's patches, the first step to reach the submucosa (Fig. 1.1) (Fàbrega and Vila, 2013). Nonetheless, *Salmonella* may reach the submucosa without crossing the epithelial layer due to the action of dendritic cells that are reported to have the ability to take up bacteria from the intestinal lumen by opening the tight junctions between the enterocytes (Fig. 1.1) (Rescigno *et al.*, 2001).

If the invasion progresses through the nonphagocytic enterocytes, first *Salmonella* causes severe internal modifications to the epithelial cells by interfering with the host cell signaling pathways. With these changes, the

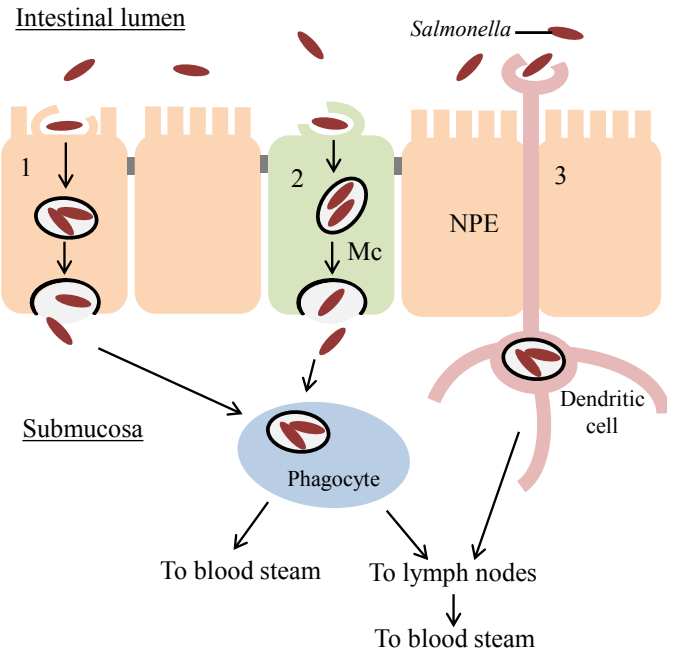

Figure 1.1. Invasion mechanism of *S. enterica*. Schematic representation of the invasion mechanism displayed by *S. enterica* spp. The infection starts with the oral ingestion of contaminated water or food. Once the bacteria reach the intestinal lumen they could use several pathways to reach the intestinal submucose and from there start to disseminate to internal organs and other parts of the organism causing a systemic infection. Invasion routes are denoted with numbers: 1, invasion through nonphagocytic endocytes; 2, invasion through Peyer's patches M-cells and 3, direct invasion through phagocytosis by dendritic cells. Nomenclature: NPE, nonphagocytic enterocyte; Mc, Peyer's patches M-cell.

bacteria promote their own endocytosis through the creation of a membrane-bounded, specialized compartment called *Salmonella*-containing vacuole (SCV). Peyer's patches M-cells are naturally phagocytic thus, the bacteria are internalized through a normal endocytosis system but they also trigger the formation of the SCV compartments. *Salmonella* is able to survive and replicate inside the host cell (either nonphagocytic epithelial cells or macrophages) while trapped in this compartment. Thanks to a tightly controlled network of effectors secreted to the host cell cytoplasm, *Salmonella* is able to alter the normal operation of the host cell vacuolar system avoiding the SCV fusion to secondary lysosomes, containing lysosomal enzymes which would kill the cells (Schleker *et al.*, 2012; Fàbrega and Vila, 2013).

Then, a fraction of the existing SCV migrate to the baso-lateral side of the enterocytes and, through a process of exocytosis, bacteria are released into the interstitial space of the lamina propia. Once there, bacteria are randomly phagocyted by either neutrophiles, macrophages or dendritic cells within SCVs thus triggering a similar process that the one previously explained. The migration of these infected phagocytic cells facilitates the rapidly dissemination of *Salmonella* either to lymph nodes and finally to the blood steam or directly to blood steam. Indistinctly of the migration system used, both cases render a systemic infection (Worley *et al.*, 2006; Velge *et al.*, 2012; Fàbrega and Vila, 2013).

1.1.3 Epidemiology and clinical relevance

In humans, there are two main diseases caused by *Salmonella*. The enteric fever (or typhoid fever) is a systemic invasive illness caused by the specific human pathogenic serovars Typhi and Paratyphi of *S. enterica* (Parry *et al.*, 2002). The other clinically relevant illness associated with

pathogenic strains of this bacteria is the diarrheal disease, mainly caused by the broad host range, nontyphoidal serovars Enteritidis and Typhimurium (Velge *et al.*, 2012). The concern for the salmonellosis goes far beyond the human health as many *Salmonella* serovars, either host-restricted or broad host, are able to infect the domestic livestock and fowl with a wide variety of possible outcomes thus becoming a cause of major economic concern (Velge *et al.*, 2012; Fàbrega and Vila, 2013).

The most common reservoir of these bacteria is the gastrointestinal tract of infected hosts. In fact, *Salmonella* spp. uses several defensive systems (such as the already mentioned ATR) to protect themselves from the the damaging conditions which are part of the host defense against the infection. These defensive systems are tightly controlled and specialized thus providing an adequate response to each specific condition found throughout the intestinal tract of the host (Alvarez-Ordóñez *et al.*, 2011; Monack, 2012).

As expected from a gastrointestinal disease, the main cause of human infection is through fecal-oral contact, either in a direct way (zoonotic) or indirect through contaminated foodstuffs. According to data obtained from the European Food and Safety Authority (EFSA., 2013), in 2011 a total number of 95548 cases of salmonellosis were reported in the European Union thus being the second most important cause of human zoonoses only after campylobacteriosis with 220209 cases. The hospitalization rate for these cases was of 45.7 % whereas the fatality rate was of 0.12 %. *S.* Enteritidis and *S.* Typhimurium were the most frequently reported serovars accounting for a 44.4 and a 24.9 % of the cases respectively.

In the period 2004-2011, *S.* Enteritidis and *S.* Infantis were the most commonly reported serovars in fowl and eggs. Also in the same period,

S. Typhimurium was the most commonly reported serovar found in bovine cattle, pigs, and meat from both origins.

If the analysis is conducted in a distinct way, *Salmonella* appears as the most important causative agent of food-borne outbreaks in 2011 in the European Union, only surpassed by the the cases where the causative agent could not be faithfully determined. All this data gives a clear view not only of the clinical relevance of *Salmonella,* but also of the economic impact this pathogen has in the agro-alminetary industry.

1.2 Motility systems

1.2.1 The flagellar system

1.2.1.1 Structure and function of the flagellar motor

In the model organisms *E. coli* and *S.* Typhimurium, cells are propelled by three or four flagella, on average, that arise randomly on its sides and extend to the external medium (Berg, 2003; Partridge and Harshey, 2013a). Each flagellum is attached to a rotary motor embedded in the cell envelope that uses the proton motive force to generate the thrust required to enable cell motility (Berg, 2003; Gabel and Berg, 2003).

During swimming, bacterial cells usually "run" in a direction parallel to their long axis for a period of approximately 1 second. Running periods are interspersed by "tumbling" periods that last approximately a tenth of a second. During tumbling periods, cells move erratically in the same place until another running period starts (Berg, 2003). Classic experiments conducted by Macnab and colleagues in the 1970s decade first correlated those so called running and tumbling periods with the direction of flagellar rotation (Macnab and Ornston, 1977; Macnab, 1977). When a cell is

running, all of its flagellar filaments are rotating counter clockwise (CCW) thus forming a flagellar bundle that pushes the cell forward. As mentioned, periodically one or more filaments start rotating clockwise (CW), these filaments leave the bundle thus provoking a tumbling movement (Berg, 2003). During the normal CCW rotation, the flagellum structure is a left handed helix. Upon rotary sense change to CW, the flagellum filament undergo a structural transformation from the left handed normal helix to a right handed curly helix where the structural tensions are higher not only within the filament structure, but also at the flagellum basis and motor (Macnab and Ornston, 1977). Despite the motor switch from CCW to CW rotation appears to be approximately a random phenomenon, relieving the torsional stress generated when the flagella filaments change their structure it is likely to be one of the main forces involved in recovering the normal state thus originating the running-tumbling cycles (Turner *et al.*, 2000).

Despite this model for the change of motor rotation is widespread, it is not a universal mechanism. Other bacteria, such as *Rhodobacter sphaeroides,* have a more complicated flagellar and chemotaxis systems. In this case, the motor rotation appears to be unidirectional and the cell reorientation occurs through a Brownian rotation during stop periods (Armitage and Macnab, 1987). *Sinorhizobium meilioti* also uses an unidirectional motor but the cell reorientation is achieved by variations in the rotation speed and not through stop periods (Attmannspacher *et al.*, 2005). *Vibrio alginolyticus* also presents an alternative mechanism that achieves the cell reorientation by a push-pull mechanism depending on flagellar rotation sense (Sowa and Berry, 2008). In summary, it seems clear that although a general and widespread model could be stated for the observations performed in organisms like *E. coli*, a higher degree of diversity is present among bacteria.

Figure 1.2 shows the schematic representation of an *E. coli* flagellum. The signaled protein constituents are named after the genes that encode them. The flagellum and the motor are a well-organized, complex structure that involves more than 35 different proteins that interact between them at different stoichiometries to form the various sub-complexes that, finally, will lead to the entire flagellum-motor structure (Berg, 2003).

The hook and the filament are formed by single polypeptides of FlgE and FliC respectively, both arranged in cylindrical structures. There exist two type of structures depending on the inclination from the vertical axis and packing of the subunits, the R- and S-types. Both are present at the same time in one flagellum thus giving them the known helical form. Whereas the hook is a flexible structure that allows the rotation, the filament is rigid and its shape depends on physicochemical conditions of the environment and of the amino acid sequence of the FliC protein (Berg, 2003). As discussed above, CCW/CW motor switches lead to structural changes that affect both the structure of the filament and the hook. The structural changes that finally lead to left- or right-handed filament helices, thus varying the movement from running to tumbling, rely heavily on how the cylindrical structures of the hook and the filament are arranged and interact to change their spatial distribution (Berg, 2003).

The hook-basal body (HBB) is the structure that spans across the membranes and the peptidoglycan layers comprising the rod, the rotor or MS-ring, the rest of ringed structures, and the export system associated to the flagellum (Samatey *et al.*, 2004).

The switch complex, comprised by the FliG, M and N proteins, constitutes the core of the motor regulatory proteins. As it will be discussed in the chemotaxis section (Section 1.2.2), the regulatory CheY protein is able

to bind FliM thus modifying the CCW/CW motor bias (Blat *et al.*, 1998; Samatey *et al.*, 2004).

In *E. coli,* the stator is thought to be comprised by MotA and MotB proteins. MotA spans across the inner membrane but the vast majority of the protein is cytoplasmatic. MotB has a membrane spanning region but the majority of the protein is found in the periplasmatic space bound to the peptidoglycan. MotB is the responsible to anchor MotA to the rigid cell wall structure in order to permit the torque to be transmitted to the flagellar filament probably through the interaction with FliG, a component of the cytoplasmatic face of the rotor system (Garza *et al.*, 1996; Berg, 2003).

The stator complex is the responsible for torque generation. This generation is dependent on the proton motive force obtained with the H^+transport from the periplasmatic space to the cytoplasm through the two channels per stator unit formed by MotAB proteins (Sharp *et al.*, 1995; Braun and Blair, 2001; Gabel and Berg, 2003). In fact, the speed of the flagellar motor is known to increase linearly with the proton motive force generated by the MotAB stator complex (Gabel and Berg, 2003). The mechanism by which protons are translocated through the inner membrane by MotAB proteins, thus generating torque, is of great complexity and some aspects still remain unclear. In summary, the protonation and deprotonation of an specific aspartate residue of MotB is believed to modulate a MotA cytoplasmatic domain conformation change and, in turn, its interaction with FliG thus generating the required mechanical movement (Braun and Blair, 2001; Kojima and Blair, 2001). This model, as happens with the flagellar rotation mechanism, could be regarded as valid for *E. coli, Salmonella, Bacillus, Rhodobacter* and *Pseudomonas* species as they all obtain the motor energy through H^+- driven motors (Terashima *et al.*, 2008) but an alternative model has been reported for the marine bacterium *Vibrio alginolyticus* that

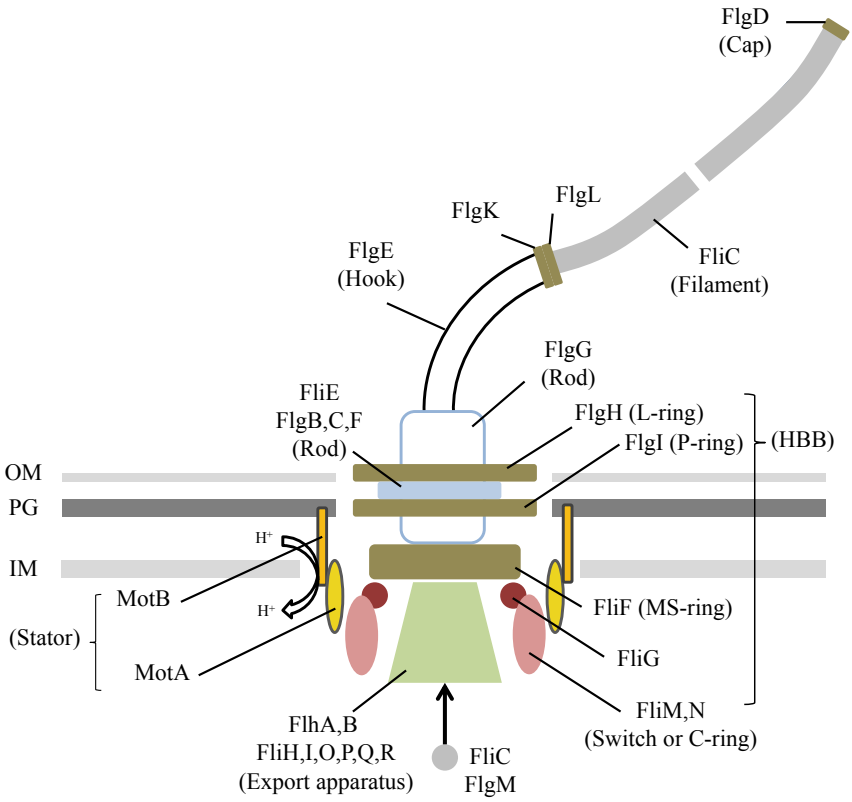

Figure 1.2. Flagellum structure. Schematic representation of the flagellum and motor structures of *E. coli*. The functional names of the main protein complexes are given within parentheses. Nomenclature: OM, outer membrane; PG, peptidoglycan; IM, inner membrane; HBB, hook-basal body.

uses a Na^+- driven flagellar motor. This variation may be explained as an adaptative mechanism to the high salt concentrations present in the habitat of this bacterium (Yorimitsu and Homma, 2001).

1.2.1.2 Flagellar operon gene expression

The flagellar regulon consists of at least 17 operons comprising more than 50 genes encoding the constituents of the flagellar and the chemotaxis systems (Chilcott and Hughes, 2000). The flagellar regulon components are organized in transcriptional hierarchies that are evolutionary conserved among Gram negative bacteria. During flagellar biogenesis, distinct groups of genes are differentially expressed depending on the synthesis stage (Soutourina and Bertin, 2003).

In *E.coli*, *S.* Typhimurium and other Gram negative bacteria, the genes of the flagellar operon are classified depending on their expression stage as early, middle or late expressed and are placed under the control of three classes of flagellar promoters: class 1, 2 and 3 (Chilcott and Hughes, 2000).

In the mentioned organisms, there exist only one class 1 promoter that is able to respond to metabolic and environmental stimuli and controls the expression of the early master regulator operon *flhDC* (Wang *et al.*, 2006b). As a crucial regulatory point, a number of global regulatory pathways and signals have input on this promoter, for example the cAMP-CRP pathway, the heat shock proteins DnaK, DnaJ and GrpE, high concentrations of inorganic compounds (such as salts or alcohols), the growth phase, the cell cycle regulators and noteworthy, the surface-liquid transition (Chilcott and Hughes, 2000). The regulatory network over the *flhDC* promoter is even more complicated if the effects of the autogenous regulation are taken into account. Under normal growth conditions FlhDC is an autogenous repressor

of the *flhDC* expression but in the presence of a σ^{28}increased activity, FlhDC acts as an autogenous activator (Kutsukake, 1997).

The FlhD and FlhC proteins (expressed from the master regulatory operon *flhDC*) are two σ^{70}- dependent transcriptional activators required for the expression of the middle genes placed under the control of the class 2 promoters (Wang *et al.*, 2006b). The genes expressed from the class 2 promoters encode for proteins required to build the hook-basal body (HBB) and also for the alternative sigma factor 28 (σ^{28}, product of *fliA*), a transcriptional regulator that confers specificity for the class 3 flagellar promoters of late genes (Ohnishi *et al.*, 1990; Kutsukake and Iino, 1994; Schaubach and Dombroski, 1999; Chilcott and Hughes, 2000). The late genes (those expressed from class 3 promoters) encode for proteins required to build the filament, the motor torque generators MotA and MotB, and the chemosensory system (Chilcott and Hughes, 2000; Wozniak *et al.*, 2010). Mention apart should be done with the FlgM protein, that is an anti-σ^{28}regulator expressed from both class 2 and class 3 promoters (Gillen and Hughes, 1991, 1993). The FlgM protein is the key player in coordinating the expression of late flagellar genes to the flagellar synthesis. One of the main components of the HBB is the excretion system located at its basis, in the cytoplasmatic side. This type III secretion system is used to secrete the FliC subunits and also FlgM (Fig. 1.2). Before the completion of the HBB the excretion system is not functional thus, FlgM accumulates in the cytoplasm and binds to σ^{28}preventing the expression of class 3 genes. When the HBB is complete, it becomes competent for secretion of the hook associated proteins and flagellin and also other filament-type substrates such as FlgM. Then, as FlgM intracellular levels decrease, more $\sigma^{28}$is available to trigger the class 3 promoters transcription (Hughes *et al.*, 1993; Kutsukake, 1994; Kutsukake and Iino, 1994; Wozniak *et al.*, 2010).

Despite the clear hierarchic scheme of gene expression of the flagellar regulon, the real picture is far from being as easy. Up to date, ten genes (*fliA, fliD, fliS, fliT, fliY, fliZ, flgK, flgL, flgM* and *flgN*) are known to be transcribed from both class 2 and class 3 promoters. Although the reason for this duplicate expression remains poorly understood, most of the cited genes encode proteins required after the completion of the HBB and before the start of filament polymerization (Wozniak *et al.*, 2010). The most well studied case of duplicate expression is the case of the *flgM* gene whose expression, as mentioned above, is found to happen from both class 2 and class 3 promoters. The class 2 FlgM is primarily found in the cytoplasm and its function as hook-basal body assembly checkpoint is well established (Hughes *et al.*, 1993; Kutsukake, 1994; Karlinsey *et al.*, 2000). The class 3 FlgM role is less clear but its production seems to be coupled with the secretion form the cell. The coupling of class 3 FlgM to secretion after HBB assembly is thought to provide a mechanism to regulate the filament length thus, the longer the filament the harder it is to excrete FlgM that then tends to accumulate at the cytoplasm leading, in turn, to class 3 genes shut down (Chilcott and Hughes, 2000). Also, class 3 FlgM has been proposed act as a sensor to test the environmental conditions for motility with a special focus on surfaces (Wang *et al.*, 2005). This represents another link between the flagellar regulon and bacterial motility. It is noteworthy that the analysis of other dual-expressed operons have revealed a role in bacterial motility. The expression of the hook-associated proteins (HAPs) FlgK, FlgL and FliD has been reported to be important for swarming motility and they have been hypothesized to play a role in broken-flagella repair (Wozniak *et al.*, 2010).

In conclusion, this hierarchic system constitutes a form to ensure that the earlier required constituents will be available before the late ones thus avoiding over-synthesis or competition between proteins for processes such

as secretion to periplasmatic space (which would be likely to happen between the HBB proteins and FliC). Overall, this genetic expression mechanism constitutes an efficient way to save the cell resources (Chilcott and Hughes, 2000).

1.2.2 The chemotaxis system

1.2.2.1 The chemotaxis system and signal transduction

The chemotaxis system is a two-component signal transduction system used by bacteria to sense the environment for the presence of attractants or repellents and to generate the adequate response (Baker *et al.*, 2006a; Krell *et al.*, 2011).

Although it is a well conserved system among *Bacteria*, evidences that a wide variety of responses could be found in distinct species have been reported. Thus, while *E. coli* is able to respond primarily to some amino acids, dipeptides and sugars, other bacteria are reported to be able to respond to an increased variety of chemical compounds including those sensed by *E. coli* (Krell *et al.*, 2011). This amplitude of sensing abilities among bacteria correlate well with the genetic analysis. A complete analysis of the sequenced bacterial genomes have shown large differences in the number of *mcp* genes, encoding for methyl-accepting chemotaxis proteins (known as chemotaxis receptors), depending primarily on the bacterial lifestyle. Thus, strict pathogens are included within a group that shows the lowest number of *mcp* genes (some *Bacillus* species have only 1 *mcp* gene) while bacteria with a complex behavior, including those with the ability to socialize with other living organisms, show a dramatically increased number of *mcp* genes (e.g. in *Myxococcus* or *Agrobacterium* species 20 to 60 *mcp* genes could be found) (Lacal *et al.*, 2010).

Despite the great variety in sensing abilities existing among bacteria, all of the components of the chemotaxis apparatus of *E. coli* and *S.* Typhimurium are functionally interchangeable and thus their chemotaxis systems are closely related (Baker *et al.*, 2006b; Krell *et al.*, 2011). From now on, the data reported here will be focused on the chemotaxis system found in *E. coli* (Fig. 1.3) which is assumed to be basically the same for *S.* Typhimurium.

The *E. coli* chemotaxis system core is formed by eleven proteins, the six Che: CheA, CheB, CheR, CheW, CheY and CheZ, and the five chemoreceptors or methyl-accepting chemotaxis proteins: Tsr, Tar, Tap, Trg and Aer.

The chemotactic response is initiated when a signal (an attractant or a repellent) is recognized by an MCP. The MCPs are proteins composed by a variable ligand binding domain and a conserved cytoplasmatic adaptative and signaling domain (Zhulin, 2001). The canonical description of the MCPs as transmembrane proteins with a periplasmatic binding domain is not used here as this is the structure observed in some MCPs, like Tar and Tsr of *E. coli,* but it is not a general model. For example, the Aer receptor also from *E. coli* shows a cytoplasmatic ligand binding region (Lacal *et al.*, 2010). This demonstrates that the structure of the MCPs have adapted to the different input signals and thus, they can be distinguished in groups regarding the location of the ligand binding region and if they are membrane-bound or cytoplasmatic (Lacal *et al.*, 2010).

The recognition of the ligand by the MCP could be achieved by direct binding of the molecule to the MCP scaffold, as happens for the Tar receptor and aspartate, or by indirect binding through other adaptor proteins. An example of indirect binding is the maltose. In *E. coli* this disaccharide is also sensed by the Tar receptor but it requires the binding to the

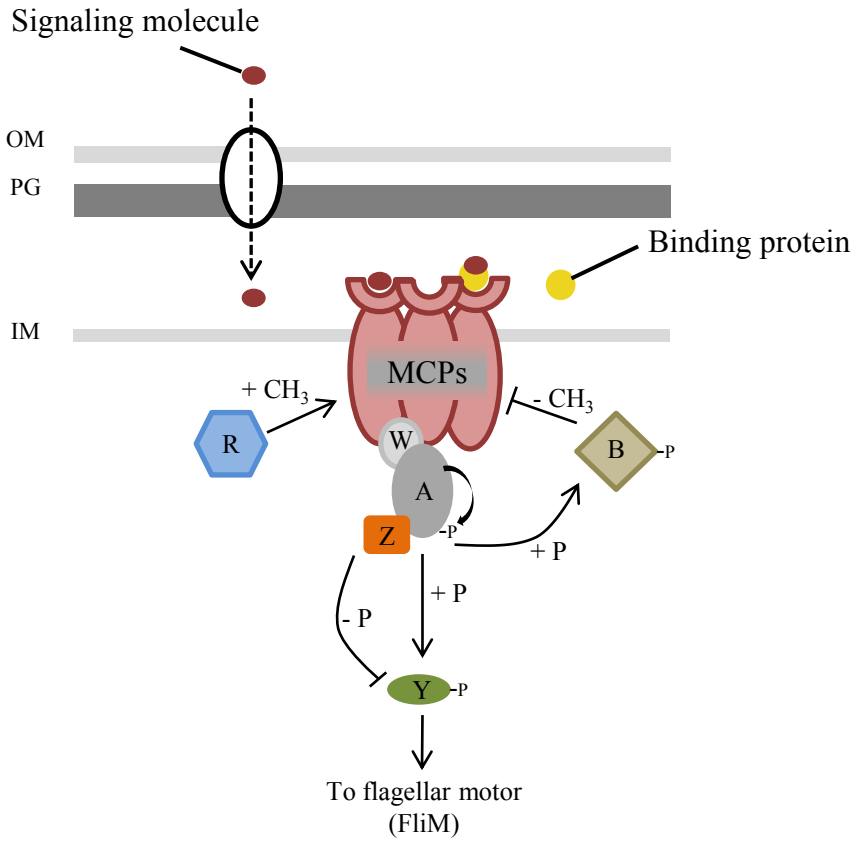

Figure 1.3. Chemotaxis system in *E. coli*. Schematic representation of the chemotaxis signaling pathway found in *E. coli* and the functional relationships existing between its constituents. Nomenclature: OM, outer membrane; PG, peptidoglycan; IM, inner membrane; MCPs, methyl-accepting chemotaxis proteins; A, B, R, W, Y and Z refers to CheA, CheB, CheR, CheW and CheZ proteins respectively. Relationships indicated with an arrow indicate an additive effect (e.g. phosphorylation) whereas relationships indicated with a cut line indicate a substractive effect (e.g. demethylation).

periplasmatic maltose-binding protein (MBP) as a prerequisite for Tar binding (Krell *et al.*, 2011).

Following the *E. coli* model for Tar-aspartate recognition, the binding of the ligand to the MCP ligand binding domain causes a molecular stimulus that modulates CheA autophosphorylation and its transphosphorylation activity towards the response regulator CheY (Baker *et al.*, 2006a). The histidine kinase CheA and the coupling protein CheW interact within a highly conserved signaling domain at the cytoplasmatic side of the MCP to form a large receptor-signaling complex that controls the CheA kinase activity. Despite CheA is the main recipient of the receptor signaling stimulus, CheW has been hypothesized to play a more complex role *in vivo* than simply serve as coupling protein to tether CheA to the MCP (Surette and Stock, 1996; Boukhvalova *et al.*, 2002b,a; Vu *et al.*, 2012).

When CheY has been phosphorylated by the CheA transphosphorylase activity (giving place to CheY-P), it undergoes a conformational change that allows it to rapidly dissociate from CheA and interact with the flagellar motor switch complex, concretely with FliM. The interaction of CheY-P with the switch complex of the flagellar motor promotes the CW rotation causing a change in the motility pattern from running to tumbling (Berg, 2003; Baker *et al.*, 2006a; Sowa and Berry, 2008). Thus, bacterial chemotaxis is the response to an attractant or a repellent given by the modulation of the CheY-P levels present in the cell that lead to changes in the CCW/CW motor bias thus re-orientating the cell during motility. An attractant compound causes the inhibition of CheA kinase activity and thereby a decrease in CheY-P concentration whereas a repellent causes the contrary (Baker *et al.*, 2006a).

Apart from the excitatory pathway already mentioned, a second component of the chemotactic response is the adaptational pathway that comprises

the mechanisms leading to the restoration of the basal state of the system or achieving a tolerance state towards an stimulus. This systems are the main reason why the chemotactic response is produced towards chemical gradients rather than absolute concentration values of chemical compounds (Baker *et al.*, 2006a).

CheY-P is reported to undergo a rapid auto-dephosphorylation (Sanders *et al.*, 1989a) but the rate at which this process takes place is not sufficient to guarantee an optimal chemotactic response. In *E. coli*, the phosphatase CheZ is the responsible for obtaining a rapid signal termination through its catalytic activity in CheY-P dephosphorylation (Zhao *et al.*, 2002).

Other adaptative mechanisms are present and lead to stimulus tolerance. CheR is a methyltransferase and CheB a methylesterase that regulate the methylation state of 4 to 6 glutamate residues of the MCPs leading them to different response states (Krell *et al.*, 2011). Attractants cause an increased methylation of the MCPs by increasing the CheR activity in detriment of the CheB activity as a feedback to counter-act the CheA kinase inhibition produced by the same signal binding. Repellents act on the contrary thus enhancing the CheB over the CheR activity. Also, the methylation state has been reported to influence the affinity of the receptor for the signaling molecule (Li and Weis, 2000; Levit and Stock, 2002; Sourjik and Berg, 2002; Baker *et al.*, 2006a). By contrast to CheR, the activity of CheB is modulated by CheA transphosphorylation giving place to the active CheB-P form. CheA phosphoryl transfer to CheY is faster than to CheB thus ensuring that the chemotactic response takes place before the adaptative response. CheB demethylation is the most influencing activity affecting the methylation state of the receptors in the CheR/CheB balance (Sourjik and Berg, 2002; Krell *et al.*, 2011).

1.2.2.2 Structure of the chemoreceptor signaling arrays

As explained above (Section 1.2.2.1), the MCPs and the CheA and CheW proteins form the initial complex whose role is to start the signaling cascade leading to the appropriate changes in the flagellar motor bias thus allowing the correct response to each situation. These components form the so called chemotaxis signaling complex. In *E. coli* a few to thousands of signaling complexes are known to arrange preferentially at the cell poles forming the so called signaling arrays or clusters that are proposed to play critical role for the generation of the chemotactic signals (Maddock and Shapiro, 1993; Bray *et al.*, 1998; Duke and Bray, 1999; Sourjik and Berg, 2000; Besschetnova *et al.*, 2008; Greenfield *et al.*, 2009). Nonetheless of the preferential polar location of the clusters, lateral clusters could also be observed in the cells (Sourjik and Berg, 2000; Kentner *et al.*, 2006). It has been proposed that, regarding to the presence of these lateral clusters, the assembly of the receptor clusters must be conducted laterally and upon several rounds of cell division they become polar (Thiem *et al.*, 2007; Thiem and Sourjik, 2008).

The MCPs composition of those clusters appear to be a mix between the different types of receptors found in the cell which are believed to act in a cooperative manner in order to integrate and amplify the chemotactic signals and also improve the sensitivity and feedback control over the system (Sourjik and Berg, 2002, 2004).

The basic unit for the formation of the chemoreceptor signaling complexes is the MCPs homodimer. Once bound, three homodimers interact to form a structure known as trimer of dimers which is the basic structure involved in the formation of the receptor arrays (Fig. 1.4) (Kim *et al.*, 1999; Studdert and Parkinson, 2004, 2005; Li and Hazelbauer, 2011). Recently, it

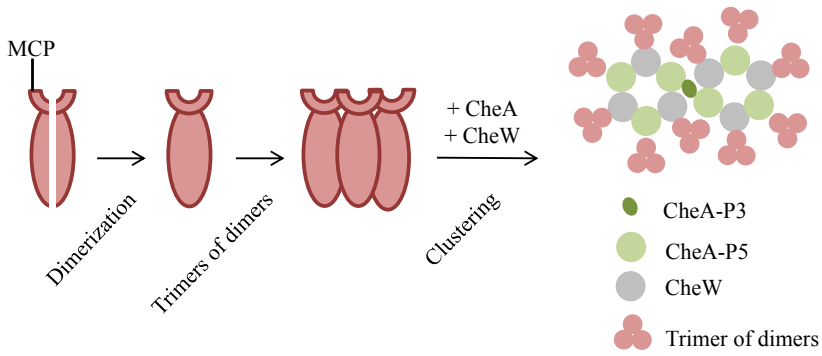

Figure 1.4. Model of the chemotaxis receptors clustering. Schematic representation of the chemotaxis receptors array formation. First an homodimerization of two MCPs occurs. After that, receptor dimers aggregate forming a trimer of dimers structure that finally forms the hexagonal chemoreceptors signaling arrays upon recruitment of CheA and CheW proteins whose function is to network the hexagonally packed trimers of dimers. Adapted from Briegel *et al.* (2012).

has been described the basic structure of the chemoreceptor signaling arrays. In this model, trimers of receptor dimers are packed in an hexagonal lattice interconnected at its basis by a ring of alternating CheA and CheW thus giving place to a high interconnected array that reinforce the cooperative behavior of the chemotaxis receptors (Fig. 1.4). The reported stoichiometry for CheA:CheW:MCPs in this model is of 1:1:6 although it may vary depending on the strain and signaling state (Briegel *et al.*, 2012). This model, which predicts that a CheA/CheW complex bridges two trimers of dimers, is reinforced by previous findings that suggest a minimal functional unit of two trimers of dimers, a dimeric CheA and two CheW proteins required to activate the CheA kinase activity (Li and Hazelbauer, 2011). The importance of CheA and CheW in the receptor structuring process remains controversial. Apparently, neither CheA nor CheW are required for the polar localization and clustering of the receptor arrays but their presence greatly enhances the compactness of the clusters and thus they are likely to be required to achieve the full packed state reported in the previously commented hexagonal-packing model (Skidmore *et al.*, 2000; Zhang *et al.*, 2004; Kentner *et al.*, 2006). In the same way, the excess of CheW is known to disrupt the chemoreceptor signaling arrays and also affect the MCP-induced CheA activation thus indicating that the stoichiometry is strictly pivotal for the correct function within the signaling arrays (Liu *et al.*, 1997; Cardozo *et al.*, 2010).

Following the structuring of the signaling complexes packed hexagonal arrays, the rest of the cytoplasmatic proteins implicated in the chemotaxis signaling pathway (as CheR and CheZ among others) are reported to co-localize also in the cell poles indicating that a stable protein complex is formed surrounding the MCPs at this physical region (Sourjik and Berg, 2000). The interactions responsible for this co-localization have also been

described in detail (Shiomi *et al.*, 2002; Cantwell *et al.*, 2003; Banno *et al.*, 2004; Kentner and Sourjik, 2009).

1.3 The swarming motility

1.3.1 Types of bacterial motility

Swarming is specialized form of flagellar-driven multicellular surface translocation movement found within *Bacteria* domain (Harshey, 2003; Kearns, 2010; Partridge and Harshey, 2013b).

By contrast to swimming, which is also defined as a flagellar-dependent translocation mechanism that takes place in liquid environments and as an individual cell behavior (Kearns, 2010), swarming is a highly coordinated displacement of groups of cells, commonly referred as rafts, over a moist surface, for example, laboratory media solidified with agar (Harshey, 2003; Kearns, 2010; Partridge and Harshey, 2013b). The expansion rate for swarming cells, about 2-10 μm/s depending on the bacterial specie, is approximately equal to the one observed in swimming cells of the same specie but on swimming agar (0.2-0.35 % agar).

However, other kind of motility mechanisms that allow the cells to move on top or within solid surfaces are known in other *Bacteria* (Fig. 1.5).

Twitching, also called retractile motility or social gliding, is a slow (0.06-0.3 μm/s) surface movement observed in species of the genera *Acinetobacter*, *Pasteurella*, *Pseudomonas*, *Streptococcus* or *Myxococcus,* among others (Harshey, 2003; Kaiser, 2007). The twitching motility is powered by the type IV pili extension and retraction (Mattick, 2002; Kaiser, 2007; Kearns, 2010). Similarly to swarming, this movement is primarily a social movement involving the formation of highly organized and compact rafts but by con-

trast to swarming motility, where individual swarmer cells do not move and rapidly lose their swarmer state, individual cells can show limited twitching on soft-agar plates (Harshey, 2003).

Gliding, also called adventurous gliding, is an active smooth movement along the long axis of the cell that does not involve the use of flagella or pili (Harshey, 2003; Kaiser, 2007; Kearns, 2010). It is a typical movement found primarily in myxobacteria, cyanobacteria and the *Cytophaga-Flavoabcterium* groups (Harshey, 2003). The expansion rate of this movement is highly variable and dependent on the bacterial group. For example, in the three mentioned groups the extension rates are 0.1, 10 and 2-4 μm/s, respectively (Harshey, 2003). Gliding usually involves the movement of the entire cell body over a slime layer through the use of focal-adhesion complexes, putative cell surface-associated complexes that may act as motors for motility (Kaiser, 2007; Mignot, 2007).

Finally, sliding or spreading is a passive surface translocation mechanism that does not involve motors but require surfactants or other molecules capable of reducing the surface tension (Kearns, 2010). Sliding is powered by expansive forces transmitted through the growing colony from the center to the edges; its expansion rate is very variable and is group-dependent, as observed in gliding motility (e.g 0.03 μm/s for *Mycobacterium smegmatis* or 2-6 μm/s for *Serratia marcescens*). *Escherichia*, *Bacillus*, *Serratia*, *Mycobacterium, Pseudomonas* or *Vibrio* are among the bacterial genera reported to use this "diffusion" mechanism (Matsuyama *et al.*, 1995; Harshey, 2003; Kinsinger *et al.*, 2005; Murray and Kazmierczak, 2008).

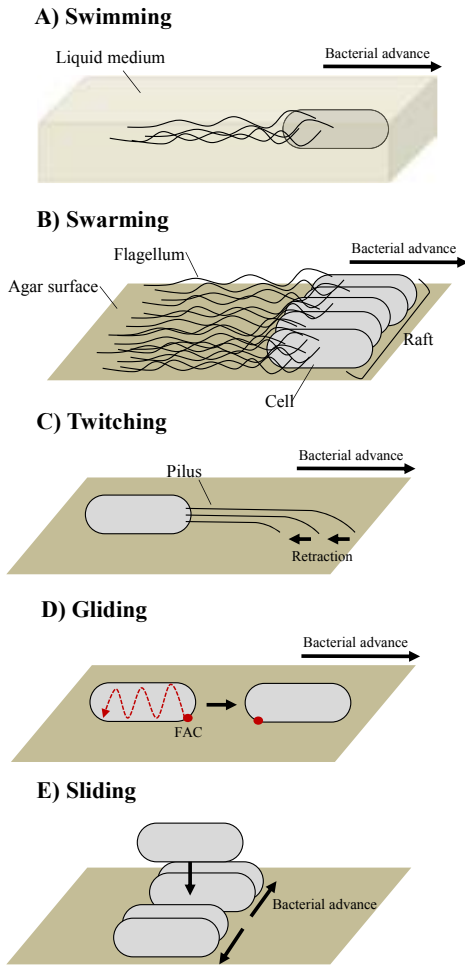

Figure 1.5. Mechanisms of bacterial motility. Schematic representation of the known types of bacterial motility: swimming, swarming, twitching, gliding and sliding. The direction of bacterial movement is shown with a black arrow in each case. FAC: Focal-adhesion complex. Modified from Kearns (2010)

1.3.2 Swarmer cell differentiation

Regarding their ability to displace over agar-solidified surfaces in the laboratory conditions, swarming bacteria may be divided in two categories: robust swarmers, that can swarm across hard agar surfaces (1.5 % agar and above) and temperate swarmers, that can only swarm over soft agar surfaces (0.4 to 0.8 % agar) (Harshey, 2003; Verstraeten *et al.*, 2008; Partridge and Harshey, 2013a).

When a bacterial colony grows on swarming medium, this triggers a cell differentiation process from vegetative (the ones found in liquid medium) to swarmer cells. In robust swarmers, such as *Proteus*, *Vibrio*, *Rhodospirillum* or *Clostridium* species, swarmer cell morphology is clearly distinguishable from their vegetative counterparts by a prominent elongation of cell bodies, usually caused by the inhibition of cell division, and by the acquisition of an hyperflagellated and polynucleate state (Fraser and Hughes, 1999; Harshey, 2003; Verstraeten *et al.*, 2008). By contrast, temperate swarmers such as *Escherichia*, *Salmonella*, *Pseudomonas*, *Serratia*, *Yersinia* or *Bacillus* species also display some cell differentiation but it is less evident than the one observed in robust swarmers. In spite of early observations that defined *E. coli* and *S.* Typhimurium swarmer cells as hyperflagellated and elongated (Harshey and Matsuyama, 1994), recent observations have demonstrated that Gram negative temperate swarmers do not display a significant swarmer cell differentiation except for modest increases in cell length as in *S.* Typhimurium (Partridge and Harshey, 2013a). This idea is consistent with the lack of swarming-associated regulation of flagellar synthesis genes observed using microarray approaches in some of the temperate swarmer species. (Wang *et al.*, 2004; Tremblay and Déziel, 2010). Some controversy arises at that point as a proteomic analysis conducted

in *S.* Typhimurium demonstrated a FliC upregulation in actively swarming cells (Kim and Surette, 2004) in contrast to transcriptomic analysis that also displayed a *fliC* upregulation but this phenomenon was attributed to a surface growth issue instead of a swarming-specific regulation (Wang *et al.*, 2004).

Mention apart should be done with the Gram positive *Bacillus* species. By contrast to other temperate swarmers, they display a significant increased cell length though not as dramatic as the observed for robust swarmers (Kearns and Losick, 2003). Also, and by contrast to Gram negative temperate swarmers, some *Bacillus* species show a differential regulation of flagellar genes on swarm agar and can display complex swarming patterns that resemble the ones observed in robust swarmers (Kearns and Losick, 2003; Salvetti *et al.*, 2011).

1.3.3 Colony patterns during swarming

One of the more striking characteristics of swarming is the wide variety of colony patterns observed (Fig. 1.6), that are usually specie-specific under certain environmental conditions. *P. mirabilis*, a robust swarmer, display a colony pattern known as terraces. This pattern is due to a phenomenon known as consolidation (Fraser and Hughes, 1999). Swarmer cells of *P. mirabilis* align in along their long axis in a structure called raft and start migrating. Periodically, swarmer cells de-differentiate into vegetative cells and starts a period of population growth but without colony expansion, named consolidation. Repeated cycles of mass migration of differentiated cells interspersed with consolidation periods gives place to the characteristic pattern of concentric circles displayed by *P. mirabilis* (Fraser and Hughes, 1999; Verstraeten *et al.*, 2008). Similar patterns could be observed in *V.*

paradoxus mobilis (McCarter, 1999; Verstraeten *et al.*, 2008; Kearns, 2010), another robust swarmer whereas temperate swarmers, like *Salmonella* or *Escherichia* species, tend to move continuously without consolidation periods thus not forming terraces (Fraser and Hughes, 1999; Verstraeten *et al.*, 2008). Again, *Bacillus* species need to be mentioned apart as some of them display a wide variety of colony patterns, ranging from featureless to dendritic, in a poorly understood fashion that has been related to media and environmental conditions (Kearns, 2010). Regarding this issue, it is hypothesized that swarming-capable bacteria can produce a wide range of colony patterns depending on the environmental conditions (Shimada *et al.*, 2004; Hiramatsu *et al.*, 2003).

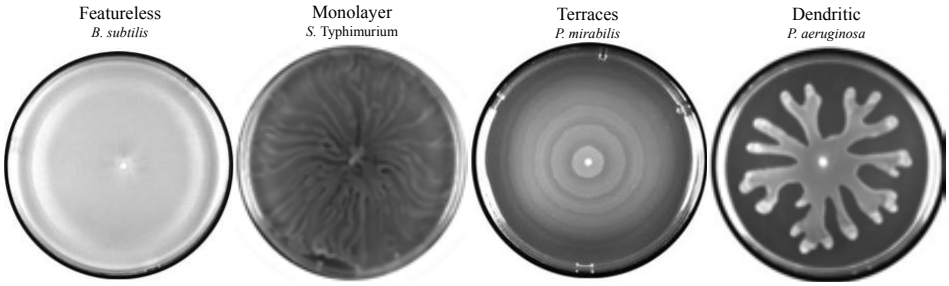

Figure 1.6. Most common colony patterns during swarming. Colony patterns displayed by *Bacillus subtilis*, *Salmonella enterica* ser. Typhimurium, *Proteus mirabilis* and *Pseudomonas aeruginosa* when grown on swarming agar plates. Images from *B.subtilis*, *P.mirabilis* and *P.aeruginosa* are adapted from Kearns (2010).

1.3.4 Conditions required to swarm

1.3.4.1 Surface moisture

The importance of surface moisture on swarming motility could be easily observed in temperate swarmers. These strains (such as *S.* Typhimurium or *E. coli*) are swarming-proficient on 0.5-0.7 % agar whereas they are unable to swarm when the agar concentration is near 1 % or above thus giving place to a less moist surface (Harshey, 2003).

The challenge on how to overcome low surface humidity arise at that point for swarmer cells. *P. mirabilis,* a well studied robust swarmer, is surrounded by a complex extra cellular matrix (ECM) during swarming. This slime is composed, among others, from an acidic capsular polysaccharide called Cmf (from Colony migration factor) and the osmolyte gliycine betaine, both linked to aid in colony hydration by extracting water from the agar medium (Fraser and Hughes, 1999; Verstraeten *et al.*, 2008; Partridge and Harshey, 2013b). In addition to its role helping in colony hydration, Cmf has been hypothesized to participate in maintaining and favoring cell-cell contacts within the swarmer cell rafts (Gygi *et al.*, 1995; Rahman *et al.*, 1999).

In temperate *Enterobacteriaceae* swarmers, like *E. coli* and *S.* Typhimurium, it has been described that lipopolysaccharide (LPS), enterobacterial common antigen (ECA) and the *flhE* gene, that belongs to the flagellar regulon, could be involved in colony hydration functions as the ones described for Cmf in *P. mirabilis* (Toguchi *et al.*, 2000; Inoue *et al.*, 2007; Stafford and Hughes, 2007). Concretely, the O-antigen of the LPS has been reported to play a critical role in *S.* Typhimurium motility (Toguchi *et al.*, 2000) and in other bacteria like *P. mirabilis* (Belas *et al.*, 1995).

In spite of the previous considerations, a model involving LPS production as a part of a swarming-specific program could not be established as LPS genes appear to be upregulated in a surface-specific instead of a swarming-specific manner (Wang *et al.*, 2004; Kim and Surette, 2004). It seems that, at least in *Salmonella*, the overproduction of LPS when living on a surface may be a characteristic used to promote swarming but not a part of a swarming-specific gene expression pattern (Partridge and Harshey, 2013b).

1.3.4.2 Frictional forces

In order to translocate over a surface, swarmer cells must overcome frictional forces generated by surface-cell charge interactions and the viscosity of the fluid between the agar surface and the cell wall (Partridge and Harshey, 2013b). Molecules discussed in the section 1.3.4.1, like LPS, have some surfactant properties that may alter the surface-cell interaction during swarming thus modifying the hardness of the frictional forces involved in this kind of motility (Partridge and Harshey, 2013b). Despite that, the mechanical approach based on an increase of the flagellar motor output to defeat frictional forces seems to be the most common and easy understandable mechanism found in bacteria (Partridge and Harshey, 2013b). Again, some differences between robust and temperate swarmers arise at that point.

Robust swarmers are known to present an hyperflagellated and elongated phenotype when doing swarming as reviewed in section 1.3.2. Thus, it has been hypothesized that increasing the cell length is a strategy to, among others, accommodate the increased number of flagella that will provide the required thrust to overcome the surface friction even in hard surfaces like 1 % agar (Partridge and Harshey, 2013b).

By contrast, temperate swarmers like *S.* Typhimurium neither overproduce flagella nor significantly increase the cell length (Partridge and Harshey, 2013a). Also in *Salmonella*, it has been reported that this modest increase in cell length could serve as a mechanism to reduce cell friction with the surface as rods have demonstrated to be more proficient in reducing the surface friction than spheres (Partridge and Harshey, 2013a). *B. subtilis* is a special case of temperate swarmer as it exhibits no increase in cell length but it promotes an increase in flagella number during swarming differentiation. Despite that, the overproduction of flagella is not as dramatic as the one observed in robust swarmers thus supporting the idea that other mechanisms to overcome frictional forces must exist (Patrick and Kearns, 2012).

As the temperate swarmers strategies against frictional forces could not be explained through the shape or the swarmer phenotype, some other mechanism to overcome this challenge must exist. *P. aeruginosa* is reported to require two sets of stator proteins (MotAB and CD) that likely transmit more power to flagellar motors allowing the bacteria to move across surfaces or swim in more viscous mediums (Doyle *et al.*, 2004; Toutain *et al.*, 2005). *E. coli* and *S.* Typhimurium only have one set of stators (MotAB) but in this case they also require the presence of the FliL protein to effectively support swarming. FliL is thought to function as an structural reinforcement of the flagellar motor allowing it to support stress produced by the higher torque necessary to overcome the frictional forces. (Attmannspacher *et al.*, 2008; Partridge and Harshey, 2013a). The theory that *S.* Typhimurium (and probably *E. coli* and others) would solve the frictional problem through a thrust increase of the existing flagellar motors is supported by the reported fact that the overproduction of MotAB alongside with FliL is equivalent to increasing the flagella number, as it happens in robust swarmers, allow-

ing *Salmonella* to swarm on hard agar substrates (Partridge and Harshey, 2013a).

1.3.4.3 Surface tension

Surface tension is a phenomenon due to the cohesive forces existing between liquid molecules and it represents a difficult challenge to overcome for moving objects like swarmer cells (Partridge and Harshey, 2013b). Surfactants, short form for surface-active agent, are amphipathic molecules that help in reducing the surface tension between the cell and the surface thus allowing an easier movement (Kearns, 2010). They are not osmolytes thus, their role is not to attract water to hydrate the colony (like the polysaccharides of the ECM) but they are involved in facilitate the colony spreading from the inoculation point (Partridge and Harshey, 2013b).

In robust swarmers, no surfactants have been described up to date and the LPS is assumed to play this role (Partridge and Harshey, 2013b). By contrast, several temperate swarmers display a variety of surfactant compounds that are secreted during swarming motility. *Bacillus* and *Serratia* are known to produce two potent surfactants known as surfactin and serrawettin respectively, and *Pseudomonas* is known to produce rhamnolipids through a modification of the core molecule HAA. Both have been shown to act as surfactants (Kearns, 2010).

E. coli and *S.* Typhimurium are not known to secrete any surfactant molecule (Chen *et al.*, 2007; Be'er and Harshey, 2011). In fact, it is reported that the wetting agent required to allow swarming motility in *Salmonella* is not a surfactant and thus LPS may play here a central role (Chen *et al.*, 2007).

1.3.4.4 Available nutrients

Nutrient availability is an important factor conditioning swarming motility (Harshey, 2003). In *S.* Typhimurium has been reported a clear dependence of the motility with the use of rich media supplemented with a carbon source such as glucose but also galactose, mannose, fructose or glycerol (Kim and Surette, 2004, 2005). Swarming motility has been observed in *Salmonella*, *Serratia* and *Proteus* in minimal media but it requires the supplement of a carbon source, usually glucose, and casamino acids (Harshey, 2003).

1.3.4.5 Temperature

Temperature is a crucial factor affecting the swarming motility. Although species like *S.* Typhimurium are able to swarm in a wide range of temperatures, usually between 30 and 37 °C (our results), others like *Serratia marcescens* are the clear example of the temperature effects over swarming. In this bacteria, swimming and swarming motility are inhibited if the temperature slightly surpasses 30 °C which could correlate with the reported inhibition of the serrawettin synthesis in a temperature-dependent fashion (Matsuyama *et al.*, 1989; Alberti and Harshey, 1990; Matsuyama *et al.*, 1995; Harshey, 2003).

1.3.5 Environment sensing and signaling pathways

1.3.5.1 Sensing and gene regulation

Before swarming-proficient cells could start moving, the surface environment must be sensed in order to trigger the required gene regulation program. The exact means by which bacteria sense the surface conditions is still poorly understood and the existence of such a program remains controversial.

In *V. parahaemolyticus*, which shows a dual flagellar system with a polar flagella commonly used in swimming and several lateral flagella induced upon surface contact (McCarter, 2004), any condition leading to a decrease in the rotary speed of the polar flagella triggers the swarmer-cell differentiation (Harshey, 2003). The polar flagellum acts here as a mechanosensor triggering the expression of the genes required to achieve the full swarmer state, such as the lateral flagella (*laf*) genes (Kawagishi *et al.*, 1996; Patrick and Kearns, 2012). The mechanism by which the mechanical signal produced by flagellum stall is transduced to an upregulation of some swarmer state related genes is still unknown (Partridge and Harshey, 2013b).

A model involving the flagella as a surface sensor for unfavorable hydration conditions have been hypothesized in *S.* Typhimurium. A mechanical impairment for flagellar rotation, primarily due to unfavorable moist conditions, is also likely to cause an interference with the filament subunit (the flagellin) secretion or with the subunit polymerization. This situation sends a feedback to the type three secretion system located at the base of the flagellum inhibiting both the flagellin and the FlgM protein, the inhibitor of flagellar class 3 genes transcription, translocation across the cell membrane and the outer membrane. This model assumes that the constant secretion of class 3 FlgM is designed to test the external environment for motility (Wang *et al.*, 2005).

Apart from the consequences of sensing unfavorable hydration conditions, which are explained above, several models exist to explain the role of the flagella in *S.* Typimurium colony hydration. Chemotaxis genes (*che*) mutants, which are impaired for the correct flagellar rotation, present a less hydrated phenotype than their wild type counterparts (Wang *et al.*, 2005; Mariconda *et al.*, 2006; Partridge and Harshey, 2013a). Two models are proposed to explain this fact. Probably, when the cell is able to freely

rotate their flagella (this is in a non-mutant background or in good moist conditions), this facilitates the capillary extraction of water from the agar thus facilitating the colony hydration. The second model accounts for a less mechanical approach. In this case, the limitation of the flagellar rotation due to a dry surface (or any mutation) leads to stalled flagellar motors which in turn send a feedback signal activating the osmolyte secretion. With this system the flagella rotation will be recovered and the colony hydration will proceed as in the first model (Partridge and Harshey, 2013a).

Finally, a sensing mechanism involving the FliL protein has been proposed in *P. mirabilis* however it still remains unclear if it is a mechanosensor mechanism or the sensing ability is dependent on any other pathway (Partridge and Harshey, 2013b).

Other less mechanical approaches to sense the conditions of the surface have been reported. In *E. coli* and *S.* Typhimurium the *flhDC* master regulator is the primary site for the integration of signals coming from the membrane associated RscBC two component system that is activated in response to outer membrane perturbations (Whitfield and Roberts, 1999; Verstraeten *et al.*, 2008; Patrick and Kearns, 2012). In *P. mirabilis*, the integration of sensing signals is known to involve also the *flhDC* master regulator and is believed to be very similar to the systems found in *E. coli* but the sensing pathways are best studied in this organism. The Umo proteins (for upregulator of the master operon *flhDC*) found in *P.mirabilis* are associated with the cell envelope and are believed to be involved in surface sensing and signal transduction to the FlhDC master regulator (Dufour *et al.*, 1998). In this organism, the Rsc pathway also plays a central role in sensing outer membrane stress and transduce the signal to the FlhDC master regulator (Patrick and Kearns, 2012). The Umo and the Rsc pathways should not be regarded as independent sensing ways as their integration

in a more complex sensing network is possible. In fact, in *S. enterica* and *S. marcescens*, an homologue of *umoB* (*yrfF* or *mucN*) have been related to the Rsc pathway (Costa *et al.*, 2003; Castelli and Véscovi, 2011). Also in *Proteus*, other proteins have been identified as central players in environmental sensing. *P. mirabilis* Lrp protein, an homologue of the *E. coli* leucine-responsive regulatory protein, has been proposed as a nutritional sensor playing a central role in swarming motility as it requires high energetic resources (Patrick and Kearns, 2012). WosA (for wild-type onset with superswarming) is a novel protein that has been involved in sensing solid surfaces via FliL interaction resulting in a final regulation of the *flhDC* master operon (Verstraeten *et al.*, 2008). Analogous strategies have been reported in *B. subtilis* through the use of the DegU proteins coupled to the SwrA master regulator but upstream sensing signals affecting this pathway are still unknown (Calvio *et al.*, 2005; Patrick and Kearns, 2012; Partridge and Harshey, 2013b).

In summary, neither a universal surface sensing mechanism nor a clear difference between the systems used by robust and temperate swarmers could be established. Cell envelope and flagella emerge as the key sensors involved in surface-sensing however, the existence of clear patterns of gene regulation in a swarming-specific manner has not been demonstrated for the known swarmer species (Partridge and Harshey, 2013b). Instead, species like *S.* Typhimurium appear to have a differential gene expression caused by surface growth rather than as a part of a swarming differentiation program (Wang *et al.*, 2004).

1.3.5.2 Signaling pathways that affect swarming motility

1.3.5.2.1 The chemotaxis system Although swarming is an extreme energy-demanding process (Harshey, 2003), the chemotactic ability of swarmer cells is reported to play a variable role within the swarming-capable species. Whereas in *V. parahaemolyticus* and *P. mirabilis* chemotaxis is required for a full proficient swarming motility but not for the swarmer-cell differentiation (Sar *et al.*, 1990; Belas *et al.*, 1991), in species like *E. coli* and *S.* Typhimurium it has been reported that the chemotaxis system but not chemotaxis is required for swarming motility (Burkart *et al.*, 1998). Indeed, an *S.* Typhimurium mutant defective in the seven known chemoreceptors and unable to swarm could be rescued by overexpressing only the cytoplasmatic domain of the Tsr receptor indicating that it is the presence of the chemotaxis pathway constituents but not the chemotaxis itself the key element controlling the swarming behavior (Mariconda *et al.*, 2006). Also, it remains unclear if all the components of the chemotaxis system are required as, for example, *cheA*, *cheR* and *cheB* mutants of *S.* Typhimurium could be rescued for swarming by expressing a constitutively active form of the CheY protein (Mariconda *et al.*, 2006).

The chemotaxis system main role is to control the flagellar motor bias between CW and CCW states which allows the cell to change the movement direction and generate a response to an attractant or a repellent (Baker *et al.*, 2006a). The flagellar motor bias has been established as an important factor affecting the swarming motility (Mariconda *et al.*, 2006). Mutations in the *che* genes cause a wide range of affectations in the motor bias. Thus, *cheA*, *cheY, cheR* and *cheW* mutations cause a bias to a CCW rotation of the flagella whereas *cheB* and *cheZ* mutations cause the bias to be displaced towards CW rotation (Sanders *et al.*, 1989b; Mariconda *et al.*, 2006). The

swarming ability of all of these mutants is impaired but in a *cheBR* mutant, which shows a nearly normal motor bias, the swarming is still supported (Mariconda *et al.*, 2006). Complementary to these evidences is the fact that *che* mutants, which show extreme motor biases, could be rescued for swarming when the surface moisture is sufficiently high in spite of the bias direction (Wang *et al.*, 2005) thus, the motor bias is a highly influential factor for swarming but only in a dry-surface situation (Mariconda *et al.*, 2006). Usually, it is believed that the CCW motor bias forms a left-handed bundle of flagella that is used for running propulsion whereas transient conversions from the left-handed form of the filament to the right-handed form caused by the CW motor bias undergo the tumbling movement (Turner *et al.*, 2000). It is proposed that CW biased mutants (like *cheB* and *cheZ*), that can not change the motor bias, are able to swarm due to a phenomenon known as inverse motility using a right-handed bundle of flagella rotating CW but only on moist surfaces (Mariconda *et al.*, 2006).

1.3.5.2.2 Quorum sensing The quorum sensing is the process by which bacteria synchronize their social activity through the release of small hormone-like molecules named autoinducers that could be sensed by the rest of the population (Waters and Bassler, 2005). In fact, cell density is believed to be a key factor controlling the swarming behavior due to the quorum sensing thus coupling swarming and social communication in bacteria (Daniels *et al.*, 2004).

In *Bacillus*, *Serratia* and *Pseudomonas* species, quorum sensing controls the production of the surfactants surfactin, serrawettin and rhamnolipids respectively, all of them closely related to swarming motility as explained in section 1.3.4.3 (Daniels *et al.*, 2004; Partridge and Harshey, 2013b). Concretely, the production of serrawettin in *Serratia* and of rhamnolipids in

Pseudomonas species has been linked to the production AHLs (*N*-acyl-homoserine lactones), a kind of autoinducers (Verstraeten *et al.*, 2008). In *P. mirabilis*, extracellular peptides or amino acids (such as glutamine) have been found to stimulate swarming motility and thus this molecules have been proposed as quorum sensing signals. Also, in the same organism, the production of putrescine, a product of amino acids break down, results in the delay of swarmer cell differentiation (Fraser and Hughes, 1999; Verstraeten *et al.*, 2008).

The role of quorum sensing during swarming in *E. coli* and *S.* Typhimurium has not been established yet (Partridge and Harshey, 2013b). However there are several evidences involving quorum sensing and motility in those species. The *E. coli* QseBC system, that shares homology with the PmrAB system of *S.* Typhimurium, has been reported to be under quorum sensing control. Also, this two-component system has been shown to regulate the expression of several flagella and motility genes by activating the transcription of *flhDC* master regulator (Sperandio *et al.*, 2002). Finally, in *S.* Typhimurium it has been reported that actively swarming cells show a significant expression of two cell-cell signaling systems (Kim and Surette, 2006). In actively migrating cells, the *pfs* and the *sdiA* genes are up-regulated. The first one is related to the control of autoinducer-2 production in *Salmonella* while the former encodes a LuxR homologue that has been linked to AHLs response also in *Salmonella* (Kim and Surette, 2006).

1.3.5.2.3 Secondary messengers The most important secondary messenger known to affect the state of mobility of bacteria is the c-di-GMP (Hengge, 2009; Krasteva *et al.*, 2012). This nucleotide-based secondary messenger have a great influence in the signaling pathways controlling the transition between motile and sessile forms of bacteria, mainly during biofilm

formation. High levels of c-di-GMP promote biofilm formation through inhibition of bacterial motility (Hengge, 2009). Thus, during swarming motility the c-di-GMP levels are maintained low. In *V. parahaemolyticus* it is known the existence of a system encoded in the *scrABC* operon which triggers a quorum sensing system and increases the phosphodiesterase activity in response to growth on a surface thus decreasing the levels of c-di-GMP and up-regulating swarming related genes (Ferreira *et al.*, 2008). This system is independent from the previously explained flagellum-driven surface sensing mechanism (Partridge and Harshey, 2013b).

In *Escherichia* and *Salmonella*, c-di-GMP is known to bind YcgR, a receptor protein, and to interact with the flagellar motor inhibiting the CW rotation thus affecting the bacterial motility (Boehm *et al.*, 2010; Paul *et al.*, 2010). In *Salmonella*, *yhjH* and *ycgR* genes, that encode a phosphodiesterase and the c-di-GMP receptor protein respectively, have been reported to be part of the class 3 flagellar regulon whose expression has been related with the surface sensing mechanisms (Frye *et al.*, 2006; Wang *et al.*, 2006a). The environmental signals that regulate the levels of c-di-GMP during swarming are still unknown but a knock-out mutant of the *yhjH* gene is unable to swarm in both *Salmonella* and *E. coli* (Wang *et al.*, 2006a; Paul *et al.*, 2010).

1.3.6 Swarming and bacterial virulence

The role of swimming and other kind of bacterial motility at different points of the infectious cycle of several pathogens have been reported throughout years (Ottemann and Miller, 1997; Fraser and Hughes, 1999; Harshey, 2003). Apart from being an important mechanism to colonize new habitats, swarming motility is a widespread ability among several bacteria with a pathogenic

lifestyle. This may be an indicator of the tight relationship between swarming ability and virulence (Harshey, 2003; Partridge and Harshey, 2013b).

As happens in other swarming-related features, the virulence-swarming relationship has been best studied in the uropathogen *P. mirabilis*. In this organism the swarming motility and swarm-cell differentiation have been reported to be essential for the invasion of the urinary tract (Allison *et al.*, 1994). During swarming in *P. mirabilis* it has been reported a significant increase in intracellular urease and extracellular heamolytic and protease activities (Allison *et al.*, 1992). Concretely, in this pathogen the expression of the *hpmA* locus, coding for the HpmA haemolysin toxin, and *zapA* locus, coding for a metalloprotease involved in resistance towards some antibacterial compounds, has been reported to be a coordinated process with the expression of the flagellar regulon which in turn is closely related to swarm-cell differentiation (Walker *et al.*, 1999; Fraser *et al.*, 2002; Belas *et al.*, 2004). In fact, variations in the *flhDC* flagellar master regulator expression have shown to affect the expression of the *hpmA* locus (Fraser *et al.*, 2002). This link between the expression of virulence factors and swarming related functions have been observed in other bacteria. In *P. aeruginosa* the swarmer population shows a significant increase in the expression of several virulence factors, such as extracellular proteases, secretion systems closely related to host invasion and toxins related to lung damage. The expression of the previously mentioned virulence factors come altogether with the up-regulation of the multidrug efflux pump MexGHI-OpmD which confers an increased antibiotic resistance (Overhage *et al.*, 2008).

In *S.* Typhimurium, the swarmer population has been reported to display an increased antibiotic resistance towards a wide variety of antibiotic classes when compared to its vegetative counterparts, specially to those that inhibit protein synthesis such as macrolides or aminoglycosides (Kim *et al.*,

2003). Although the main resistance mechanism to several of the antibiotics that showed a distinct profile between swarmer and vegetative cells is through enzymatic modifications, it is argued that the elevated resistance observed may be related to changes in the cell envelope. As explained above, the LPS has been demonstrated to play a central role in the swarming motility of *S.* Typhimurium affecting the colony hydration (Toguchi *et al.*, 2000). The LPS is a known factor affecting bacterial virulence and the expression of several genes involved in its biosynthesis is affected in a surface-specific manner in *Salmonella* (Finlay and Falkow, 1988; Wang *et al.*, 2004). Also, the expression of several outer membrane proteins (OmpA, OmpD and OmpW) is known to be down-regulated in swarmer cells (Kim and Surette, 2004). Thus, it is believed that swarmer cells present a modified and less permeable cell envelope when compared to vegetative cells that indirectly could block the entry of the antimicrobial compounds (Kim *et al.*, 2003).

Also in *S.* Typhimurium, it has been demonstrated that genes related to the iron metabolism (tightly related to *Salmonella* pathogenicity) are up-regulated in a swarming-specific manner. Also, the expression of the pathogenicity island 1 (SPI-1), a large cluster of virulence genes found in *Salmonella*, is influenced in a surface-specific manner indicating its close relationship with surface motility mechanisms and thus with the swarming motility (Wang *et al.*, 2004; Teixidó *et al.*, 2011).

1.4 The RecA protein

1.4.1 General Characteristics

The RecA protein is universally known to be the main bacterial recombinase involved in non-mutagenic repair of stalled replication forks in several bac-

terial species such as *E. coli* and *S.* Typhimurium (Kowalczykowski *et al.*, 1994; Lusetti and Cox, 2002). Also, it is the activator of the SOS system, the emergency repair mechanism that allows bacteria to surpass the effects of being subject to DNA damaging conditions such as UV radiation or the presence of antimicrobial agents. Upon the appearance of ssDNA in the cell (e.g. due to unrecoverable stalled replication forks or DNA repairing processes) RecA turns into its active form (RecA*) by binding to this ssDNA and forming nucleofilaments around it. RecA* is then able to trigger the autohydrolysis of the SOS repressor, LexA, thus increasing the expression of the SOS genes (Erill *et al.*, 2007; Janion, 2008).

The RecA protein is also involved in several other cellular processes such as the control of integron dynamics (Guerin *et al.*, 2009; Cambray *et al.*, 2010), the appearance and horizontal transfer of antibiotic resistances (Blázquez *et al.*, 2012), the prophage induction (Sauer *et al.*, 1982; Shearwin *et al.*, 1998; Campoy *et al.*, 2006), the induction and horizontal transfer of pathogenicity islands and other virulence factors (Zhang *et al.*, 2000; Ubeda *et al.*, 2005; Maiques *et al.*, 2006) and finally to the control of bacterial motility as it is discussed in the next section (Section 1.4.2).

Structurally, RecA is a monomeric protein that could be divided in a central major domain flanked by two smaller subdomains at the N- and C-terminus respectively. Its active form is formed by an helical polymer of 6 monomers that binds around ssDNA forming the so called nucleofilament (Story *et al.*, 1992).

The monomer is constituted by four functional domains distributed along the different structural parts of the protein (Story *et al.*, 1992). The first one, located at the major structural domain of the protein, harbors the ATP binding and hydrolysis active sites. ATP is required for the RecA binding and stabilization to ssDNA thus it is required for RecA activa-

tion. The second, located at the so called loops 1 and 2 within the major structural domain of the protein, contains the ssDNA binding region. The third, located at the smaller N- and C-terminus subdomains, contains the monomer-monomer and polymer-monomer contact sites. Finally, the fourth functional domain harbors the LexA binding site. This region has also been reported to be a key player to the interaction with other proteins (Story *et al.*, 1992; Karlin and Brocchieri, 1996; Rehrauer and Kowalczykowski, 1996; Lusetti and Cox, 2002; Kim *et al.*, 2013).

1.4.2 Influence over swarming motility

As mentioned above (Section 1.4.1), RecA is known to be the activator of the SOS system among other functions. The first evidences that pointed towards an interaction between the RecA protein and the motility systems of the cells came from the work developed by Arifuzzaman *et al.* (2006). In this large-scale immunoprecipitation work, whose aim was to define the network of protein-protein interactions in *E. coli,* it was reported that RecA co-immunoprecipitates alongside CheW, one of the main component of the chemotaxis signaling arrays and a protein known to be deeply involved in the bacterial motility (Section 1.2.2).

Although the relationship between the RecA protein and the swarming motility has been clearly established in the recent years (Gómez-Gómez *et al.*, 2007; Medina-Ruiz *et al.*, 2010), little is known about the molecular details of this relation.

In *E. coli* and *S.* Typhimurium, *recA* mutants are unable to swarm (Gómez-Gómez *et al.*, 2007; Medina-Ruiz *et al.*, 2010). In addition, the overexpression of *recA* also causes a swarming motility deficiency in *S.* Typhimurium (Medina-Ruiz *et al.*, 2010). Altogether, this results show that,

at least phenotypically, both the excess and the absence of RecA are equivalent situations.

Moreover, RecA is presumed to be the only responsible of the control of swarming motility within the entire SOS regulon (Medina-Ruiz *et al.*, 2010). In detail, it has been reported that the induction of the SOS system with mitomycin C causes a swarming deficiency in a dose-dependent fashion (Medina-Ruiz *et al.*, 2010) but also, a detailed microarray analysis of the SOS regulon genes indicate that only the presence or absence of *recA* but not any other SOS genes have an effect over the swarming motility (Gómez-Gómez *et al.*, 2007). To reinforce this idea, it is known that swarming defective strains of *E. coli* lacking the *recA* gene could be phenotypically restored by expressing a plasmid-borne copy of the *recA* gene (Gómez-Gómez *et al.*, 2007). In the same way, the swarming ability in an *S.* Typhimurium proficient strain could be impaired by overexpressing a plasmid-encoded copy of the *recA* gene (Medina-Ruiz *et al.*, 2010).

In addition, none of the already known RecA activities, such as genetic recombination, promotion of cell survival after DNA damage and DNA-dependent ATP hydrolysis, is required for the observed RecA control over swarming motility and thus a novel and non-canonical pathway for RecA as a motility modulator arises (Gómez-Gómez *et al.*, 2007).

All these results point towards an implication of the SOS system, through RecA, in controlling or at least modulating the bacterial swarming motility. As mentioned above, the putative relationship between RecA and CheW might be at the core of this novel regulating activity of RecA. In fact, an *S.* Typhimurium strain that constitutively expresses *recA*, and thus it shows a swarming deficient profile, could be rescued for swarming by overexpressing the *cheW* gene to a certain level (Medina-Ruiz *et al.*, 2010). Beyond that level, the *cheW* excess causes the loss of the swarming ability

again as expected (Sanders *et al.*, 1989b). These data confirmed the importance of an equilibrium between RecA and CheW for swarming motility *in vivo* thus reinforcing the idea of an existing bridge between the SOS system and the bacterial motility through this protein-protein interaction.

Chapter 2

Objectives

As stated on Chapter 1, there are sufficient evidences that point towards a direct implication of the SOS system, and in particular the RecA protein, as key regulators or modulators of the swarming behavior.

The main aim of the present work is to elucidate the role of the SOS system, through the RecA protein, in the bacterial motility and specifically the swarming behavior of *Salmonella enterica* sv. Typhimurium.

Subsequently, derived objectives are:

1. To confirm the interaction between RecA and CheW proteins through other approaches than two-hybrid.

2. To determine the molecular ratio between RecA and CheW in swarming conditions.

3. To evaluate the effect of an increase of RecA concentration in the swarming behavior of *S.* Typhimurium.

4. To elucidate the molecular mechanism whereby RecA modulates the swarming motility.

Chapter 3

Materials & Methods

3.1 Strains, plasmids and bacteriophages

Strains, plasmids and bacteriophages used in this study are listed in Table 3.1.

Table 3.1. Strains, plasmids and bacteriophages used in this study.

Strain, plasmid or phage	**Relevant genotype/phenotype**	**Source**
Strains		
S. Typhimurium		
ATCC 14028	Wild type strain	ATCC
LT2	Wild type strain	ATCC
MA5975	as as ATCC 14028, but ΔGifsy-1, ΔGifsy-2	Figueroa-Bossi and Bossi (1999)

Strain, plasmid or phage	**Relevant genotype/phenotype**	**Source**
UA1582	as LT2 but $\Delta sulA::\Omega$, Rif^R	Lab. collection
UA1685	as LT2 but $\Delta sulA::\Omega$ $\Delta lexA11::\Omega$-Km, Rif^R, Km^R	Lab. collection
UA1826	as ATCC 14028 but pKOBEGA, Ap^R	Lab. collection
UA1876	as ATCC 14028 but *recAo6869*, Km^R	Lab. collection
UA1907	as ATCC 14028 but $\Delta cheW\Omega$Cm, Cm^R	Lab. collection
UA1908	as ATCC 14028 but $\Delta cheW$	This work
UA1909	as ATCC 14028 but $\Delta cheR\Omega$Cm, Cm^R	This work
UA1910	as ATCC 14028 but $\Delta cheR$	This work
UA1911	as ATCC 14028 but $\Delta recA\Omega$Cm, Cm^R	This work
UA1912	as ATCC 14028 but $\Delta recA$	This work
UA1913	as ATCC 14028 but $\Delta cheR$ $\Delta recA$	This work
UA1914	as ATCC 14028 but $\Delta cheR$ *recAo6869*	This work
UA1915	as ATCC 14028 but $\Delta cheR$ $\Delta cheW\Omega$Cm, Cm^R	This work
UA1916	as ATCC 14028 but *cheW*::FLAG	This work

Strain, plasmid or phage	**Relevant genotype/phenotype**	**Source**
UA1917	as ATCC 14028 but *cheW*::FLAG *recAo6869*, Km^R	This work
UA1918	as ATCC 14028 but *cheW*::FLAG Δ*recAΩ*Cm, Cm^R	This work
UA1919	as ATCC 14028 but Δ*sulAΩ*Cm, Cm^R	This work
UA1920	as ATCC 14028 but Δ*ysdABΩ*Cm, Cm^R	This work
UA1921	as MA5975 but Δ*sulAΩ*Cm, Cm^R	This work
UA1922	as MA5975 but Δ*sulA*	This work
UA1923	as MA5975 but Δ*sulA* Δ*ysdABΩ*Cm, Cm^R	This work
UA1924	as MA5975 but Δ*sulA* Δ*sicPΩ*Cm , Cm^R	This work
UA1925	as MA5975 but Δ*sulA* Δ*ysdABΩ*Cm Δ*lexA11*::*Ω*Km, Cm^R, Km^R	This work
UA1926	as ATCC 14028 but Δ*cheY*	Lab. collection

Strain, plasmid or phage	**Relevant genotype/phenotype**	**Source**
E. coli		
DH5α	*supE4 ΔlacU169* (φ80d*lacZ*ΔM15) *hsdR17 recA1 endA1 gyrA96 thi-1 relA1*	Clontech
BL21 (DE3) pLysS	*F- dcm ompT lon hsdS* (r_B-m_B-) *gal* λ(DE3) [pLysS, Cm^R]	Stratagene
Plasmids		
pKOBEGA	λ red recombinase expression plasmid, P_{BAD} promoter, Ts origin of replication, Ap^R	Chaveroche *et al.* (2000)
pKD3	Vector carrying FRT-Cm construction, Ap^R, Cm^R	Datsenko and Wanner (2000)
pKD4	Vector carrying FRT-Km construction, Ap^R, Km^R	Datsenko and Wanner (2000)
pCP20	Vector carrying FLP system, OriVts, Ap^R, Cm^R	Datsenko and Wanner (2000)
pGEM-T	Cloning vector, Ap^R	Promega
pGEX 4T-1	Expression vector, P_{tac} promoter, *lacIq*, GST fusion tag, Ap^R	Amersham Biosci-ences
pET15b	Expression vector, P_{T7lac}, $lacI^+$, N-terminal 6xHis tag, Ap^R	Novagen

Strain, plasmid or phage	**Relevant genotype/phenotype**	**Source**
pET22b	Expression vector, P_{T7lac}, $lacI^+$, C-terminal 6xHis tag, Ap^R	Novagen
pKO3	Shuttle vector for homologous recombination, OriVts, *sacB*, Cm^R	Latasa *et al.* (2012)
pUA1108	pGEX4T-1 derivative, P_{tac} promoter, *lacIq*, Ap^R	Lab. collection
pUA1120	pGEM-T derivative carrying *S.* Typhimurium ATCC 14028 *cheW*::1xFLAG fusion, Ap^R	This work
pUA1121	pKO3 derivative carrying *S.* Typhimurium ATCC 14028 *cheW*::1xFLAG fusion, Cm^R	This work
pUA1122	pET22b derivative carrying *S.* Typhimurium ATCC 14028 *recA*, Ap^R	Lab. collection
pUA1123	pGEX 4T-1 derivative carrying *S.* Typhimurium ATCC 14028 *cheW*, Ap^R	This work
pUA1125	pGEX 4T-1 derivative carrying *S.* Typhimurium ATCC 14028 *recA*, Ap^R	This work
pUA1126	pUA1108 derivative carrying *eYFP* gene, Ap^R	This work

Strain, plasmid or phage	**Relevant genotype/phenotype**	**Source**
pUA1127	pUA1108 derivative carrying *eYFP::cheR* fusion, Ap^R	This work
pUA1128	pUA1108 derivative carrying *cheW*::1xFLAG fusion, Ap^R	This work
pUA1129	pUA1108 derivative carrying *S.* Typhimurium ATCC 14028 *recA*, Ap^R	Lab. collection
Bacteriophages		
P22HT	High transduction efficiency P22	J.L.Ingraham
P22*vir*	P22 virulent derivative, spontaneous isolate	Lab. collection

ATCC, American Type Culture collection; Cm, chloramphenicol; Ap, ampicillin; Km, kanamicyn; OriVts, thermosensible origin of replication.

For long term storage, strains of *S.* Typhimurium and *E. coli* were frozen at -80 °C in cryoprotective fluid vials (*Protect*, Ferrer Farma). Culture supernatants containing bacteriophages were filtered (0.45 µm pore diameter filters, Whatman) to ensure sterility and stored in production medium at -4 °C.

3.2 Oligonucleotides

Oligonucleotides used in this study are listed in Table 3.2. Unless otherwise noted, Invitrogen is the oligonucleotide supplier. All oligonucleotides were received in lyophilized form and were reconstituted with MQ-water to a final concentration of 100 µM.

Table 3.2. Oligonucleotides used in this study.

Oligonucleotide	5'-3' Sequence[a]	Application
Construction of mutant strains of *S.* Typhimurium ATCC 14028		
P1cheR	CATCTCTGCCCTCCGGGCAAACGTCAGTATT GTTACAGATGACACAGCGCCTCGCGCTGTCC GACGCGCATTTTCGTCGG**GTGTAGGCTGG AGCTGCTTC**	One-step deletion of *S.* Typhimurium *cheR* gene.
P2cheR	CTTACTTAGCGCATACACCGTCTGTCCGCGC AGGCTAAACTCGCGCACGAGGTTGCTAAAGT TTTCTGAGTGACCGGCAA**ATGGGAATTAG CCATGGTCC**	One-step deletion of *S.* Typhimurium *cheR* gene.
cheRstm extF	CAGTCATTAGCCGCCAGGGA	Confirmation of *S.* Typhimurium *cheR* gene mutagenesis.

Oligonucleotide	**5'-3' Sequence**[a]	**Application**
cheRstm extR	TCGGAACCTTTCCCGGTCAG	Confirmation of *S.* Typhimurium *cheR* gene mutagenesis.
cheWF-F	CGGGATCCATGACCGGTATGAGTAATG	FLAG-tag insertional mutagenesis. (*Bam*HI site)
cheWF-R	CGGGATCCGCTGCTCTGCTGGTTAG	FLAG-tag insertional mutagenesis. (*Bam*HI site)
cheWF-F1	GGCGGCGGCGACTACAAAGACGACGACGA CAAATAATAACGTTGCCGGATGGCGTCG	FLAG-tag insertional mutagenesis.
cheWF-R1	TTTGTCGTCGTCGTCTTTGTAGTC GCCGCCGCCCGCGACGTGTGATGCTGCG	FLAG-tag insertional mutagenesis.
FLAGori	GACTACAAAGACGACGACG	Confirmation of FLAG-tag insertional mutagenesis.
cheWextF	GTCACGTTGAGATCCAGTCA	Confirmation of *S.* Typhimurium *cheW* gene mutagenesis.

Oligonucleotide	5'-3' Sequence[a]	Application
cheWextR	TCGCTGGCAATGGCGTCATA	Confirmation of *S.* Typhimurium *cheW* gene mutagenesis.
P1sulA	CGTCATTTCCTACCACTACCCACAACGCTGC GCGCACCGCTACGGAAAATGCCGCGGCAGGA CTGGTCAGTGAAGTTGTC**GTGTAGGCTGG AGCTGCTTC**	One-step deletion of *S.* Typhimurium *sulA* gene.
P2sulA	GCCCGGAATGCTGTCTCCTGGGTAAAGCGTG CGCACGTACAGGGCGCATGATAAACCCTACC GCATTACCTACCTTCGCT**ATGGGAATTAGC CATGGTCC**	One-step deletion of *S.* Typhimurium *sulA* gene.
sulAextF	GTCACGTTGAGATCCAGTCA	Confirmation of *S.* Typhimurium *sulA* gene mutagenesis.
sulAextR	TCGCTGGCAATGGCGTCATA	Confirmation of *S.* Typhimurium *sulA* gene mutagenesis.

Oligonucleotide	5'-3' Sequence[a]	Application
P1ysdAB	TCGTAAACCGGCGCAACGAAGTCCTGGCTGA AACGGGTGGTGCCGTCAGCGCCTTAACCCCC TCGTGAGCACACTGTGTT**GTGTAGGCTGG AGCTGCTTC**	One-step deletion of *S.* Typhimurium *ysdAB* gene.
P2ysdAB	TACCCGGGAAGCGAAAGACCAGCGGATAAGG TGAAAGGGGAGCGGTTGCCCGCTCCCCTTCG GTGCGGCTTGAATCTGAA**ATGGGAATTAG CCATGGTCC**	One-step deletion of *S.* Typhimurium *ysdAB* gene.
ysdABextF	CCGAAGCGAGGTTCTTACAGC	Confirmation of *S.* Typhimurium *ysdAB* gene mutagenesis.
ysdABextR	ATCGCGGCGTAGAGCTTATCG	Confirmation of *S.* Typhimurium *ysdAB* gene mutagenesis.
lexAstmF1	GGCGGAATGAAAGCGTT	Confirmation of *S.* Typhimurium *lexA* gene mutagenesis. (partial *Hinc*III site)

Oligonucleotide	5'-3' Sequence[a]	Application
lexAstmR	CTACAACCATTCCCCGTTG	Confirmation of *S.* Typhimurium *lexA* gene mutagenesis.
lexAstmexF	GATGCGATTACCCGTGTGTT	Confirmation of *S.* Typhimurium *lexA* gene mutagenesis.
lexAstmexR	TCAGGAACTGCATTCCCGTA	Confirmation of *S.* Typhimurium *lexA* gene mutagenesis.
STM2583 F	GATAATACGGTCAGACAG	Confirmation of *S.* Typhimurium Gifsy 1 presence.
STM2637 R	TTCAGATGCTGTTTGGATCT	Confirmation of *S.* Typhimurium Gifsy 1 presence.
STM1004 F	CTTGAGCTGGGTTATAGC	Confirmation of *S.* Typhimurium Gifsy 2 presence.

Oligonucleotide	5'-3' Sequence[a]	Application
STM1057 R	AAGGTCAAGTCAATATCAGT	Confirmation of *S.* Typhimurium Gifsy 2 presence.
oraAint dw	CGTGCCATTTCACTCCAGTC	Positive control for Gifsy 1/2 presence confirmation PCR.
oraAint up	CCTTTTGGCATTTCTCCCTG	Positive control for Gifsy 1/2 presence confirmation PCR.
Construction and cloning of *eyfp::cheR* fusion		
eYFP F	GGGGTACCATGGTGAGCAAGGGCGAGGA	Overlap extension PCR of the *eYFP* fragment. (*Kpn*I site)
eYFP R	GATGTTCCGCCTCCGCCTCCCTTGTACA GCTCGTCCATGC	Overlap extension PCR of the *eYFP* fragment.
cheRstm F	ACAAGGGAGGCGGAGGCGGAACATC ATCTCTGCCCTCCGG	Overlap extension PCR of the *cheR* fragment.
cheRstm R	GGGGTACCTCATGCTTTATCCTTACTTA	Overlap extension PCR of the *cheR* fragment. (*KpnI* site)

Oligonucleotide	5'-3' Sequence[a]	Application
eYFP NdeI	GGAATTCCATATGGTGAGCAAGGGCGAGGA	Cloning of *eYFP::cheR* and *eYFP* into pUA1108. (*Nde*I site)
Fusio BamHI	CGGGATCCTCATGCTTTATCCTTACTTA	Cloning of *eYFP::cheR* into pUA1108. (*Bam*HI site)
eYFP BamHI	CGGGATCCTTACTTGTACAGCTCGTCCA	Cloning of *eYFP* into pUA1108. (*Bam*HI site)
Cloning of *recA* gene		
recApGEXF	CGCGGATCCATGGCTATCGACGAAAACAA	*recA* gene cloning into pGEX-4T-1. (*Bam*HI site)
recApGEXR	CCGCTCGAGTTAAAAATCTTCGTTGGTTT	*recA* gene cloning into pGEX-4T-1. (*Xho*I site)
Cloning of *cheW* and *cheW::*FLAG genes		
cheWApGEXF	CGCGGATCCATGACCGGTATGAGTAATGT	Cloning of the *S.* Typhimurium *cheW* gene into pGEX-4T-1. (*Bam*HI site)

Oligonucleotide	**5'-3' Sequence**[a]	**Application**
cheWpGEXR	CCGCTCGAGTTACGCGACGTGTGATGCTG	Cloning of the *S.* Typhimurium *cheW* gene into pGEX-4T-1. (*Xho*I site).
cheW3xFxXho	CCGCTCGAGTTATTTGTCGTCGTCGTC	Cloning of the *S.* Typhimurium *cheW* ::FLAG fusion into pGEX-4T-1. (*Xho*I site)
cheWstNdeI	GGAATTCCATATGACCGGTATGAGTAATG	Cloning of the *S.* Typhimurium *cheW* ::FLAG fusion into pUA1108. (*Nde*I site)
cheW1xFBam	CGCGGATCCTTATTTGTCGTCGTCGTC	Cloning of the *S.* Typhimurium *cheW* ::FLAG fusion into pUA1108. (*Bam*HI site)

a) Underlined: Restriction endonuclease site; double underlined: FLAG tag; undulating underlined: glycine linker; **bold**: pKD3 hybridization site.

3.3 Microbiological methods

3.3.1 Media and culture conditions

During this study, either solid, liquid or semisolid media were used. The composition of every medium and solution used in this study is described in detail in Annex A.

Unless otherwise noted, *S.* Typhimurium and *E. coli* were cultured in LB-Miller (A.1.4). Other media used in this study are: LB-Lennox (A.1.3), used to obtain electrocompetent cells; brain heart infusion (BHI) medium (A.1.1), used in electrotransformation protocol; LB-swarming (A.1.5), used in swarming assays; SOB medium (A.1.6.1), used in one-step inactivation procedure; terrific broth (TB) (A.1.7), used in plasmid extractions and tryptone broth (TBr) (A.1.8), used in fluorescence and chemotaxis experiments. When required, special growth conditions used are explained.

When necessary, ampicillin (100 µg/ml for *S.* Typhimurium; 50 µg/ml for *E. coli*), chloramphenicol (34 µg/ml) and/or kanamycin (100 µg/ml for *S.* Typhimurium; 50 µg/ml for *E. coli*) were added to growth medium. Other supplements used in different applications are mentioned in each specific case (see below).

In all cases, culture media were sterilized by wet heat at 121 °C during 15 minutes in an autoclave. Antibiotics and other non-autoclavable supplements were sterilized by filtration with 0.45 µm pore diameter filters (Whatman).

After sterilization, liquid culture media were allowed to cool progressively at room temperature and stored at 4 °C until needed. Solid media were allowed to cool to 50 °C and, when required, antibiotics or other supplements were added while shaking. After that, media were plated into 9 cm

Petri dishes (Sterillin), allowed to solidify at room temperature and stored at 4 °C.

The vast majority of experiments made in this work required the use of liquid cultures growing in early or mid-exponential phase. Over-night cultures (approx. 16 h) were diluted, usually 1/100, and incubated at 37 °C with a constant shaking at 150 rpm (*Excella® shaker E5*, New Brunswick Scientific) until the growth phase required was achieved. For those strains harboring thermosensible plasmids, incubations were made at 30 °C to maintain the plasmid or at 43 °C to eliminate it. When solid cultures were needed, the strains were streaked on the desired media and incubated over-night upside down at 37 °C or 30 °C as required.

3.3.2 Growth kinetics

The growth kinetics of several mutant strains were conducted to allow a direct and fast correlation between the optical density and the number of viable cells.

For these experiments, a 250 mL erlenmeyer containing 100 mL of the appropriate medium was used to ensure enough volume to take the sufficient amount of samples required and enough free volume to allow a good aeration thus allowing an optimal growth.

Briefly, an over-night culture in the desired medium containing the required antibiotics was diluted 1/100 in 100 mL of fresh medium (the same as the over-night). The initial optical density (OD) measured at the appropriate wavelength was of 0.04-0.06. The culture was then incubated at 37 °C, or 30 °C depending on the strain and the desired conditions, with constant shaking at 150 rpm (*Excella® shaker E5*, New Brunswick Scientific).

Samples were taken every 20-30 minutes during the lag and stationary phases and every 10-15 minutes during the exponential growth. The OD was measured and appropriate dilutions were plated on LB plates (containing antibiotic if required). After an over-night incubation at 30 °C or 37 °C (as required) the CFUs/mL at every time point were calculated. The experiment was conducted until the stationary phase was reached.

3.3.3 Swarming motility assays

Swarming motility assays were conducted to test *S.* Typhimurium behavior regarding on different mutant backgrounds. Fresh solid LB plates (A.1.4) were streaked with different *S.* Typhimurium strains and incubated overnight.

Fresh LB-swarming plates (A.1.5) were prepared the day of the assay. Small volume bottles were prepared and sterilized as described before. After sterilization, the medium was plated on 9 cm Petri dishes while constantly shaking to ensure homogenization of the agar. Supplements, like IPTG (A.2.16), should be added at that point. After solidification, plates were placed with the lid ajar in an airflow cabin and allowed to dry during 15 minutes.

The inoculum was applied with a sterile toothpick. A single colony was picked and inoculated at the center of the plate avoiding medium penetration. After inoculation, plates were incubated at 37 °C during a controlled period of time, usually 9 to 12 hours. This time is required for the wild type strain to reach the plate border under our experimental conditions.

If the degree of movement of study strains had to be evaluated, plates were photographed (*ChemiDoc™ XRS+* system, Bio-Rad) and the diameter of the colony was measured using ImageJ software (National Institutes

of Health). Then, the relative movement was calculated as the ratio between the colony diameter of the study strain and that of the wild type strain under the same experimental conditions.

3.3.4 Chemotaxis assays

Chemotaxis assays were conducted essentially as described by Adler (1973) but modified, where necessary, to adapt to *S.* Typhimurium particularities (Melton *et al.*, 1978; Lazova *et al.*, 2012).

Previously to the preparation of the strains, the chemotaxis chamber set and the capillary tubes were prepared. The final set-up is presented in Figure 3.1 A.

The chemotaxis chamber set was formed by laying three V-shaped needles (bent from a 40 mm 18G needle, Nipro) on the surface of an aseptic 140 mm Petri dish (Deltalab) and then by covering them with a 24 x 65 mm microscope cover slip (Menzel-Glässer). The needles and the cover slips were previously autoclaved to ensure the sterility.

Capillary tubes (*1 µL - 3 cm long Microcaps*, Drummond Scientific Co.) were used to contain the chemotactic substance to test. The capillaries were handled with forceps during the whole procedure. First, one end of the capillaries was heat-sealed in a flame and then the capillaries were autoclaved to ensure the sterility. After that, the sealed capillaries were passed four times through a flame and immediately plunged, open end down, into a small vial containing 2 mL of the chemotactic substance dissolved at the desired concentration. In this work, substances used to evaluate the chemotactic response of *S.* Typhimurium were either tethering buffer (A.3.19) or L-aspartate at a concentration of 10 mM dissolved in tethering buffer. Cap-

illaries were allowed to cool-down inside the vials for at least 30 minutes before using them in the chemotaxis assays.

For the preparation of cell suspensions, overnight cultures of *S.* Typhimurium in tryptone broth (A.1.8) were diluted 1/100 in the same medium but without antibiotics and incubated at 30 °C with constant shaking. When an OD_{600} of approximately 0.5 was reached, 10 mL of the cultures were pelleted by low speed centrifuging (4500 g) for 10 minutes at room temperature. Then, the pellet was resuspended in 1 mL of tethering buffer at room temperature and the cells were centrifuged again in the same conditions. After the wash, the pellets were resuspended in 1 mL of tethering buffer at room temperature.

Washed cell suspensions were diluted to approximately $6{\cdot}10^7$ CFUs/mL and approximately 0.2 mL of the resultant suspensions were applied into every chemotaxis chamber. Then, one filled capillary was inserted, open end first, into the every chemotaxis chamber containing the cell suspension and finally the chemotaxis chamber set was covered with the Petri dish cover. The incubation was conducted for 1 hour at 30 °C unless otherwise noted.

After the incubation, the exterior of the capillaries was rinsed with a steam of sterile MQ-water. Then, the sealed end of the capillaries was broken off over an 1.5 mL microcentrifuge tube filled with saline solution (A.2.22). The content of the capillaries was emptied using the rubber bulb supplied with the capillaries and an 1 mL sterile syringe (Fig. 3.1 B).

Suitable dilutions were plated on LB plates (A.1.4). After an over-night at 37 °C incubation, the colonies were counted and the CFUs/mL were calculated.

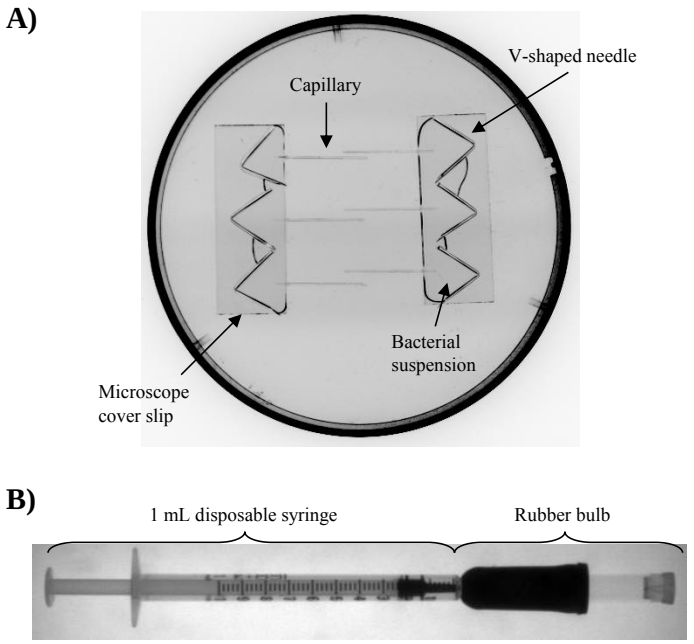

Figure 3.1. Adler's modified chemotaxis chamber set. A) Six chemotaxis chambers with the basic design as the one proposed by Adler (1973) arranged in a unique chamber set developed over a 140 mm Petri dish. **B)** One milliliter disposable syringe coupled to the rubber bulb supplied with the capillaries. This construction is used for a more efficient recuperation of the liquid inside of the capillaries.

3.3.5 Electrocompetent cell preparation

Preparation of electrocompetent cells for transformation at high voltages requires the final cell suspension to have a very low conductivity. The preparation method was described by Dower *et al.* (1988) and was used with some slight modifications.

Over-night cultures of *S.* Typhimurium or *E. coli* were made and incubated at 37 °C, or 30 °C for thermosensible plasmids. The day after, the required volume of LB-Lennox medium (100 mL to 1 L, A.1.3) was inoculated (1/100 dilution from the over-night) and allowed to growth at a convenient temperature with constant shaking until an OD_{550} of 0.5-0.6 was reached. The culture was then transferred to previously chilled 80 mL polypropylene tubes and centrifuged for 10 minutes at 12300 g and 4 °C (standard centrifuging conditions for this procedure). After that, the pellet was washed twice with 1 volume of cold MQ-water (*Ultra-pure water system plus 185*, Millipore). Cells were washed one more time with 0.02 volumes of ice cold 10 % glycerol (A.2.12). Finally, cells were harvested and resuspended in 0.001 volumes of ice cold 10 % glycerol. The resulting suspension was distributed in 50 µL aliquots and frozen at -80 °C until needed.

3.3.6 Electrotransformation

Electrotransformation was conducted following the methods described by Dower *et al.* (1988), O'Callaghan and Charbit (1990) and Green and Sambrook (2012)with some modifications.

The desired amount of DNA (Plasmid DNA, 100-200 ng; linear fragments, 1 µg) was mixed with competent cells previously thawed on ice. The mix was then transferred to a 2 mm gap electroporation cuvette (*Electroporation Cuvettes*, Cell Projects).

The cells-DNA mix was then subjected to an electrical pulse *(Bio-Rad Gene Pulser*, Bio-Rad) of 2.5 kV/cm^2 for *S.* Typhimurium or 2 kV/cm^2 for *E. coli* and immediately recovered with 1 mL of BHI medium. Transformed cells were transferred to a glass tube, incubated at 37 °C (or 30 °C for thermosensible plasmids) for 45 minutes and finally spreaded into appropriate selective LB-Miller plates (A.1.4).

3.4 Nucleic acids manipulation methods

3.4.1 Nucleic acids quantification

Nucleic acids were quantified by spectrophotometry measuring the absorbance at 260 nm wavelength (*Nanodrop 2000*; Thermo Scientific). Purity and cleanness were evaluated regarding the following absorbance relationships respectively: $1.8 \leq A_{260}/A_{280} \leq 2.0$ and $2.0 \leq A_{260}/A_{230} \leq 2.2$.

3.4.2 Agarose gel electrophoresis

Agarose gel electrophoresis was performed regularly to check DNA integrity, size or to recover PCR products.

Briefly, the required amount of conventional agarose (*D1 Low EEO*; Pronadisa) was mixed with TAE 1X (A.3.16) buffer in an erlenmeyer, heated to 90 °C and allowed to dissolve while stirring. When the agarose was completely dissolved the recipient was cooled down to approximately 50 °C under a running faucet and then ethidium bromide (*Ethidium Bromide-Solution 1 %*; AppliChem) was added to a final concentration of 0.5 µg/mL while mixing slightly to avoid air bubbles generation. The solution was then poured into a previously assembled support and allowed to solidify at room temperature.

Agarose concentration used ranges between 0.4 % and 2.5 % (w/v) depending on the DNA size of the samples. For PCR fragment recovery, a 3:1 mix of conventional agarose with low melting point agarose (*LM-SIEVE*; Laboratorios Conda) was used and prepared as explained above.

When completely solidified, gels were submerged in running buffer (TAE 1X; A.3.16) inside a horizontal tray system (*Mini-Sub Cell GT CEII*; Bio-Rad).

Samples were prepared by adding the required amount of 5X loading buffer (A.3.3) and loaded into gel wells. Electrophoresis was conducted at 100 V during sufficient time to allow correct DNA bands separation.

Visualization of DNA in pre-stained gels was conducted by placing them on a UV-transillumination and image capture device (*E-box-1000/20 M*; Vilber Loumat).

3.4.3 Genomic DNA extraction

Genomic DNA extractions of *S.* Typhimurium and *E. coli* were performed using the commercial kit *Easy-DNA*^{TM} (Invitrogen).

In short, 5 mL over-night cultures of *S.* Typhimurium or *E. coli* were prepared and incubated at 37 °C. Genomic DNA extractions were conducted directly from 1 mL of those cultures and following manufacturer's instructions

Concentration, purity and integrity of DNA were determined as previously explained. Genomic DNA was then stored at 4 °C for short-term use or at -20 °C for long-term storage.

3.4.4 Plasmidic DNA extraction

3.4.4.1 Plasmid mini preps

Small volume plasmidic DNA extractions were performed using *Genejet*^{TM} *Plasmid Miniprep Kit* (Thermo Scientific).

Briefly, cultures of *S.* Typhimurium or *E. coli* were prepared in 3-5 mL of LB (A.1.4) or TB (for low-copy number plasmids; A.1.7) including the required antibiotic/s and incubated over-night at 37 °C, or 30 °C for thermosensible plasmids. Plasmid extractions were performed from these cultures following manufacturer's instructions.

Concentration, purity and integrity of plasmids were determined as previously explained. Plasmid mini preps were stored at 4 °C for short-term use or at -20 °C for long-term storage.

3.4.4.2 Plasmid maxi preps

Large volume plasmidic DNA extractions were performed using the alkaline lysis method (Birnboim and Doly, 1979).

The day before the extraction, a 10 mL TB (A.1.7) plus antibiotic/s over-day culture of *S.* Typhimurium or *E. coli* was made and incubated at 37 °C, or 30 °C for thermosensible plasmids. The over-day culture was then used to inoculate an over-night culture of 90 mL of TB plus antibiotic/s. The over-night culture was incubated at 37 °C (30 °C if thermosensible) with constant shaking for no more than 16 hours.

Starting from the 100 ml over-night culture, the extraction was performed as explained below.

Culture was divided among two 80 mL polypropylene centrifuge tubes and then centrifuged at 12300 g and 4 °C during 10 minutes (standard conditions). After that, the supernatant was discarded and the pellet resuspended

by adding 2 mL of solution I (A.2.24) to each tube. Both suspensions were put together in one tube. Then, 8 mL of solution II (A.2.25) were added and the tubes were mixed by inversion and chilled on ice for 5 minutes. Next, 6 mL of solution III (A.2.26) were added and the tubes were mixed by inversion and chilled on ice for 10 minutes. At that point the cells should be lysed and the plasmid recovery starts.

After centrifuging at standard conditions the supernatant was recovered and 0.6 volumes of absolute isopropanol were added. The tube was mixed by inversion and incubated at room temperature for 15 minutes to allow DNA precipitation. Then, the tube was centrifuged at standard conditions but at 20 °C and the supernatant was discarded. Pelleted plasmidic DNA was allowed to dry at room temperature. The pellet was then resuspended in 1 mL of MQ-water containing 20 mg/mL of RNAse at 37 °C while shaking.

Finally, diatomaceous earth matrix (A.2.8) was used to bind plasmidic DNA. A *Wizard® Minicolumn* (Promega) was used to trap the diatomaceous earth bed containing the plasmid and to perform a washing step by passing 3 mL of ethanol 70 % (A.2.11) through the column. The column was then centrifuged at 12000 g during 5 minutes on a top table centrifuge to eliminate remaining ethanol. Two 50 µL elution steps using preheated (50 °C) MQ-water were required to obtain the maximum yield. Centrifugings were conducted at 12000 g during 5 minutes on a top table centrifuge after incubation periods of 5 minutes.

Concentration, purity and integrity of plasmids were determined as previously explained. Plasmid maxi preps were stored at 4 °C for short-term use or at -20 °C for long-term storage.

3.4.5 Polymerase chain reaction

3.4.5.1 DNA amplification for cloning

For routine amplifications, the kit *Expand^{TM} High Fidelity PCR System* (Roche) was used following manufacturer's recommendations. Final concentrations of the reaction mixture constituents were: oligonucleotides, 0.5 µM; magnesium chloride, 2.5 mM; deoxyribonucleotides triphosphate (dNTPs), 200 µM; DNA, 2 ng/µL. The final reaction volume was 25 µL. When a high amount of amplified DNA was required the final reaction volume was set to 100-200 µL maintaining concentration ratios between master mix constituents.

For those amplifications requiring very high fidelity (such as ORF cloning) or for some difficult templates, *Phusion® High Fidelity DNA polymerase* (Thermo Scientific) was used following manufacturer's instructions. Final concentrations of reaction mixture constituents for this polymerase were: oligonucleotides, 0.5 µM; dNTPs, 200 µM; DNA, 1 ng/µL. The maximum final reaction volume used was 50 µL. When a high amount of amplified DNA was needed, several 50 µL reactions were placed and recovered together.

3.4.5.2 Colony PCR

Colony PCR was used for screening purposes when performing cloning steps. In short, a single colony was picked using a sterile toothpick and resuspended in 50 µL of MQ-water in a 0.2 mL PCR tube. Then, the tube was subjected to a 99 °C for 10 minutes heat shock in a thermocycler to lysate the cells. After that, samples were centrifuged at 12000 g during 1 minute to pellet the cell debris and 10 µL of the supernatant were used as PCR template.

PCR reaction was performed using the kit *Expand^{TM} High Fidelity PCR System* (Roche) following manufacturer's recommendations. Final concentrations of reaction mixture constituents were: oligonucleotides, 0.5 µM; magnesium chloride, 2.5 mM; deoxyribonucleotides triphosphate (dNTPs), 200 µM. The final reaction volume was always 25 µL.

3.4.6 DNA recovery and purification

In order to either recover or purify DNA, the kit *Illustra*$^{\text{TM}}$ *GFX*$^{\text{TM}}$ *PCR DNA and Gel Band Purification Kit* (GE Healthcare) was used according to manufacturer's instructions.

Concentration, purity and integrity of DNA was determined as previously explained and then stored at 4 °C ready for subsequent applications.

3.4.7 Restriction endonuclease digestions

New England Biolabs and Roche were the main suppliers of restriction endonucleases. Every reaction was performed following the manufacturers recommendations for each enzyme. The reaction volume was usually set to 20 µL. When a large amount of DNA needs to be processed, the reaction volume was set to 100 µL maintaining the concentrations of the reaction constituents.

3.4.8 DNA cloning

3.4.8.1 DNA dephosphorylation

Digested vectors were dephosphorylated to prevent re-ligation during cloning procedures. Briefly, 1.5 U of calf intestine alkaline phosphatase (Roche) was mixed with DNA and 10X dephosphorylation buffer (supplied)

in a final volume of 100 µL adjusted with MQ-water. The mix was then incubated for 30 minutes at 37 °C. After that, another 1.5 U of phosphatase were added to the mix, gently agitated and incubated 30 minutes more at the same temperature. Finally, the phosphatase was inactivated by placing the mixture at 65 °C during 10 minutes and the DNA was recovered as previously explained.

3.4.8.2 DNA phosphorylation

Non-digested PCR amplified DNA fragments require a phosphorylation step to allow the ligation into previously dephosphorylated vectors. In short, 20 U of T4 polynucleotide kinase (Promega), 5X kinase buffer (supplied) and ATP to a final concentration of 5 µM were added to previously recovered DNA and the volume was adjusted to 50 µL with MQ-water. The mix was incubated for 45 minutes at 37 °C. After that, another 20 U of T4 polynucleotide kinase and 2 µL of 100 µM ATP were added to the mix, gently agitated and incubated for another 45 minutes at the same temperature. Finally, the kinase was inactivated by placing the mixture at 70 °C during 10 minutes and the DNA was recovered as previously explained.

3.4.8.3 Sticky-end filling

When necessary, sticky-end filling was performed to allow blunt-end ligation.

In short, previously recovered DNA was mixed with 5 U of T4 polymerase (Roche), 5X polymerase buffer (supplied) and dNTPs to a final concentration of 100 mM. The volume was then adjusted with MQ-water to 100 µL. The mix was then incubated for 30 minutes at 37 °C. At the end, the polymerase was inactivated by placing the mixture at 70 °C during 10 minutes and the DNA was recovered as previously explained.

3.4.8.4 DNA ligation

DNA fragments were ligated into previously prepared plasmidic vectors by using T4 DNA ligase (Fermentas) and following the manufacturer's recommendations on reaction mixture preparation. The insert:vector ratio was set to 3:1 or 5:1 to perform sticky-end ligation or to 1:1 to do blunt-end ligation. The final ligation volume was 20 µL.

Reaction time and temperature were critical parameters to achieve a good ligation yield. After a setting-up procedure, the reaction conditions were set to 90 minutes at 22 °C. Reactions were carried out using a thermocycler (Applied Biosystems).

If PCR product was obtained by using *Expand^{TM} High Fidelity PCR System* (Roche), the fast T/A cloning method was available. In those cases, if necessary, *pGEM®-T Vector System I* (Promega) was used following manufacturer's instructions. No additional steps were required between PCR amplification and ligation when using this system.

3.4.9 Sequencing of *S.* Typhimurium LT2 Δ*lexA* strain

Previous work conducted in our laboratory by Clerch *et al.* (1996) resulted in the construction of an *S.* Typhimurium LT2 mutant derivative carrying knock-out allele for *lexA* gene (UA1685).

To elucidate the compensatory mutations that allow the generation of a Δ*lexA* strain on *S.* Typhimurium, strain UA1685 was sequenced alongside her isogenic strain (UA1582) using Illumina® technology. Sequencing procedure was conducted by ServiceXS B.V. in The Netherlands.

Genomic DNA of each strain was extracted as explained into section 3.4.3. Service provider required at least 5 µg of genomic DNA meeting at least two quality parameters: a minimum concentration of 50 ng/µL

and an A_{260}/A_{280} absorbance ratio between 1.8 and 2.0. In-house quality assessment is summarized in Figure 3.2 and in Table 3.4. A total of 20 µg of UA1685 and 35 µg of UA1582 genomic DNA were sent to the provider.

Table 3.4. Quality parameters for strains UA1582 and UA1685 genomic DNA extractions.

Strain	Concentration (ng/µL)	A_{260}/A_{280}	A_{260}/A_{230}
UA1582	1880.6	1.99	2.31
UA1685	1064.6	1.94	2.24

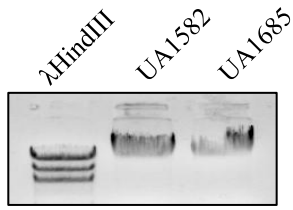

Figure 3.2. Strains UA1582 and UA1685 genomic DNA extractions. Genomic DNA extractions of strains UA1582 ($\Delta sulA$) and UA1685 ($\Delta sulA\ \Delta lexA$) were loaded on a 0.4% agarose gel to check for DNA integrity.

According to provider's information, genomic DNA was prepared for sequencing using the *Illumina® Paired-End DNA sequencing Sample Prep*

Kit (Illumina Inc.). Fragmentation (using Covaris), ligation of sequencing adapters and PCR amplification of resulting products was performed according a procedure based an already published Illumina sample preparation protocol (1005063 Rev.A). Quality and yield checks after sample preparation was conducted using Lab-on-a-Chip analysis.

Sequencing was conducted using a *HiSeq 2000* sequencer (Illumina Inc.). A total of 6.5 pmol of each pre-processed genomic DNA was used. Two sequencing reads of 100 cycles using two different primer pairs was performed with the flow cell.

After DNA sequencing, raw reads were prepared for analysis. Adapter sequences and low quality reads were removed. Remaining reads had a minimal length of 36 bp and a phred quality score of 22. Approximately 87 % of the reads passed the quality filter in every case.

Filtered reads were then aligned against *S.* Typhimurium LT2 genome (NC_003197.1) and pSLT (NC_003277.1) plasmid sequence both obtained from NCBI database. After alignment, indels and SNPs finding was performed and reported.

Differences among wild type LT2, UA1582 and UA1685 strains were then analyzed searching for differential genetic facts.

3.5 Mutant construction

3.5.1 λ Red recombination procedure

3.5.1.1 DNA preparation

λ Red one-step inactivation procedure was primarily described by Datsenko and Wanner (2000) to generate gene deletions in a fast and reliable fashion in *E. coli* K-12. In this work, one-step inactivation has been used with

some slight modifications to generate some of the *S.* Typhimurium mutant strains.

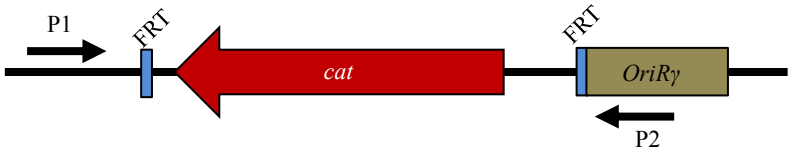

Figure 3.3. pKD3 plasmid structure. Linear scheme showing the main features of the pKD3 plasmid used in the λ Red one-step recombination procedure. Arrows denoted as P1 and P2 show the hybridization site of the 100 bp primers used during the procedure. The amplified area comprises the two FRT sequences which are recognized by the FLP recombinase and the *cat* gene conferring chloramphenicol resistance.

The chloramphenicol resistance was amplified from the pKD3 plasmid. This vector contains a chloramphenicol resistance gene (*cat*) as selectable marker flanked by two FRT, the target sequences for the FLP recombinase (Fig. 3.3).

Figure 3.4 shows a schematic representation of the overall one-step procedure as conducted in this work.

First, the antibiotic resistance gene was PCR amplified from the flanking P1 and P2 sites in a 100 µL reaction as previously explained. Primer pairs used to amplify from those sites and conduct the one-step inactivation procedure also contain an homology region within the target gene. Usually, oligonucleotide that binds the P1 site also carries the 5' target gene ho-

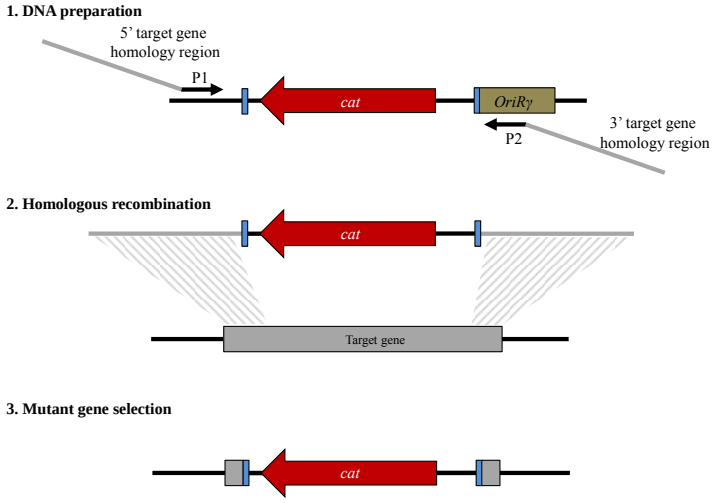

Figure 3.4. Scheme of the λ Red one-step inactivation procedure. Scheme of the three steps necessary to obtain a mutant strain using the λ Red one-step recombination procedure: 1. preparation of the mutant DNA construction, 2. transformation and homologous recombination of the linear fragment and 3. selection of the mutant colonies using the chloramphenicol marker and colony PCR.

mologous sequence. On the contrary, the oligonucleotide containing the P2 binding site carries the 3' target gene homologous sequence.

The PCR product was then loaded into an agarose gel and recovered in 90 µL volume (2 x 45 µL elution steps).

After that, the recovered product was digested with *Dpn*I endonuclease for 16 hours at 37 °C . This restriction endonuclease requires the target sequence to be methylated thus cutting the remaining pKD3 plasmid but not the amplified DNA.

After digestion, DNA was directly recovered from solution in 15 µL final volume and quantified as explained before. The remaining product was finally transformed into an *S.* Typhimurium strain harboring the pKOBEGA plasmid as explained below.

3.5.1.2 Electrocompetent cell preparation

S. Typhimurium UA1826 strain carrying the pKOBEGA plasmid was used to prepare competent cells for one-step inactivation method.

An over-night culture of UA1826 strain grown in LB-Miller (A.1.4) supplemented with 100 µg/mL ampicillin was placed. The day after, 50 mL of SOB medium (A.1.6.1) supplemented with 100 µg/mL ampicillin and with 20 mM DL-arabinose (A.2.9) were inoculated and incubated at 30 °C while shaking until an OD_{600} of 0.5 was reached. The culture was then transferred to previously chilled 80 mL polypropylene tubes and centrifuged for 15 minutes at 9200 g and 4 °C (standard conditions). Then three washing steps of 0.4, 0.2 and 0.1 volumes of 10 % glycerol (A.2.12) were conducted. Finally, cells were resuspended in 300 µL 10 % glycerol, divided into 100 µL aliquots and immediately used to maximize the efficiency. Competent cells could be stored at -80 °C for a long period of time if necessary.

3.5.1.3 Electrotransformation

In order to maximize one-step procedure efficiency at least two aliquots of competent *S.* Typhimurium UA1826 cells were used in each inactivation attempt for each target gene. 1 to 2 µg of linear DNA was mixed with electrocompetent aliquots and incubated on ice for 15 minutes. The cells-linear DNA mix was then subjected to an electrical pulse *(Bio-Rad Gene Pulser*, Bio-Rad) of 2.5 kV/cm^2 and immediately recovered with 1 mL of

SOC medium (A.1.6.2). Transformed cells were transferred to a glass tube, incubated at 37 °C for 1.5 hours and finally spreaded into selective LB-Miller plates.

3.5.1.4 Antibiotic marker removal

When necessary, pCP20 plasmid harboring FLP recombinase activity was transformed into the desired recipient strain using the electrotransformation procedure as described on section 3.3.6. However, incubations (phenotypic expression and over-night on selective plates) were conducted at 30 °C as pCP20 has a thermosensible replication origin. The day after, 5 mL of fresh LB (A.1.4) were inoculated without cloning and then incubated over-night at 42 °C. The next day, an 1/100 dilution of the culture was placed over day and allowed to grow at 42 °C to stationary phase (approx. 8 hours). Then, dilutions 10^{-5}, 10^{-6} and 10^{-7} were plated on LB and the plates were incubated over-night at 42 °C. This procedure allowed the elimination of the pCP20 plasmid due to its temperature conditional origin of replication.

Finally, individual colonies were picked and replica plated onto LB and LB containing ampicillin (to select for the loss of the plasmid) and chloramphenicol (to select for the loss of the *cat* gene). Colonies growing on LB but not on LB-ampicillin and LB-chloramphenicol were selected and PCR-checked.

3.5.2 P22 transduction

Generalized transduction using the P22HT phage was used to move several resistance markers between *S.* Typhimurium strains. The overall procedure is based on the guidelines published by Davis *et al.* (1980).

First, a phage lysate on the donor strain was obtained. The day before the lysate preparation, an over-night culture of the donor strain was placed. To prepare the lysate, the over-night culture of the donor strain and a $1{\cdot}10^8$ pfu/mL suspension prepared in LB broth (A.1.4) were mixed in a 1:5 (v/v) proportion. The MOI would be about 0.01-0.1 pfu/cell. The mix was incubated at 37 °C (or 30 °C if required) for 12 to 16 hours.

To recover the phage lysate, the mix was centrifuged at 12000 g for 10 minutes at 4 °C to pellet the cell debris. Supernatant containing transducing phages was recovered, filtered (0.45 µm pore diameter filters, Whatman) and stored at 4 °C until needed.

Previously to their use, lysates were quantified by the simple spot titering method. A mixture of 10 µL of an over-night culture of a wild type *S.* Typhimurium and 3 mL of melted top agar was spread over a green plate (A.1.2). Once solidified, 20 µL of dilutions 10^{-6}, 10^{-7}, 10^{-8} and 10^{-9} of the phage lysate were spotted on the plate and allowed to dry with the lid ajar. The plates were then incubated over-night at 30-37 °C. The number of plaques in each spot was counted and the average number of pfu/mL was calculated.

To perform phage transduction, an over-night culture of the receptor strain was placed the day before the procedure. Three infection mixtures corresponding approximately to MOI 0.5, 2.5 and 10 were prepared by adding the required amount of phage lysate over 200 µL of the over-night culture of the receptor strain. Corresponding controls with no phage and no cells were also placed. Infections were then incubated 15 minutes at room temperature to allow phage adsorption and after that for 1 hour at 37 °C to ensure phenotypic expression of antibiotic marker.

Mixtures were then centrifuged at 12000 g for 1 minute in a top-table centrifuge and the supernatant containing phage excess was removed. Pel-

leted cells were resuspended in 100 μL of fresh LB broth and spreaded on LB plates (A.1.4) containing the corresponding antibiotic. Plates were incubated over-night at 37 °C (or 30 °C if required).

Next, transductant colonies growing on the LB-antibiotic plates were cleaned-up. This step is necessary to avoid the selection of strains carrying a pseudolysogenic or lysogenic P22 which would prevent any transduction that may be required in the future. Selected colonies were streaked on green plates and incubated over-night at 30-37 °C. Those plates help in differentiate between pseudolysogen (dark green) and non-lysogen or lysogen (light green) colonies. Pseduolysogeny is an unstable state achieved after infection where the phage genome is maintained in an extrachromosomal form within the cell. Pseudolysogens may develop to either uninfected, lysogen or lytic cells.

Two more clean-up steps were conducted by selecting light green colonies. Finally, purified colonies were cross-streaked against the P22*vir* phage. This procedure allows to select for P22 sensitive (free) or resistant (lysogen) colonies. Two light green and P22 sensitive colonies were selected from every transduction experiment for further work once the presence of the antibiotic marker at the correct place was confirmed by PCR.

3.5.3 FLAG-tag genomic insertion

In order to perform either co-immunoprecipitation or ELISA assays, *cheW* gene was tagged with the small FLAG polypeptide (DYKDDDDK, 1012 Da). This allows the detection of CheW::FLAG protein with specific anti-FLAG antibodies without major disruptions in protein structure or function.

In this work, the method described by Link *et al.* (1997) is used with the modifications reported by Latasa *et al.* (2012) to obtain the *S.* Typhimurium UA1916 (*cheW*::FLAG) strain.

An overlap-extension PCR-generated *cheW::*FLAG gene fusion was introduced to the *Bam*HI restriction site of the pKO3 shuttle vector giving place to pUA1121. The vector was then confirmed by sequencing and electroporated into *S.* Typhimurium ATCC 14028 wild type strain. After electroporation, cells were allowed to recover for 1 hour at 30 °C. As pKO3 contains a temperature-sensitive OriV, cells were plated on LB chloramphenicol plates (A.1.4) and incubated at restrictive temperature (43°C) to facilitate the homologous recombination. Five colonies able to grow under restrictive conditions were picked into 5 mL LB broth (A.1.4) and incubated for 24 hours at 30 °C. As pKO3 also contains *sacB* selection marker, serial dilutions of these cultures were plated on freshly prepared 5 % (w/v) sucrose-LB plates and incubated at 30 °C. Sucrose resistant colonies were selected and replica plated on LB chloramphenicol to test for the loss of the pKO3 vector. Those colonies that were able to grow in the presence of sucrose but resulted chloramphenicol sensitive were selected and tested for FLAG insertion using colony PCR.

3.5.4 *S.* Typhimurium ATCC 14028 Δ*lexA* mutant construction

To evaluate the effect of SOS induction on swarming movement but in the absence of any DNA-damaging compound (like the commonly used mitomycin C) a Δ*lexA* mutant strain of *S.* Typhimurium was generated.

First, the *sulA* and *ysdAB* loci of MA5975 strain were knocked-out using the one-step inactivation procedure as previously described (Section 3.5.1).

The generated UA1923 strain was then used as receptor for the Δ*lexA11::Ω-Km* allele transduction obtained from the UA1685 donor strain. Transduction procedure was conducted as explained on section 3.5.2.

As a result of the transduction, two colony morphologies were observed on the plates: big round-shaped colonies and small irregular-shaped ones. Five colonies of each type were selected and a colony PCR was conducted using external primers for the *lexA* locus. Small irregular-shaped colonies proved to have acquired the Δ*lexA* mutant allele and thus were selected for subsequent clean-up steps of the transduction procedure. As a result of this procedure, the UA1925 (Δ*sulA* Δ*ysdAB* Δ*lexA* ΔGifsy1,2) strain was generated.

3.6 Protein manipulation methods

3.6.1 Whole-cell lysates preparation

Cell lysates to perform ELISA assays were obtained by recovering the cells directly from LB-swarming plates (A.1.5) following the procedure previously described by Kim and Surette (2004). Wild type *S.* Typhimurium cells and, in general, swarming-capable cells reach the plate edge within 12-15 hours of incubation at 37 °C. When the swarm-front reached near the edges of the plate, the cells were suspended in 1 mL of sonication buffer (A.3.14). By gently tilting the plates back and forth, actively migrating cells were easily unstucked from the surface. Next, the suspension was recovered in a microcentrifuge tube and the volume was adjusted to 1 mL.

Non-swarming-capable cultures were recovered using the same method but due to the fewer cell amount present on the plates the final volume was adjusted to 0.5 mL.

Cell suspensions were then lysed by sonication. Five pulses of 30 second length and 20 % amplitude were used (*Digital Sonifier® 450*, Branson). After sonication, the tubes were centrifuged at 12000 g during 10 minutes to remove cell debris and impurities from the plate. Supernatant was recovered in a clean, autoclaved microcentrifuge tube.

Sonicate volumes were then approximated by using a pipette and glycerol was added to a final 15 % (v/v) concentration. Cell lysates were stored at -20 °C until needed.

3.6.2 Protein quantification

Proteins were quantified using a modified Bradford method (Bradford, 1976). BSA in a range of 1,5 to 200 ug/mL was used as standard (A.2.6) and *BioRad Protein Reagent Dye®* (BioRad) was used as Bradford reagent.

Briefly, four serial dilutions of unknown samples were placed in a 96-well flat bottom microtiter plate. The standards and at least four blank replicates were also included.

Samples and standards were diluted in 140 µL final volume of MQ-water. Next, 20 µL of 1 M NaOH (A.2.23) were added to each well. NaOH is used to ensure that the sample does not precipitate upon addition of Bradford reagent as it facilitates protein solubility, especially for membrane proteins (Stoscheck, 1990).

Finally, 40 µL of concentrated Bradford reagent were added to each well and pipette-mixed. After a 15 minutes incubation, the A_{595} was measured using a microtiter plate reader (*Sunrise*, Tecan).

The BSA standard curve was fitted using a 4-parameter logistic non-linear regression and sample values were taken from the curve.

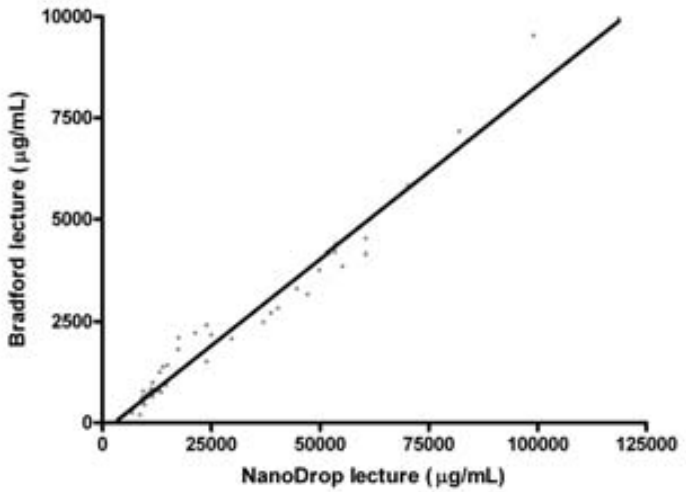

Figure 3.5. NanoDrop-Bradford Calibration Curve. NanoDrop lectures obtained using the A_{280} BSA method are plotted against values obtained for the same samples using the Bradford assay (grey dots). The NanoDrop lecture correlates the Bradford lecture in a linear fashion (black line) and thus it could be used to approximate the sample protein concentration to determine the suitable dilutions for the Bradford assay.

As obtaining whole-cell lysates for ELISA quantifications was a laborious procedure, a calibration method between Bradford and NanoDrop (*Nanodrop 2000*; Thermo Scientific) lectures was developed in order to use as little sample's amount as possible. A calibration curve was obtained by using data from previously analyzed lysates (Fig. 3.5). Calibration lysates were quantified by Bradford method and by using the A_{280} BSA quantification mode of the NanoDrop. Note that in BSA quantification mode, NanoDrop software uses the BSA molar extinction coefficient to return the

protein concentration, thus lectures obtained from the lysates were only rough estimates of relative protein amounts between fractions and could not be used as absolute values. Bradford method quantifications were then plotted against NanoDrop lectures.

Equation A was calculated from Figure 3.5 linear regression and was used to determine a rough Bradford value estimate for every sample previously to the quantification assay.

$$Bradford\,lecture = 0.085 \cdot NanoDrop\,lecture - 230 \qquad \text{(A)}$$

Using the concentration values obtained, appropriate dilutions for the Bradford quantification assay were calculated.

3.6.3 Protein overexpression and purification

3.6.3.1 Overexpression

RecA and CheW proteins were overexpressed and purified from either pET or pGEX series vectors. *E. coli* BL21 (DE3) pLysS were used as host for these expression plasmids.

First, an over-night culture of the required overexpression strain was placed. The day after, an 1/20 dilution in fresh LB (A.1.4) without antibiotics was made. The culture was incubated at 37 °C for about 2 hours ($OD_{550} \approx 0.6$) while shaking at 180-200 rpm. After that, overexpression was induced by adding IPTG to 1 mM (A.2.16) final concentration. The culture was then allowed to express for 3 hours at 37 °C while shaking at 180-200 rpm. Once the desired expression time was reached, culture was divided among several 10 mL tubes and centrifuged at 12300 g and 4 °C for

10 minutes. Supernatant was completely removed and pelleted cells were stored at -20 °C until needed for protein purification.

3.6.3.2 Sonication

Frozen cell pellets prepared from overexpressed cultures were thawed on ice. After that, 3 mL (pET vectors) or 2 mL (pGEX vectors) of sonication buffer (A.3.14) per 50 mL of pelleted culture was used to resuspend all the pellets and put them together in one tube. Four pulses of 30 second length and 20 % amplitude were used (*Digital Sonifier® 450*, Branson). Tubes were then centrifuged at 12000 g and 4 °C for 20 minutes to remove cell debris. Supernatant was recovered in a clean tube.

3.6.3.3 Protein purification from pET series vectors

Proteins expressed from either pET15b or pET22 vectors were histidine tagged. *Talon Metal Affinity resin*®(Clontech) was used for IMAC chromatography. Before purification procedure, resin was prepared for subsequent steps by washing two times with TALON wash buffer (A.3.18) following manufacturer's recommendations. The required amount of resin was 2 mL for 50 mL of overexpression culture. This gave approximately 1 mL bed volume capable to retain about 3 mg of protein.

Purification was performed following manufacturer's recommendations with some slight modification for a better yield.

Equilibrated resin and sonication supernatant were mixed and incubated at room temperature for 40 minutes while gently balancing to allow a proper interaction to occur. After that, the tube was centrifuged at 700 g and 4 °C for 5 minutes to settle the resin. Supernatant was removed but conserved in a new tube as flow through fraction. Resin was then washed with 10

bed volumes of PBS 1X pH 7 (A.3.10) by gently shaking the tube at room temperature for 10 minutes. Wash procedure was repeated one more time.

After washing steps, resin was resuspended in 1 mL of PBS 1X, transferred to a 2 mL gravity flow column (*TALON® 2 mL Disposable Gravity Column*, Clontech) and allowed to settle. The column was then washed with 5 bed volumes of PBS 1X. Finally, protein was eluted by passing through the column 5 bed volumes of TALON elution buffer (A.3.17) and recovering 500 µL fractions. Protein fractions were then analyzed by the A_{280} method to determine the maximum concentration fraction.

3.6.3.4 Protein purification from pGEX series vectors

Proteins expressed from pGEX-4T-1 vector were GST tagged. *Sepharose 4B®* resin (GE Healthcare) was used for glutathione affinity chromatography. Before the purification procedure, resin was prepared for subsequent steps by concentrating and washing two times with PBS 1X pH 7.3 (A.3.10) following manufacturer's instructions. The required amount of 50 % resin was 1.33 mL for 50 mL of overexpression culture. This gave approximately 1 mL bed volume capable to retain about 5 mg of GST fused protein.

Purification was performed following manufacturer's instructions with some modifications for a better final yield.

Equilibrated resin and sonication supernatant were mixed and incubated at room temperature for 1 hour while gently shaking to allow a proper interaction to occur. Glutathione-GST interaction is relatively weak so vigorous shaking might result in low yields. After that, the tube was centrifuged at 500 g and 4 °C for 5 minutes to settle the resin. Supernatant was removed but conserved in a new tube as flow through fraction. Resin was then washed with 10 bed volumes of PBS 1X pH 7.3 by gently inverting the

tube at room temperature for 6 to 8 times. Wash procedure was repeated two more times.

After washing steps, PBS was completely removed avoiding the upper resin too dry and then 230 µL of PBS 1X pH 7.3 were added. Elution of GST-tagged proteins was performed by adding 20 µL of thrombin 1 U/µL. This produced the cleavage of the polypeptide chain between GST and the expressed protein. The thrombin-resin mix was incubated for 16 hours at 22-25 °C. Finally, the tube was centrifuged at 500 g and 4 °C for 5 minutes and the supernatant containing the recombinant protein was recovered in a clean microcentrifuge tube. The centrifuging step was repeated to ensure the complete elimination of the sepharose resin.

3.6.4 SDS-PAGE

SDS-PAGE was routinely used to visualize protein presence and integrity. Polyacrylamide gels were prepared as described in Appendix A sections A.2.27.1 and A.2.27.2. Gels were prepared and electrophoresed using the *MiniVE Vertical Electrophoresis System*®(GE Healthcare). For general purposes, like cell lysates loading, 12 % acrylamide gels were used. RecA protein (approx. 38 kDa) was visualized using a 12 % acrylamide gel while CheW protein (approx. 18 kDa) was visualized in a 15 % acrylamide gel.

First, samples were prepared to load into gel wells. Negative and positive controls from an overexpression procedure were pelleted at 12000 g for 2 minutes. Next, the supernatant was discarded and the pellet was resuspended in 90 µL of MQ-water. Then, 30 µL of Laemmli 4X buffer (A.3.9) were added and the mix was subjected to 3 freeze-boil cycles to allow cell disruption. If the sample was purified protein, a lysate or any of the fractions

obtained during the purification procedure sample was prepared directly by mixing with Laemmli 4X buffer to the desired final volume, usually 12 µL.

Before gel loading, samples were boiled at 100 °C for 5 minutes. Usually, 10 µL of samples (5 µL if overexpression positive controls) were loaded into gel wells and allowed to settle. The electrophoresis was conducted in tris-glycine-SDS buffer (*TGS 10X*, Laboratorios Conda) at 150 V for 90 minutes. After that, acrylamide gels were stained using Coomasie staining solution (A.2.7) for 10 minutes at room temperature while shaking. To visualize the protein bands, gels were destained in 10 % acetic acid solution (A.2.1) until the gel become transparent.

3.6.5 Far-Western blot

Far-Western blotting experiments were conducted to confirm the interaction between RecA and CheW proteins. In this study, a dot-blot version rather than a common gel and transfer procedure was used. This procedure proved to be simpler and more reliable in our conditions (Lee and Alani, 2006; Li *et al.*, 2008 and Cheng *et al.*, 2010).

First, a PVDF membrane was activated by soaking it in methanol 100 % for 15 seconds. Next, the membrane was washed by immersion in MQ-water for 2 minutes. Finally, an equilibration step of 5 minutes by soaking the membrane in TBS 1X buffer (A.3.20) was performed.

The PVDF membrane must be activated but not wet to inoculate it. The membrane was stretched over two 3MM filter papers. The first one of them, in direct contact with the membrane, was previously soaked in TBS 1X buffer and put over a second but dry strip of filter paper. The membrane buffer excess was allowed to absorb until the surface brightness decreased

and the surface became matte. Then, several 5 µL drops of different dilutions of purified proteins were spotted over the membrane.

Protein amounts used were: RecA at 2.5, 5, 10, 20 and 40 pmoles; CheW at 40, 80, 100, 200 and 400 pmoles and BSA, as negative control, at 10, 20, 40, 80 and 100 pmoles.

After the inoculation, the membrane was air-dried for 1.5 hours at room temperature stretched over a dry 3MM filter paper. This allows protein retention over the membrane surface.

The dried membrane was then blocked in Western blot blocking buffer (A.3.23) for 3 hours at room temperature while gently shaking. After that, the membrane was directly incubated for 16 hours at room temperature with 400 nM of His-tagged RecA protein in Western blot blocking buffer while gently shaking. Then, the membrane was washed three times during 10 minutes in TBS wash buffer (A.3.21) while vigorously shaking. Next, the membrane was incubated for 1 hour at room temperature with 0.5 µg/mL of anti-His_6 mouse monoclonal antibody (*Anti-His_6 mouse monoclonal antibody 100 µg*, Roche) in Western blot blocking buffer. Then, the membrane was washed again as explained above and incubated for 1 hour at room temperature with a 1/10000 dilution of the secondary anti-mouse IgG antibody (*Anti-Mouse IgG (Fc specific)-Alkaline Phosphatase*, Sigma) in Western blot blocking buffer. Finally the membrane was washed again as previously explained and equilibrated for 5 minutes in alkaline buffer (A.3.1). After that, alkaline phosphatase substrate solution (A.2.2) was added and the membrane was allowed to develop until sufficient contrast between samples and background was observed. For storage, membranes were washed with distilled water and air-dried at room temperature.

3.6.6 Co-immunoprecipitation

3.6.6.1 Cell lysis

A mild lysis step is required to extract *S.* Typhimurium proteins without disrupting protein-protein interactions and therefore sonication is not a recommended methodology for co-immunoprecipitation lysate preparation. In this work, method described by D'Ulisse *et al.* (2007) was used. Briefly, *S.* Typhimurium strains *cheW::FLAG* (UA1916), Δ*cheW* (UA1907) and Δ*recA cheW::FLAG* (UA1918) were resuspended in TBS 1X buffer (A.3.20) in an 1.5 mL microcentrifuge tube and centrifuged at 12000 g during 1 minute. Approximately a 25 µL volume pellet is required for a correct protein extraction. Then, the supernatants were discarded and the pellets were resuspended in 200 µL of ice-cold immunoprecipitation lysis buffer (A.3.8). Cells were then incubated on ice for 40 minutes and gently vortexing steps were applied at 5 minutes intervals to ensure a correct mix. Finally, the tubes were centrifuged at 12000 g and 4 °C for 15 minutes to pellet the cell debris and the supernatants were recovered in previously chilled 1.5 mL microcentrifuge tubes. Protein amounts were then quantified by Bradford method (Section 3.6.2) as previously explained.

3.6.6.2 Protein A magnetic beads pre-coating and blocking

Pre-coated protein A magnetic beads (*PureProteome*^{TM} *Protein A Magnetic Beads*, Millipore) were used to bind and precipitate the capture antibody.

Briefly, 50 µL of suspended beads were pipetted into a clean 1.5 mL microcentrifuge tube placed into a magnetic stand. Storage buffer was removed and the beads were washed once with 500 µL of immunoprecipitation wash buffer (A.3.7). Then, the wash buffer was removed and the beads were resuspended in 100 µL of wash buffer. Next, 2 µL of anti-FLAG monoclonal

antibody (*Monoclonal Antibody to DYKDDDDK Epitope Tag*, Acris) were added. The beads-antibody mix was then incubated for 1 hour at room temperature to allow the adsorption of the antibody to protein A coated beads. Next, the beads were washed twice with 500 µL of immunoprecipitation wash buffer.

After the second wash, wash buffer was completely removed and 400 µL of immunoprecipitation blocking buffer (A.3.6) were added. Beads were incubated in blocking buffer at 4 °C for 1 hour while gently shaking (*Polymax 1040*, Heidolph). Finally, the beads were washed twice with 500 µL of immunoprecipitation wash buffer. Next, the wash buffer was removed and beads could either be directly mixed with cell lysates or resuspended in 100 µL of immunoprecipitation wash buffer and stored several days at 4 °C until needed.

3.6.6.3 Co-immunoprecipitation

Co-immunoprecipitation experiments were conducted by developing an in-house protocol based on previously published guidelines by Thermo (2008) and Abcam (2012).

A pre-clearing step using non-coated protein A magnetic beads was performed to account for non-specific interactions occurring between lysate proteins and magnetic beads used to immunoprecipitate. In short, 50 µL of suspended beads were washed as previously explained in section 3.6.6.2. Then, the beads were mixed with approximately 300 µg of cell lysate and incubated for 30 minutes at 4 °C while gently shaking (*Polymax 1040*, Heidolph). Finally, the tubes were centrifuged at 12000 g and 4 °C for 2 minutes and pre-cleared lysates were recovered in pre-chilled 1.5 mL microcentrifuge tubes.

The pre-cleared lysate was then mixed with pre-coated and blocked protein A magnetic beads. The lysate-beads mix was incubated at 4 °C overnight while gently shaking (*MR Hei-Mix D*, Heidolph). The day after, the beads were recovered by placing the tubes into a magnetic stand and washing them twice with 500 µL of immunoprecipitation wash buffer (A.3.7). Next, the beads were resuspended in 45 µL of immunoprecipitation wash buffer and 15 µL of Laemmlli 4X buffer (A.3.9) were added. Elution was performed by incubating the resuspended beads at 90 °C for 10 minutes. Finally, tubes were centrifuged at 12000 g for 1 minute to pellet the magnetic beads and the supernatant containing the immunoprecipitated fraction was recovered into a clean 1.5 mL microcentrifuge tube.

Immunoprecipitated fractions were then analyzed using a common Western blot procedure (Gallagher *et al.*, 2008). In short, immunoprecipitated samples were loaded alongside with the input fraction into a 15 % SDS-PAGE gel (A.2.27.1 and A.2.27.2) and electrophoresed as explained above. Then, proteins were wet-transferred for 1.5 hours at 350 mA to a previously activated PVDF membrane. Next, the membrane was blocked at 4 °C for 1 hour in Western blot blocking buffer (A.3.23).

The blocked membrane was washed 3 times with TBS wash buffer (A.3.21) and then incubated with a 1/2000 dilution in Western blot blocking buffer of either an anti-FLAG (*Monoclonal Antibody to DYKDDDDK Epitope Tag*, Acris) or an anti-RecA (*Anti-RecA antibody*, Abcam). Incubation lasted 1 hour at room temperature while gently shaking.

After that, the membrane was washed again as previously explained and then incubated with either a 1/5000 dilution in Western blot blocking buffer of an anti-mouse IgG (*Polyclonal Antibody to Mouse IgG (H&L)-HRP*, Acris) to detect the anti-FLAG antibody or a 1/10000 dilution in Western blot blocking buffer of an anti-rabbit IgG (*Polyclonal Antibody to*

Rabbit IgG (H&L)-HRP, Acris) to detect anti-RecA antibody. Incubation lasted 1 hour at room temperature while gently shaking.

Finally, the membrane was washed as previously explained and developed using an HRP luminiscent substrate (*Luminata Forte™ Western HRP substrate*, Millipore) following manufacturer's instructions. Membrane images were taken using a *ChemiDoc™ XRS+* system (Bio-Rad).

3.6.7 ELISA

Indirect ELISA quantifications were conducted to determine the relative amounts of RecA and CheW proteins in several study strains.

Pre-treated 96-well flat bottom microtiter plates (*Nunc-Immunoplate F96 Maxisorp*, Nunc) were coated with four replicates of different amounts of whole-cell lysates from study strains in a final well volume of 100 µL. Coating concentrations used to detect either RecA or FLAG-tagged CheW are summarized in Table 3.5 and Table 3.6 respectively.

Apart from samples, every ELISA plate was coated with at least two replicates of a two-fold serial dilution standard curve of purified RecA or purified FLAG-tagged CheW. Standard concentrations used were: RecA, from 0.625 to 80 ng/mL and FLAG-tagged CheW, from 0.156 to 20 ng/mL.

Lysates from strains UA1912 ($\Delta recA$) and UA1908 ($\Delta cheW$) were used as background controls for RecA and CheW quantifications respectively. Background controls were coated at the same concentration that samples and at least in four replicates. This controls were necessary to correct absorbance lectures for unspecific binding to other cellular components of the lysates.

Table 3.5. ELISA coating concentrations (μg/mL) for RecA detection.

		IPTG induction (μM)					
		0	**10**	**20**	**30**	**40**	**50**
Strain	**Plasmid**						
UA1916	pUA1108	2.5	2.5	2.5	2.5	2.5	2.5
UA1916	pUA1129	0.16	0.04	0.04	0.04	0.04	0.04
UA1916	pUA1128	2.5	2.5	2.5	2.5	2.5	2.5
UA1917	pUA1108	0.08	0.08	0.08	0.08	0.08	0.08
UA1917	pUA1128	0.08	0.08	0.08	0.08	0.08	0.08

Table 3.6. ELISA coating concentrations (μg/mL) for CheW detection.

		IPTG induction (μM)					
		0	**10**	**20**	**30**	**40**	**50**
Strain	**Plasmid**						
UA1916	pUA1108	2.5	2.5	2.5	2.5	2.5	2.5
UA1916	pUA1129	2.5	2.5	2.5	2.5	2.5	2.5
UA1916	pUA1128	0.16	0.08	0.08	0.04	0.04	0.04
UA1917	pUA1108	2.5	2.5	2.5	2.5	2.5	2.5
UA1917	pUA1128	0.16	0.08	0.08	0.08	0.04	0.04

Coated plates were covered with aluminum foil and incubated for 16 hours at 4 °C. The day after, plates were washed with 200 µL/well of wash buffer 1X (A.3.21) for 4 times with 5 minutes incubation each. Incubations were performed by placing the plates on a microtiter plate shaker (*Kline K3 E*, Ovan) at 600 rpm. Next, 200 µL/well of ELISA blocking buffer (A.3.4) were added and the plates were covered and incubated at room temperature for 2 hours while gently shaking at 300 rpm. After the blocking step, assay plates were washed as previously explained and then 100 µL/well of a 1/2000 dilution in wash buffer 1X of either an anti-RecA antibody (*Anti-RecA antibody*, Abcam) or an anti-FLAG (*Monoclonal Antibody to DYKDDDDK Epitope Tag*, Acris) were added. Plates were covered and incubated for 1 hour at room temperature while gently shaking at 300 rpm. After that, plates were washed again as previously explained and then 100 µL/well of the corresponding secondary antibody diluted in wash buffer 1X were added. For RecA detection, a 1/15000 dilution of an anti-rabbit IgG (*Polyclonal Antibody to Rabbit IgG (H&L)-HRP*, Acris) was used. For FLAG-tagged CheW detection, a 1/10000 dilution of the anti-mouse IgG (*Polyclonal Antibody to Mouse IgG (H&L)-HRP*, Acris) was used. Plates were then covered and incubated for 1 hour at room temperature while gently shaking at 300 rpm. Finally, plates were washed as explained above and 100 µL/well of developing solution was added (*BD OptEIA^{TM} TMB Substrate Reagent Set*, BD Biosciences). Developing solution was prepared according to manufacturer's instructions.

Plate lectures were taken every 10 minutes at 650 nm wavelength using a multititer plate reader (*Sunrise*, Tecan) for a total time of 40 minutes after adding the developing solution. The best signal-to-noise ratio lecture (usually the 30 minutes lecture) was then used for further analysis.

3.7 Microscopy methods

3.7.1 Agarose pads preparation

For fluorescence microscopy assays, cells were immobilized and fixed at the same focal plane using thin agarose pads. On-slide agarose pads preparation procedure is shown in Figure 3.6. A 1 % (w/v) agarose suspension (*D1 Low EEO*; Pronadisa) in tethering buffer (A.3.19) was prepared in a clean, sterile, 5 mL plastic tube. The mix was then heated at 90 °C using a thermal block to allow the agarose to completely melt. Temperature was maintained during the whole agarose pads preparation procedure to ensure that no solidification occurs inside the tube.

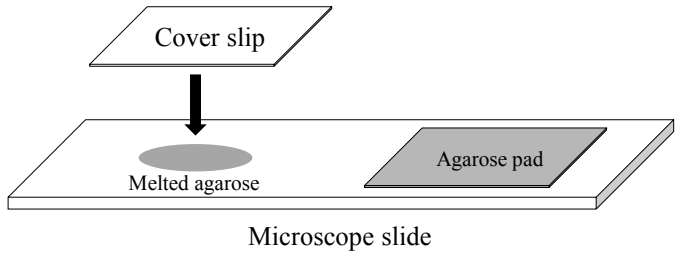

Figure 3.6. Agarose pads preparation. Preparation of the agarose pads is conducted on temperate microscope slides by applying the melted agarose, covering it with a microscope cover slip and allowing the agarose to slowly solidify at room temperature.

A microscope slide was placed on the thermal block at 90 °C and heated for 2 minutes. Then, 70 µL of melted 1 % agarose were applied over the hot slide and immediately covered with a 20 x 20 mm cover slip. The cover

slip was placed over the agarose without applying any pressure. Presence of leant areas were checked before agarose solidification and if needed were corrected by applying a slight pressure to the area. Agarose pads were allowed to solidify for 30 minutes at room temperature.

3.7.2 Chemoreceptor clustering assay

Receptor clustering experiments were performed essentially as described by Sourjik and Berg (2000) and Kentner *et al.* (2006).

S. Typhimurium over-night cultures of strains carrying the pUA1127 (*eYFP::cheR*) plasmid were grown in tryptone broth (A.1.8) supplemented with ampicillin at 30 °C under constant agitation. The day after, over-night cultures were diluted 1/100 in tryptone broth supplemented with ampicillin and IPTG 25 µM to induce *eYFP::cheR* fusion expression. Cultures were then incubated at 30 °C until an OD_{600} of ≈ 0.5 was reached .

Cells were then harvested by low speed centrifuging (5300 g) for 15 minutes, washed once in cold tethering buffer (A.3.19) and resuspended in 100 µL of ice cold tethering buffer. Cells were maintained on ice during the whole assay.

Thin 1 % agarose pads were prepared as described above. When solidified, 3 µL of cells were applied on the pad and covered with a clean cover slip.

Fluorescence microscopy was performed using a *Zeiss AxioImager M2* microscope (Carl Zeiss Microscopy) equipped with a *Zeiss AxioCam MRm* monochrome cam (Carl Zeiss Microscopy) and a filter set for eYFP (Excitation BP 500/25; Beamsplitter FT 515; Emission BP535/30). Each experiment was performed in triplicate on independent cultures. Images presented here were chosen to be representative fields of the entire image.

ImageJ software (National Institutes of Health) was used to either quantify cluster amounts or to prepare images for publication.

3.8 Informatic methods

3.8.1 Statistical methods

Hypothesis testing was performed using the one- or two-way ANOVA test plus Tukey's or Dunnett's multiple comparison *post hoc* tests to differentiate between data sets. Significance was reported when the p-value for a given comparison was found to be less than 0.05 as conventionally accepted.

For the Bradford and ELISA assays (described before) data fitting was conducted using the common linear regression fitting for linear shaped data or a 4-parameter logistic fitting for sigmoid shaped data. In both cases accepted fittings had an r^2 coefficient of at least 0.90.

In order to adjust the CFUs/mL value for the chemotaxis assays, growth kinetics of every strain of interest were conducted and finally adjusted using the Gompertz sigmoidal model. Then, the exponential growth phase was selected and plotted against the optical density. The resultant scatter plot was adjusted with a fourth order polynomial function that allowed a direct calculation of the CFUs/mL using the optical density value.

3.8.2 Protein docking

A basic RecA-CheW docking was performed using the ClusPro server (Comeau *et al.*, 2004b,a; Kozakov *et al.*, 2006, 2010). *E. coli* three dimensional protein structures were obtained in ".pdb" format from RCSB Protein Data Bank (PDB). Accession numbers for the resolved structures used in this work were: 2REB for RecA and 2HO9 for CheW.

The docking results and protein structures were visualized and analyzed using PyMOL software (Schrödinger, LLC, 2010).

Chapter 4

Results

4.1 Construction of a *cheW::FLAG* strain

To reach the main objectives of the present work it was imperative to develop a useful way to detect RecA and CheW proteins of *S.* Typhimurium. Western blot and ELISA protocols were implemented to conduct several experimental steps and thus, anti-RecA and anti-CheW antibodies were required. Commercial antibodies against *E.coli* RecA (which can recognize *S.* Typhimurium RecA) are available but they are not for CheW protein.

To overcome this handicap it was decided to generate a strain with a FLAG tagged version of the CheW protein. The widely used FLAG epitope has only 11 amino acid residues including a glycine spacer (Terpe, 2003). Due to it's small size and hydrophilic composition, it is unlikely to affect neither the folding nor the functionality of CheW protein making it a good choice for protein tagging, specially for small ones. To further prevent any folding issue, the FLAG tag was placed at the C-terminus of the protein.

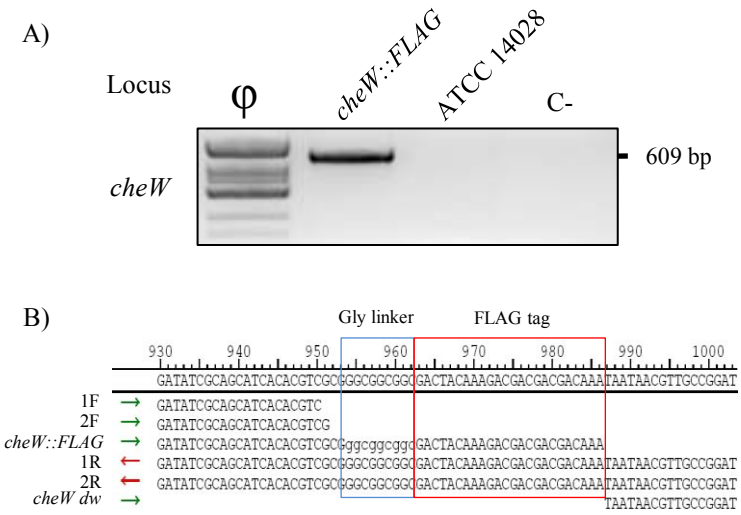

Figure 4.1. *S*. Typhimurium *cheW::FLAG* mutant strain confirmation. **A)** PCR amplification of *cheW* locus of either *cheW::FLAG* (UA1916) strain or wild type strain using the FLAGoricheWextF primer pair (Section 3.2). PCR products were loaded on an 1.5 % (w/v) agarose gel. Amplification was only possible if the FLAG epitope was placed at the expected site. **B)** Contig assembly from sequences obtained by capillary sequencing of *cheW* locus using the same external primers as in figure A. Consensus sequence for the locus in UA1916 strain is retrieved based on data from two experiments. FLAG sequence presence is included into the red square. Blue square includes the 3 x glycine spacer. Nomenclature: 1 and 2, sequencing replicates; F, cheWextF forward primer; R, cheWextR reverse primer; *cheW::FLAG*, hypothetical FLAG tagged *cheW* sequence; *cheW dw*, downstream region of the *cheW* gene.

Apart from functional and experimental considerations, highly purified monoclonal antibodies against the FLAG epitope are available from several suppliers thus making experimental procedures easy.

The FLAG epitope was introduced using a scarless mutation system based on the pKO3 plasmid as explained in materials and methods section (Section 3.5.3) and following the procedure described by Latasa *et al.* (2012). The FLAG epitope incorporation was checked by PCR amplification using a forward oligonucleotide priming within the FLAG tag and an external reverse oligonucleotide priming downstream of *cheW* locus (Fig. 4.1 A). If the FLAG epitope is present, a 609 bp product is observed whereas no amplification product is detected when the FLAG tag is absent like in the wild type ATCC 14028 strain.

Strain UA1916 carrying the *cheW::FLAG* allele was further confirmed by sequencing using construction-external oligonucleotides. Figure 4.1 B shows the consensus sequence for *cheW* locus of the *cheW::FLAG* strain based on two sequencing replicates and compared with both the expected *cheW*::*FLAG* gene sequence and the *cheW* locus downstream sequence.

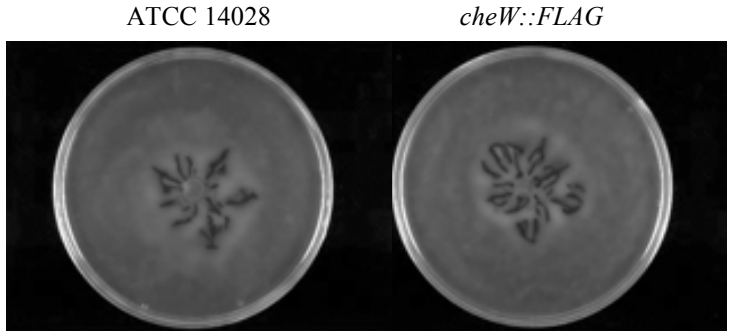

Figure 4.2. UA1916 strain swarming pattern. Swarming pattern on 0.5 % soft agar of UA1916 strain *(cheW::FLAG)*. Wild type ATCC 14028 strain under the same experimental conditions is shown as a control.

To determine if the *cheW::FLAG* strain is phenotypically equivalent to the wild type *S.* Typhimurium, a swarming assay comparing both strains was conducted. Figure 4.2 shows the swarming patterns of the wild type and UA1916 strains under the same incubation conditions. As it should be noticed, no differences are detected among strains and thus no phenotypic effect is attributable to *cheW* tagging.

Based on this result, the *cheW::FLAG* tested clone was selected as genetic basis to generate further constructions.

4.2 Determination of RecA-CheW relationship

4.2.1 RecA and CheW interaction

Previous work on protein-protein interaction conducted in *E.coli* K-12 by Arifuzzaman *et al.* (2006) reported the interaction between RecA and CheW proteins. Also, previous work developed in our laboratory by Medina-Ruiz *et al.* (2010) showed that a swarming defect on a *S.* Typhimurium *recAo6869* (constitutive expression of *recA*) strain could be phenotypically complemented by overexpressing the *cheW* gene from a plasmid. Besides, other work conducted by Medina-Ruiz (2012) revealed a positive interaction result in a two hybrid experiment based on the coexpression of *lacZ* fusion variants of RecA and CheW proteins in *E. coli* MC1061.

As a part of the objectives of the present work, it was decided to further investigate and confirm these previous results through two complementary methods: a far-Western blot and a co-immunoprecipitation.

Figure 4.3 shows the result of a dot-blot version of a far-Western blot. RecA, CheW and BSA proteins were immobilized on top of a PVDF membrane and the interaction of each one of them with RecA was tested.

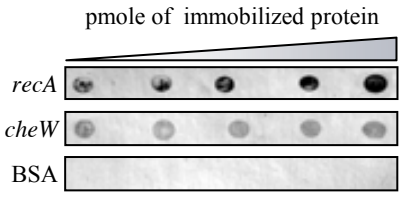

Figure 4.3. Far-Western blot interaction assay of RecA and CheW. Different concentrations of RecA and CheW from *S.* Typhimurium and BSA were applied to a PVDF membrane and then incubated with 400 nM of 6 x His-tagged RecA. Protein complexes were detected as explained in materials and methods. The RecA-RecA interaction is here used as positive control while the BSA-RecA absence of interaction is used as negative control.

As expected, RecA protein is able to interact with himself (Story *et al.*, 1992) and with CheW but not with BSA thereby, RecA and CheW are able to interact *in vitro* confirming the results previously obtained in the two hybrid assay.

To further elucidate the behavior of RecA and CheW interaction in a real environment, a co-immunoprecipitation from a whole-cell lysate of *S.* Typhimurium UA1618 strain was conducted. The chosen strain expresses both *recA* and *cheW* at physiological levels. Strains lacking either Δ*recA* (UA1618) or Δ*cheW* (UA1605) were used here as controls.

The results presented in Figure 4.4 clearly show that when CheW::FLAG was immunoprecipitated, RecA was also detected in the resulting supernatant indicating that CheW and RecA are interacting in their common environment. Some remaining RecA signal was detected in the strain lacking *cheW::FLAG*. This could be attributed to unspecific binding of RecA either to anti-FLAG antibody or to magnetic beads used during immunoprecipitation. Despite this, and because the intensity of RecA band detected

in the *recA+ cheW::FLAG+* strain is clearly higher than the observed in the *recA+ cheW:FLAG-* strain, the binding was assumed to be specific. As expected, in the strain lacking *recA* gene no RecA signal was found confirming that no other unspecific protein could be detected by this procedure at the same location.

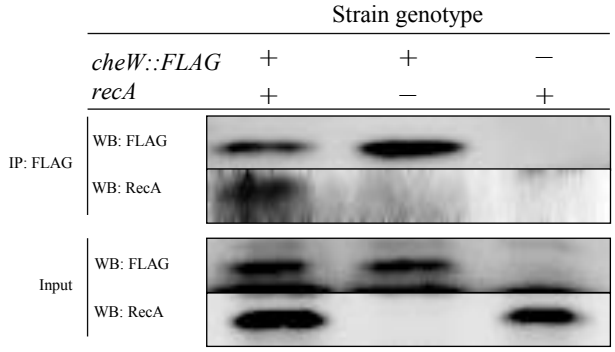

Figure 4.4. Co-immunoprecipitation of CheW::FLAG. FLAG tagged CheW was immunoprecipitated from *S.* Typhimurium ATCC 14028 *cheW::FLAG* (UA1916), Δ*recA cheW::FLAG* (UA1918) and Δ*cheW* (UA1908) whole-cell lysates. The resultant supernatant was analyzed by immunobloting with anti-RecA (WB:RecA) and anti-FLAG (WB:FLAG) antibodies. Non-immunoprecipitated whole-cell lysates are shown as load controls to confirm the presence/absence of either RecA or CheW::FLAG. Nomenclature: IP, immunoprecipitated; WB, immunoblotted .

Finally, a simple protein-protein docking was conducted to generate an *in silico* model for the RecA-CheW interaction using the available resolved structures of the *E. coli* RecA (PDB: 2REB) and CheW (PDB: 2HO9) proteins (Fig. 4.5 A). The resultant model is believed to be reliable also for *S.* Typhimurium as the reported BLAST identity between *E. coli* K-12 and

S. Typhimurium ATCC 14028 proteins is of 97 % for RecA and 92 % for CheW.

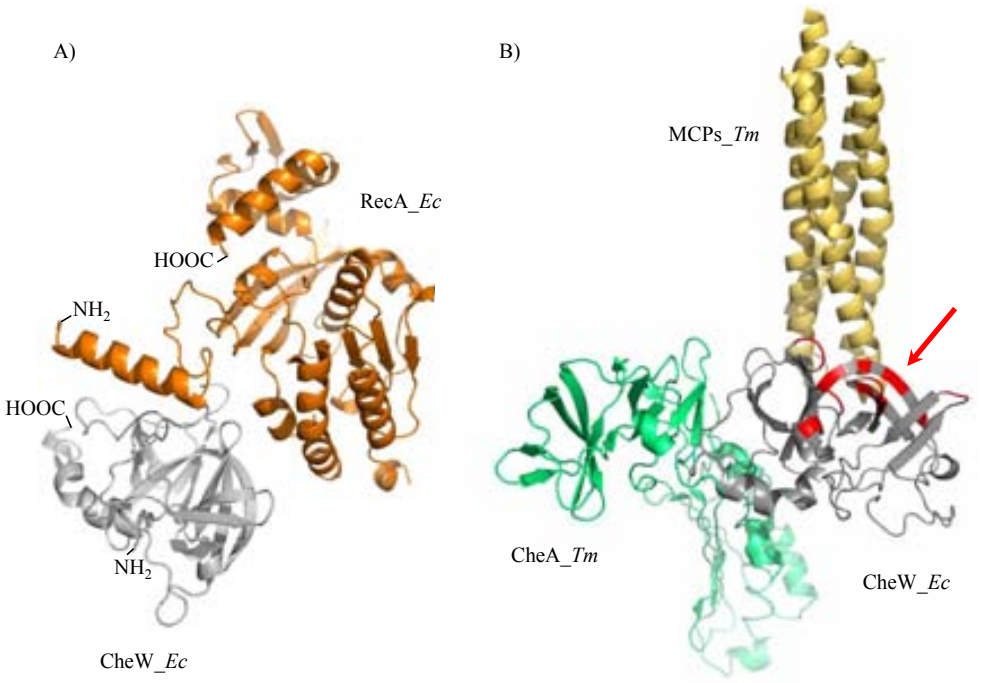

Figure 4.5. Protein docking of RecA and CheW. A) Protein-Protein docking using RecA and CheW resolved structures from *E. coli*. Source: Irazoki O, not published. **B)** Three dimensional model of the expected MCP-CheA-CheW complex. The model was generated *in silico* by substituting the *T. maritima* CheW protein in the PDB: 3UR1 model by the *E. coli* CheW (PDB: 2H09) as their three dimensional structures are very similar. Regions that were determined to support polar contacts within RecA and CheW in the docking model are highlighted in red.

Previous work conducted by Briegel *et al.* (2012) and Li *et al.* (2013) resolved the three dimensional structure of the MCP-CheA-CheW complex of *Thermatoga maritima* (PDB: 3UR1). This structure was reported as a generic model for signaling complexes within bacterial chemosensory arrays. *Thermatoga* proteins had been used for crystallographic assays due to the difficulty in performing structural studies using the *E. coli* CheW protein. Also, this thermophilic bacteria have a chemotaxis system structure similar to the one found in several mesophilic bacteria, including *E. coli.* (Swanson *et al.*, 1996; Griswold *et al.*, 2002).

A simple *in silico* analysis of the RecA-CheW docking model allowed the identification of those amino acids on the CheW that more likely support polar contacts with RecA. To evaluate the spatial location of these amino acids, the *E. coli* CheW three dimensional model was used to substitute the *T. maritima* CheW within the MCP-CheA-CheW model (PDB: 3UR1) for this organism (Fig. 4.5 B). Remarkably, the putative residues involved in the contact with RecA were found to be located either on β-strand structured zones or on unstructured loops but the putative interaction area formed by its combination was found to be completely solvent exposed (Fig. 4.5 B, red highlighted zones).

4.2.2 RecA and CheW cellular stoichiometry

Once it was demonstrated that RecA and CheW proteins of *S.* Typhimurium were able to interact, the next goal for this work was to quantitatively describe the *in vivo* relationship between them. The objective of this part of the present work was to determine the relative amounts of each protein and to try to define the swarming behavior as a function of the molecular ratio between RecA and CheW.

4.2.2.1 Swarming behavior and stoichiometry variations

As previously stated, RecA and CheW proteins interact in the cells, thus a controlled relationship in their abundances could be expected and might be important for swarming motility. In fact, previous results obtained in our laboratory showed that over-expression of *recA* abolishes swarming motility in *S.* Typhimurium (Medina-Ruiz *et al.*, 2010). Similar effects are reported in *E. coli* for *cheW* gene (Cardozo *et al.*, 2010).

S. Typhimurium *cheW::FLAG* (UA1916) was transformed with either *cheW::FLAG* (pUA1128) or *recA* (pUA1129) overexpression plasmids and placed onto soft agar plates to check for the swarming motility. In addition, plates were supplemented with IPTG concentrations ranging from 0 to 50 µM to induce the expression of the plasmid-encoded genes.

Figure 4.6 shows the swarming behavior of *S.* Typhimurium under IPTG induction conditions when none, *recA* or *cheW::FLAG* genes are overexpressed. As it could be noticed, neither the empty plasmid (pUA1108) nor the presence of rising IPTG amounts showed any effect on the swarming motility of the *cheW::FLAG* strain. Thus, any difference could be directly attributed to the expression of the study genes. To quantitatively assess the movement ability of the different studied strains and to allow a ready comparison between them, in this experiment the relative motility was calculated as the ratio between the colony diameter of the study strain and that of the control strain under the same experimental conditions following the previously described methodology (Harshey and Matsuyama, 1994; Sourjik and Berg, 2000; Toguchi *et al.*, 2000).

When carrying the *recA* overexpression plasmid (pUA1129), swarming motility is clearly affected as the induction level increases indicating that the overexpression of *recA* produces an impairment on swarming ability

(Fig. 4.6 A). The relative motility of *cheW::FLAG* strain harboring the *recA* overexpression plasmid is dramatically diminished at 10 μM IPTG being only of 0.3 (corresponding to a 30 % of the maximum displacement held by the control strain). After that, a quick decrease in swarming ability is shown and when inducing at 30 μM or more the minimum extension area (relative motility of 0.15) in our experimental conditions is reached (Fig. 4.6 B).

The same pattern is observed when carrying the *cheW::FLAG* overexpression plasmid (pUA1128). In this case, swarming ability also decreases as IPTG concentration increases (Fig. 4.6 A) but in a more progressive fashion than what previously shown for *recA* overexpression. In fact, the behavior of the *cheW::FLAG* strain is almost normal at 10 μM with a relative motility of 0.9, thus nearly as the control strain. At 30 μM the *cheW::FLAG* strain still have a relative motility around 0.3 whereas to reach the minimum extension area (relative motility of 0.15) a minimum of 50 μM IPTG is required (Fig. 4.6 B) in contrast to what is previously stated for *recA* induction.

To further investigate, a phenotypic complementation experiment with *recAo6869 cheW::FLAG* (UA1917) strain was conducted. This strain carries a mutation into the *recA* SOS-box which prevents LexA binding thus causing the constitutive expression of the *recA* gene product. This mutant showed to be swarming defective when carrying the empty overexpression plasmid at any induction level (Fig. 4.7 A). When harboring the *cheW::FLAG* overexpression plasmid (pUA1128) the strain remained swarming deficient (relative motility of 0.1-0.15) with no induction but colony diameter increased as IPTG concentration does until 20 μM when a relative motility of 1 was quantified (Fig. 4.7 A and B). This confirmed that a phenotypic complementation of the *recAo6869 cheW::FLAG* strain

is possible by means of *cheW::FLAG* overexpression to a certain level. At 30 µM IPTG, the swarming was still present and relative motility was high (0.6-0.7) but beyond this point the swarming motility rapidly decreases and at 50 µM IPTG a relative motility of around 0.15 was reached again.

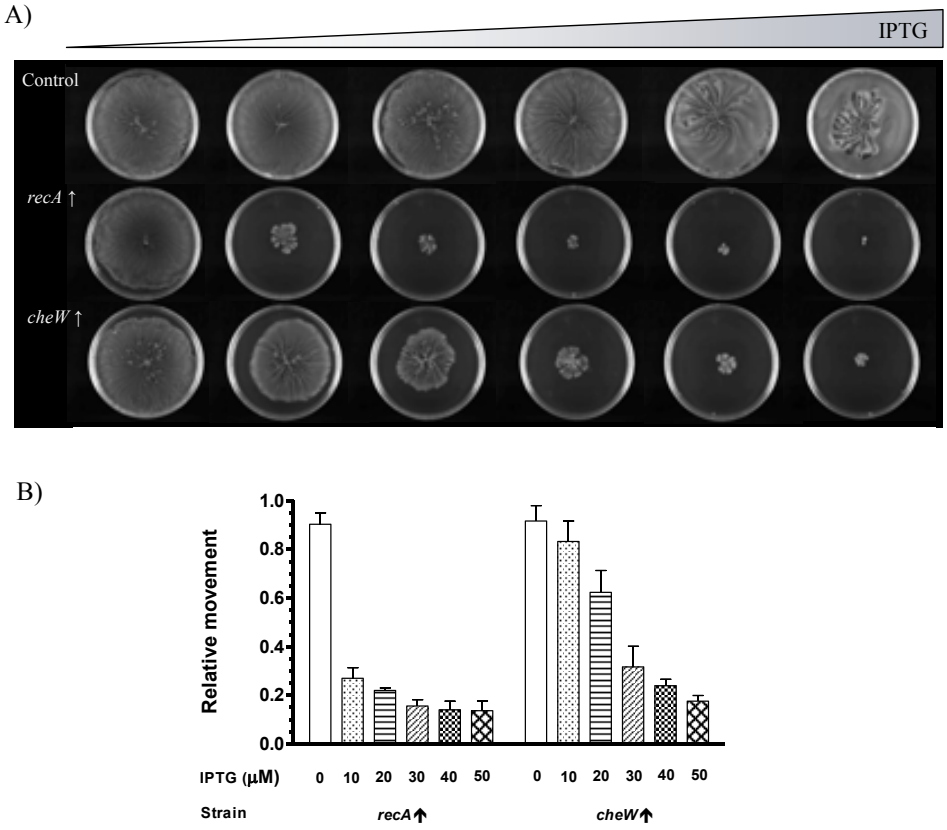

Figure 4.6. Effects of RecA and CheW overexpression in the swarming ability of the UA1916 strain. A) Swarming ability of the *S.* Typhimurium *eda W::FL1G* strain harboring either the empty expression vector (Control, UA1516 pUA1108), the *recA* expression vector (*recA*↑, UA1516 pUA1125) or the *eda W::FL1G* expression vector (*eda W*↑, UA1516 pUA1128). Plates shown were supplemented with 0, 10, 20, 30, 40 and 50 μM IPTG. **B)** Quantification of the relative colony motility of each strain under each induction condition tested. The relative motility is defined as the ratio between the colony diameter of the study strain and that of the *eda W::FL1G* strain under the same experimental conditions. Results are the mean (SD) of three independent experiments.

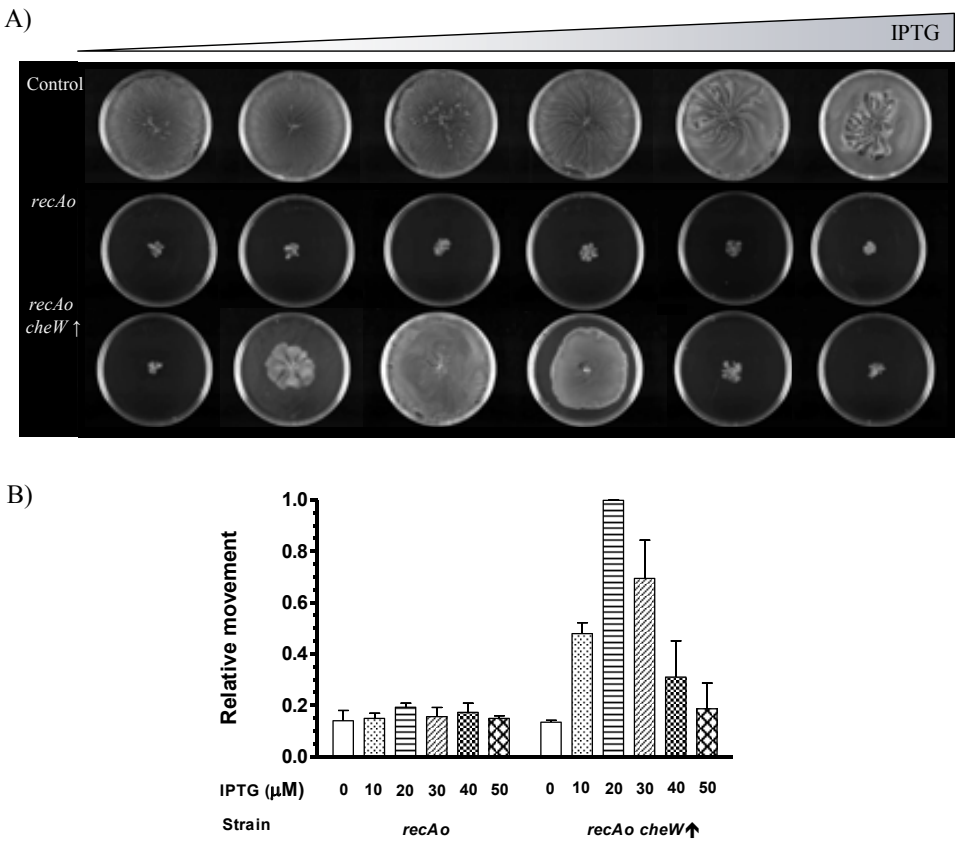

Figure 4.7. Effects of RecA and CheW overexpression in the swarming ability of the UA1917 strain. A) Swarming ability of *S.* Typhimurium strains *cheW::FL4G* harboring the empty expression vector (Control, UA1516 pUA1108) and *recA6605 cheW::FL4G* strain harboring either the empty (*recA6605*, UA1517 pUA1108) or the *cheW::FL4G* (*recA6605 cheW*↑, UA1517 pUA1128) expression vectors. Plates shown were supplemented with 0, 10, 20, 30, 40 and 50 μM IPTG. B) Quantification of the relative colony motility of each strain under each induction condition tested. The relative motility is defined as the ratio between the colony diameter of the study strain and that of the *cheW::FL4G* strain under the same experimental conditions. Results are the mean (SD) of three independent experiments.

4.2.2.2 Quantification of RecA and CheW

To go in depth with the importance of stoichiometry in the swarming behavior of *S.* Typhimurium it was decided to quantify the cellular amount of RecA and CheW::FLAG under the same conditions previously tested to obtain the phenotypic results shown in Figures 4.6 A and 4.7 A. Thereby, ELISA quantifications of whole-cell lysates obtained from swarming plates under different IPTG induction conditions were conducted.

4.2.2.2.1 Quantification in the *cheW::FLAG* strain The amount of RecA in *cheW::FLAG* (UA1916) strain harboring the empty expression vector (pUA1108) was found to be, on average, of $2.43 \cdot 10^{10}$ molecules/µg of total protein. The amount of RecA quantified in this strain is very similar to the one previously quantified in *E. coli* AB1157 strain by Karu and Belk (1982). In that work, the amount of RecA was found to be approximately $1.58 \cdot 10^{10}$ molecules/µg of total protein by using a competitive ELISA method. Accounting for the phylogenetic proximity between *E. coli* and *S.* Typhimurium, the similarity between ELISA methods used and the close similarity between values obtained for that control strain, a very reliable quantification of RecA is expected for the rest of the samples analyzed in this work.

Furthermore, no variation in RecA amount was observed for this strain under the six induction conditions tested (Fig. 4.8). This indicates that the effect on swarming motility could be directly attributed to the protein expressed from the plasmid and not to IPTG or the plasmid backbone itself.

The amount of CheW::FLAG in this strain was quantified to be, on average, $2.44 \cdot 10^{10}$ molecules/µg of total protein (Fig. 4.9) in the whole IPTG induction range tested with nearly no variation. This value matches well

with the approximately $1.32 \cdot 10^{10}$ molecules/µg of total protein previously quantified in *E. coli* RP437 strain using semi-quantitative Western blot (Li and Hazelbauer, 2004). As the quantification value obtained for *S.* Typhimurium is of the same order as the value already published for *E. coli* and accounting for the small phylogenetic distance between both strains, a very reliable quantification of CheW::FLAG is expected in the samples analyzed in the present work.

4.2.2.2.2 Quantification in the *cheW::FLAG* strain harboring the *recA* overexpression plasmid When carrying the *recA* overexpression vector (pUA1129), the basal expression (without induction) of the RecA protein in the *cheW::FLAG* (UA1916) strain is of 27 times higher ($6.74 \cdot 10^{11}$ molecules/µg of total protein) than the same strain harboring the empty plasmid (pUA1108). When IPTG is added, an average expression level of $8.22 \cdot 10^{12}$ molecules/µg of total protein is rapidly reached even at 10 µM IPTG. Expression level does not vary substantially throughout the whole IPTG induction range as an expression plateau seems to be reached rapidly (Fig. 4.8).

Quantified levels of CheW::FLAG in this strain were of $2.08 \cdot 10^{10}$ molecules/µg of total protein on average (Fig. 4.9) and thus, non significant differences were observed when compared to the same strain but harboring the empty expression vector ($2.44 \cdot 10^{10}$ molecules/µg of total protein). As it could be noticed, no significant variation occurs throughout the IPTG induction range tested suggesting that harboring the *recA* expression vector had no effect over *cheW::FLAG* endogenous expression.

4.2.2.2.3 Quantification in the *cheW::FLAG* strain harboring the *cheW::FLAG* overexpression plasmid The *cheW::FLAG* (UA1916)

strain carrying the *cheW::FLAG* overexpression vector (pUA1128) showed a RecA level of $1.62 \cdot 10^{10}$ molecules/µg of total protein on average (Fig. 4.8), very similar to those value previously observed in the control strain ($2.43 \cdot 10^{10}$ molecules/µg of total protein) harboring the empty expression vector (pUA1108). This value remains constant throughout the whole IPTG induction interval. As expected, harboring an expression plasmid for *cheW::FLAG* allele does not have any effect on the RecA amount.

Quantified levels of CheW::FLAG in this strain were of $4.48 \cdot 10^{11}$ molecules/µg of total protein if no IPTG was present. This basal value is approximately 20 times higher than in the same strain with the empty expression vector and it could be attributed to the increased genetic dosage. As expected after the induction, the detected CheW::FLAG amount progressively rises as the inductor concentration does. At 10 µM IPTG the amount of CheW::FLAG is of $1.73 \cdot 10^{12}$ molecules/µg of total protein and it rises to $1.25 \cdot 10^{13}$molecules/µg of total protein when 50 µM IPTG is added (Fig. 4.9). In contrast to what is explained for RecA induction in section 4.2.2.2.2, in this case no plateau is reached and the amount of protein detected describes a positive tendency depending on the IPTG concentration for the whole interval studied.

4.2.2.2.4 Quantification in the *recAo6869 cheW::FLAG* strain

As expected given the presence of a mutation in the *recA* gene promoter leading to its constitutive expression, the amount of RecA in the *recAo6869 cheW::FLAG* (UA1917) strain harboring the empty expression vector (pUA1108) was found to be, on average, $2.76 \cdot 10^{12}$ molecules/µg of total protein. This is more than a hundred times higher than in the *cheW::FLAG* strain harboring the empty expression vector and under the same experimental conditions (Section 4.2.2.2.1).

As previously observed, in this case no variation of the RecA amount was observed throughout the whole IPTG induction interval (Fig. 4.8) indicating that there is no interaction attributable to a side effect of neither IPTG nor the plasmid backbone.

The CheW::FLAG amount quantified in this strain was, on average, $6.92 \cdot 10^9$ molecules/µg of total protein (Fig. 4.9). This value is 3.5 times lower that the one observed for *CheW::FLAG* strain harboring the empty expression vector (here used as control for endogenous levels). In addition, no significant change in CheW::FLAG amount is detected as the IPTG concentration rises indicating that, as expected, no side effects due to IPTG or the expression plasmid are occurring.

4.2.2.2.5 Quantification in the *recAo6869 cheW::FLAG* strain harboring the *cheW::FLAG* overexpression plasmid The amount of RecA in the *recAo6869 cheW::FLAG* (UA1917) strain harboring the *cheW::FLAG* (pUA1128) expression vector was found to be, on average, $1.71 \cdot 10^{12}$ molecules/µg of total protein. This value is close to the one previously found for the same strain but harboring the empty expression vector ($2.76 \cdot 10^{12}$ molecules/µg of total protein). As expected, no variation of the RecA amount occurred throughout the induction range tested (Fig. 4.8) suggesting that variations in *cheW::FLAG* amount had no effect on RecA quantification.

The CheW::FLAG amount quantified for this strain at zero IPTG induction is of $1.19 \cdot 10^{12}$ molecules/µg of total protein thus, the basal value is approximately 170 times higher than the one reported for the same strain but harboring the empty expression vector (Section 4.2.2.2.4). At 10 µM IPTG the amount of CheW::FLAG increases to $2.97 \cdot 10^{12}$ molecules/µg of total protein. Beyond that point, the amount of protein quantified rises

progressively as the IPTG concentration does until 50 µM IPTG is reached. At that point the amount of CheW::FLAG is $1.17 \cdot 10^{13}$ molecules/µg of total protein, close to the maximum value obtained for the cheW::FLAG strain harboring the same plasmid and at the same conditions (Section 4.2.2.2.3).

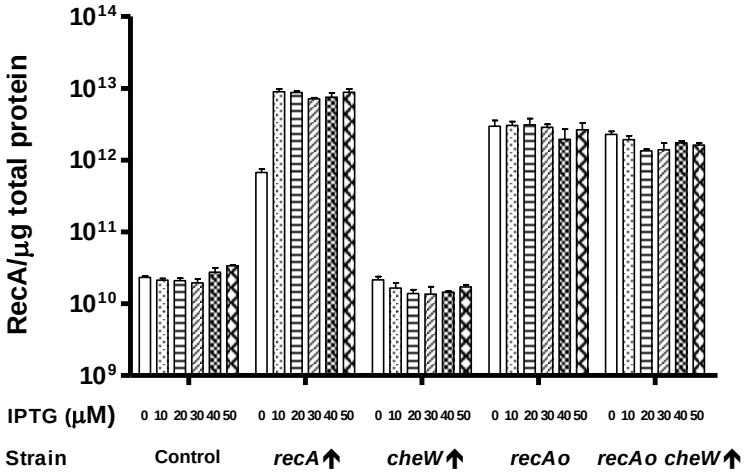

Figure 4.8. RecA quantification in several *S.* Typhimurium strains that overexpress either *recA*, *cheW* or both. Indirect ELISA quantifications of RecA protein of several strains growing on 0.5 % soft agar plates supplemented with 0, 10, 20, 30, 40 and 50 µM IPTG. Tested strains are: the *cheW::FLAG* strain carrying either the empty expression vector (Control, UA1916 pUA1108), the *recA* expression vector (*recA*↑, UA1916 pUA1129) or the *cheW::FLAG* expression vector (*cheW*↑, UA1916 pUA1128) and the *recAo6869 cheW::FLAG* strain carrying either the empty expression vector (*recAo*, UA1917 pUA1108) or the *cheW::FLAG* expression vector (*recAo cheW*↑, UA1917 pUA1128). Results are the mean (SD) of three independent experiments.

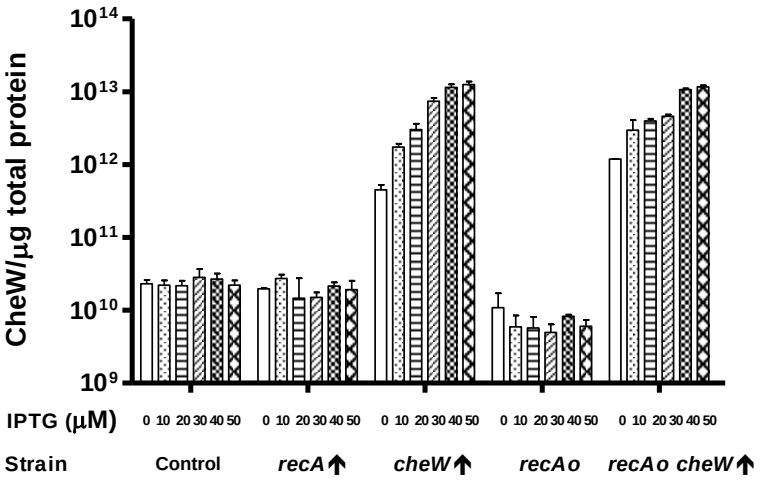

Figure 4.9. CheW quantification in several *S.* Typhimurium strains that overexpress either *recA*, *cheW* or both.. Indirect ELISA quantifications of CheW::FLAG protein of several strains growing on 0.5 % soft agar plates supplemented with 0, 10, 20, 30, 40 and 50 µM IPTG. Tested strains are: the *cheW::FLAG* strain carrying either the empty expression vector (Control, UA1916 pUA1108), the *recA* expression vector (*recA*↑, UA1916 pUA1129) or the *cheW::FLAG* expression vector (*cheW*↑, UA1916 pUA1128) and the *recAo6869 cheW::FLAG* strain carrying either the empty expression vector (*recAo*, UA1917 pUA1108) or the *cheW::FLAG* expression vector (*recAo cheW*↑, UA1917 pUA1128). Results are the mean (SD) of three independent experiments.

4.2.2.2.6 Summary of the quantification of RecA and CheW::FLAG and its relation with the swarming motility The quantification experiments conducted in this work allowed to precisely determine the amount of RecA and CheW::FLAG proteins present in the study strains when placed under swarming conditions. As reported in the previous section (Section 4.2.2.1), the swarming ability of the *cheW::FLAG* (UA1916) and the *recAo6869 cheW::FLAG* (UA1917) is affected by variations in the *recA* and *cheW:FLAG* genes expression thus, a correlation between the amount of each protein in the cell and the ability of given strain to swarm could be established. Results summarized in Table 4.1 show the correlation between the amount of RecA and CheW and the ability of the given strains to swarm.

The 20 μM IPTG induction concentration has been chosen as the reference concentration to compare the distinct strains as at this induction level the *recAo6869 cheW::FLAG* (UA1917) harboring the *cheW::FLAG* (pUA1128) expression vector showed a complete restoration of its swarming ability.

As it could be noticed, variations of two orders of magnitude in the amount of RecA or CheW::FLAG had a clear inhibiting effect over the swarming motility. However, when both proteins were expressed again at approximately the same level (as seen in the *recAo6869 cheW::FLAG* harboring the *cheW::FLAG* expression vector) the swarming motility was fully restored. This is consistent with the previous observations that pointed towards the existence of a strict stoichiometry relationship between RecA and CheW controlling the swarming motility.

Table 4.1. Summary of the swarming ability of *S.* Typhimurium related with the RecA and CheW amount at 20 μM IPTG.

Strain [a]	OE gene[b]	Situation at 20 μM IPTG		
		RecA amount[c]	CheW::FLAG amount[c]	Swarming ability [d]
cheW::FLAG	none	2.09 (0.18) $\cdot 10^{10}$	2.17 (0.36) $\cdot 10^{10}$	+++
cheW::FLAG	*recA*	8.74 (0.45) $\cdot 10^{12}$	2.19 (0.36) $\cdot 10^{10}$	+
cheW::FLAG	*cheW::FLAG*	1.38 (0.18) $\cdot 10^{10}$	3.02 (0.61) $\cdot 10^{12}$	++
recAo6869 cheW::FLAG	none	3.11 (0.67) $\cdot 10^{12}$	5.71 (2.41) $\cdot 10^{9}$	ns
recAo6869 cheW::FLAG	*cheW::FLAG*	1.34 (0.07) $\cdot 10^{12}$	3.95 (0.28) $\cdot 10^{12}$	+++

[a] *cheW::FLAG* (UA1916); *recAo6869 cheW::FLAG* (UA1917).

[b] Plasmid encoded genes that are overexpressed (OE): none (pUA1108); *cheW::FLAG* (pUA1128); *recA* (pUA1129).

[c] Values are the mean (SD) of three independent experiments expressed as molecules/μg of total protein.

[d] Based on the relative movement of each strain when compared to the control strain under the same experimental conditions. <0.2, ns; 0.2-0.5, +; 0.51-0.75, ++ and 0.76-1, +++.

4.2.2.3 Molecular ratio of RecA and CheW

From the results presented in section 4.2.2.2, the molecular ratio of RecA over CheW::FLAG was calculated for each strain in order to elucidate if a limited stoichiometric relationship is required for swarming motility.

4.2.2.3.1 RecA/CheW molecular ratio in the *cheW::FLAG* strain The strain *cheW::FLAG* (UA1916) harboring the empty expression vector (pUA1108) showed a molecular ratio of, on average, 1.02 in the whole range of IPTG concentrations tested. This means that in this strain, the same amount of RecA and CheW::FLAG is present and that no variation in this ratio occurs as the IPTG concentration increased.

This strain exhibited a normal swarming pattern for the whole range of IPTG concentrations tested (Section 4.2.2.1, Fig. 4.6) and thus, having a ratio of 1 should be considered the wild type situation in the experimental conditions tested.

4.2.2.3.2 RecA/CheW molecular ratio in the *cheW::FLAG* strain overexpressing *recA* When the *cheW::FLAG* (UA1916) strain is complemented with the *recA* expression vector (pUA1129), the molecular ratio in absence of IPTG raised to 34 on average (Fig. 4.10). At that point, this strain still showed a normal swarming displacement thus, little or no effect could be attributed to the excess of *recA* caused by the increase in the genetic dosage (Section 4.2.2.1, Fig. 4.6). When even as less as 10 µM IPTG is added, the ratio dramatically increases to more than 300. Beyond that point, and as the production of RecA reached a plateau (Shown in section 4.2.2.2.2) the molecular excess of RecA over CheW::FLAG is maintained, on average, at 405 for the induction interval tested (Fig. 4.10). The swarming ability of this strain is also rapidly depleted and basal motility

ratios are reached and maintained throughout the whole induction interval (Section 4.2.2.1, Fig. 4.6).

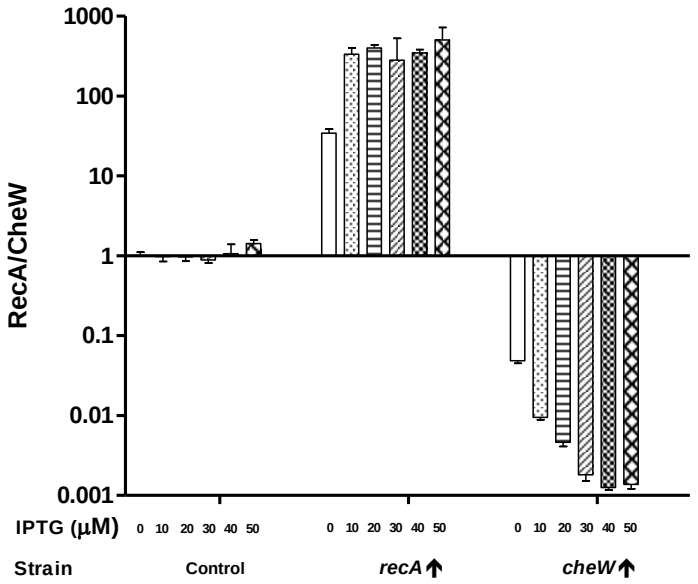

Figure 4.10. Molecular ratio of RecA over CheW in UA1916 strain. The molecular ratio between RecA and CheW was calculated for the *cheW::FLAG* strain carrying either the empty expression vector (Control, UA1916 pUA1108), the *recA* expression vector (*recA*↑, UA1916 pUA1129) or the *cheW::FLAG* expression vector (*cheW*↑, UA1916 pUA1128) on 0.5 % soft agar plates supplemented with 0, 10, 20, 30, 40 and 50 µM IPTG. Results are the mean (SD) of three ratios obtained from three independent ELISA quantification experiments.

4.2.2.3.3 RecA/CheW molecular ratio in the *cheW::FLAG* strain overexpressing *cheW::FLAG* When *cheW::FLAG* (UA1916) strain is complemented with the *cheW::FLAG* expression vector (pUA1128) the molecular ratio under non-induction conditions is of 0.05 and thus, the magnitude of change is the same than the one previously observed for the same strain but harboring the *recA* expression plasmid (Section 4.2.2.3.2). At that point, the swarming ability of this strain is nearly normal, thus only a little effect for this excess of CheW::FLAG is observed (Section 4.2.2.1, Fig. 4.6). Between 10-40 μM IPTG, the ratio decreases gradually from approximately 0.01 to 0.001 where it stabilizes as observed at 50 μM (Fig. 4.10). A close link between the molecular excess of CheW::FLAG and the decrease in swarming ability could be established but, when compared to the overexpression of *recA* (Section 4.2.2.1, Fig. 4.6), in this case the decrease in swarming motility is more progressive.

4.2.2.3.4 RecA/CheW molecular ratio in the *recAo6869 cheW::FLAG* strain Strain *recAo6869 cheW::FLAG* (UA1917) carrying the empty expression vector (pUA1108) was found to have a molecular ratio of RecA over CheW::FLAG of, on average, 491 for the whole range of IPTG concentrations tested (Fig. 4.11). This indicates that due to *recAo6869* mutation this strain has a basal ratio highly displaced towards RecA excess. Also, this strain is unable to swarm as previously shown and no IPTG level from the interval tested is able to revert this situation (Section 4.2.2.1, Fig. 4.7).

4.2.2.3.5 RecA/CheW molecular ratio in the *recAo6869 cheW::FLAG* strain overexpressing *cheW::FLAG* When the *recAo6869 cheW::FLAG* (UA1917) strain is complemented with the

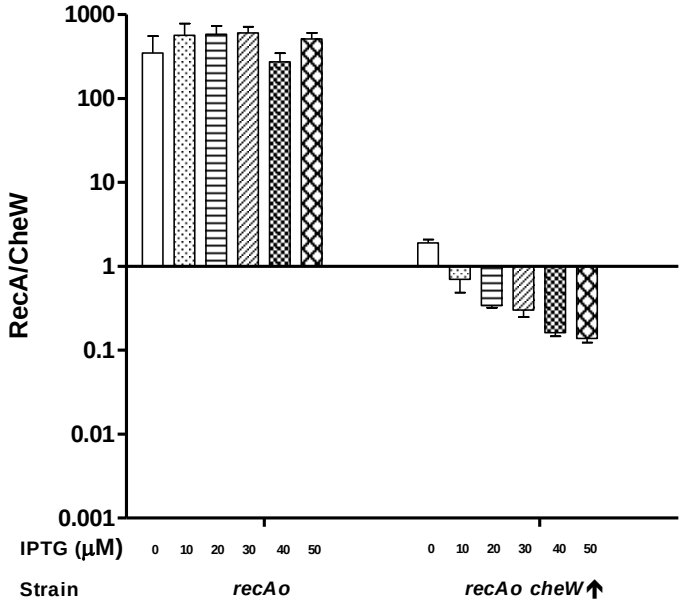

Figure 4.11. Molecular ratio of RecA over CheW in UA1917 strain. The molecular ratio between RecA and CheW was calculated for the *recAo6869* strain carrying either the empty expression vector (*recAo*, UA1917 pUA1108) or the *cheW::FLAG* expression vector (*recAo cheW*↑, UA1917 pUA1128) on 0.5 % soft agar plates supplemented with 0, 10, 20, 30, 40 and 50 µM IPTG. Results are the mean (SD) of three ratios obtained from three independent ELISA quantification experiments.

cheW::FLAG expression vector (pUA1128), the ratio under non-IPTG conditions is of 1.9 (Fig. 4.11). At this point, the molecular ratio is still displaced towards RecA excess. By the next induction concentration (10 µM IPTG) the ratio is of 0.7 thus it is already displaced towards CheW excess (Fig. 4.11). Then, a progressive decreasing tendency (to CheW::FLAG

excess) is maintained during the whole interval of IPTG concentrations. The minimum quantified ratio is of 0.15 at 50 µM IPTG (Fig. 4.11).

The swarming ability of this strain varies throughout the IPTG interval tested (Section 4.2.2.1, Fig. 4.7). As seen before, when the ratio points towards a RecA excess the swarming ability is depleted but, by contrast to what previously stated for *cheW::FLAG* strain harboring the *recA* expression vector (Section 4.2.2.3.2), the excess of RecA required to disable the swarming motility is lower in this case. Beyond the zero IPTG point, the swarming ability slowly recovers until a normal relative motility is reached again when 20 µM IPTG is added (ratio of 0.34). Then, the relative motility started falling progressively again and when 50 µM IPTG is added, and thus the ratio is completely displaced towards CheW::FLAG excess, no significant swarm ability is observed (Section 4.2.2.1, Fig. 4.7).

4.2.2.4 Summary of the stoichiometric relationship between RecA and CheW

ELISA quantifications conducted in the present work allowed a reliable calculation of the stoichiometric relationship existing between RecA and CheW in two distinct *S.* Typhimurium strains when being placed under swarming conditions.

For the strain considered as the reference, the *cheW::FLAG* (UA1916) harboring the empty expression vector (pUA1108) the molecular ratio of RecA over CheW was found to be around 1 regardless of the IPTG concentration present in the medium. This means that the same amount of RecA and CheW is expected to be found in *S.* Typhimurium when doing swarming at what has been defined as normal conditions.

In this work, imbalances in swarming ability caused by either RecA or CheW excess were assessed by quantifying both proteins and establishing the molecular ratio under several IPTG induction conditions. For the previously mentioned reference strain, the overexpression of both *recA* or *cheW* ended with the complete depletion of swarming ability. When there was around 30 times more RecA than CheW, the swarming ability of the reference strain was seriously affected while when the ratio was approximately 400, this is an order of magnitude higher, the swarming motility was completely depleted. A similar behavior was observed in the same strain when *cheW* was overexpressed. When there was around 20 times more CheW than RecA, the swarming ability of this strain was nearly normal but then the swarming ability progressively decreased until no significant motility could be observed. At that point, CheW was around 700 times more abundant than RecA.

For the other strain tested, the *recAo6869 cheW::FLAG* (UA1917) a molecular excess of 500 times RecA over CheW was calculated when harboring the empty expression vector (pUA1108) in the whole IPTG induction range. As expected this strain was completely unable to swarm due to the excess of RecA. A recovery of the swarming ability is possible in this strain by overexpressing *cheW*. When the molecular ratio fell within 0.3-0.7, this strain recovered the swarming motility reaching the maximum relative motility at a ratio of approximately 0.35. The swarming ability was depleted again when a bigger excess of CheW was achieved.

This results indicate that a strong relationship exists between the swarming ability and the RecA/CheW stoichiometry but also show a certain strain dependency. Implications of this fact will be discussed later in section 5.2.

4.3 Swarming behavior under SOS induction

One of the main objectives of the present work was to get a complete view of the interaction between the SOS system and the swarming motility. The classical approach to study the effects of the SOS system over other cellular processes has been to cause the induction of the system by treating the cells with some damaging agent (like mitomycin C) or to put them under stressing conditions (like UV irradiation). In fact, in previous work conducted by Medina-Ruiz *et al.* (2010), mitomycin C was used to demonstrate that the induction of the SOS system abolishes the swarming motility in *S.* Typhimurium (Section 1.4.2). All these strategies have clear major issues against them but the most important is that cells are under stress conditions and their behavior could be affected not only by the SOS system induction but also for the direct toxicity of the agent used.

The aim of this work was to study the swarming ability of *S.* Typhimurium under SOS induction but in the absence of damaging conditions to ensure that the observed effects over the swarming motility were a consequence of the system induction rather than a toxicity problem due to the experimental conditions. To achieve this goal, a strain with a completely unregulated SOS system ($\Delta lexA$) was necessary.

S. Typhimurium $\Delta lexA$ strains are known to be non-viable unless some compensatory mutations are present. The work conducted by Bunny *et al.* (2002) put insight into that fact and pointed towards the responsibility of Fels-2 and both Gifsy-1 and 2 prophages in the lethality of the *S.* Typhimurium *lexA* deficient strains. An *S.* Typhimurium LT2 $\Delta lexA$ strain (UA1685) has been available in our laboratory for many years (Clerch *et al.*, 1996). This strain was obtained by a classical mutagenesis procedure and it is believed to carry some compensatory mutations for $\Delta lexA$ lethality.

To maintain an isogenic background between every strain tested in this study, the generation of an ATCC 14028 strain carrying the Δ*lexA11::Ω*Km allele was attempted by using P22 transduction from the donor UA1685 strain. It should be noticed that some genetic differences exist between the ATCC 14028 and LT2 strains (Jarvik *et al.*, 2010). The most important for the purpose of this work is the absence of both Fels prophages in the ATCC 14028 strain. This, according to Bunny *et al.* (2002), should have prevented the lethality of the Δ*lexA* mutation but attempts to obtain a phage clean ATCC 14028 Δ*lexA* strain failed. This pointed to other compensatory mutations in addition to Fels-2 absence and therefore it was decided to conduct a whole-genome sequencing of the LT2 Δ*lexA* strain (UA1685) to find out other mutations susceptible to be involved in this process.

4.3.1 UA1685 strain sequencing-by-synthesis

S. Typhimurium LT2 strains UA1685 (Δ*sulA* Δ*lexA*) and its isogenic strain except for the *lexA* locus, UA1582 (Δ*sulA*), were sequenced by ServiceXS B.V. to certainly determine the genetic combination of factors that allow the viability of a *lexA* null strain in *S.* Typhimurium.

Table 4.2. Strains UA1582 and UA1685 genomic DNA sequencing results.

		Reads		
Strain	**Min-Max coverage[a]**	**Raw ($\cdot 10^6$)**	**Aligned ($\cdot 10^6$)**	**Missmatch (%)**
UA1582	400-1000x	66.76	55.03	0.143
UA1685	300-900x	57.24	45.73	0.191

[a] Estimated coverages. Minimum read length, 36 bp; maximum read length, 100 bp.

Sequencing and data analysis was conducted as briefly explained in materials and methods (Section 3.4.9). After aligning the resultant reads to the LT2 wild type reference genome, the parameters shown in Table 4.2 were calculated. Coverage values obtained were the typical for an Illumina sequencing experiment.

Accounting for the whole genome, the percent coverage obtained for the LT2 Δ*sulA* (UA1582) strain was of 100 % whereas for the LT2 Δ*sulA* Δ*lexA* (UA1685) strain was of 98 %. The lack of coverage in some areas of the LT2 Δ*sulA* Δ*lexA* strain corresponds to the location of Gifsy-2 and Fels-2 prophages insertion sites (Fig. 4.12) thus indicating that they are both missing in this strain but not in the LT2 Δ*sulA* strain. This fact demonstrates that the Fels-2 absence is necessary to isolate a *lexA* deficient *S.* Typhimurium as proposed by Bunny *et al.* (2002) but remains unclear if it is a sufficient condition. Also, it should be noticed that Gifsy-2 was almost completely absent but Gifsy-1 was not (Fig. 4.12). This is consistent with previous studies that stated the presence of the Gifsy prophages as a secondary lethality factor in a Δ*lexA* background after the presence of Fels-2 prophage. The lack of the Gifsy prophages showed to improve the growth rate of *S.* Typhimurium Δ*lexA* strains already lacking the Fels-2 prophage but was not a necessary condition for the viability of these strains (Bunny *et al.*, 2002).

A search for indels and SNPs was conducted after assembly. When compared to wild type LT2 strain, a total of 31 and 32 small indels were found for the LT2 Δ*sulA* and LT2 Δ*sulA* Δ*lexA* strains respectively. Of those, only two indels were unique for the LT2 Δ*sulA* Δ*lexA* strain (Table 4.3). The first one is localized at the intergenic region between *pps* and *ydiD* genes. Both genes are opposed thus this mutation is unlikely to cause an impairment in either of them. The second one is a guanine insertion

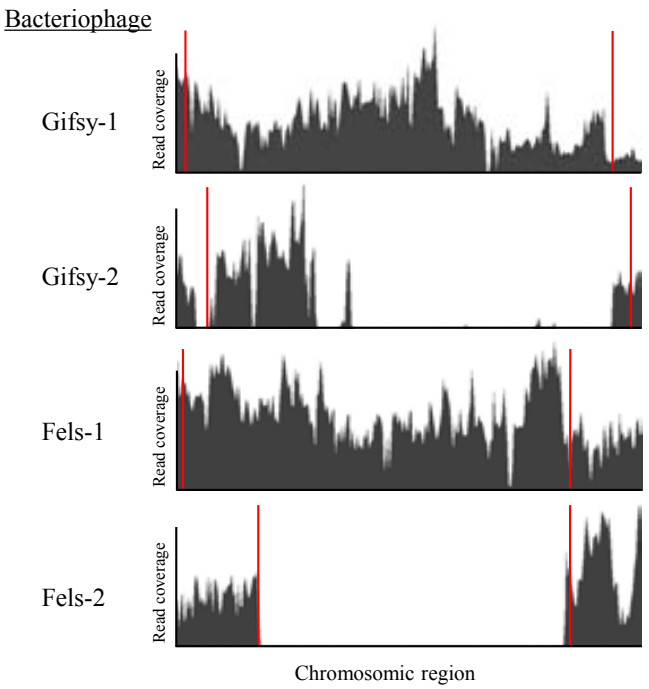

Figure 4.12. Coverage map of the four bacteriophage insertion sites in UA1685 strain genome. Read coverage maps of the chromosomic regions containing the insertion sites for the Gifsy-1, Gifsy-2, Fels-1 and Fels-2 prophages in the UA1685 ($\Delta sulA$ $\Delta lexA$) strain aligned against the *S.* Typhimurium LT2 wild type genome. The area between the red bars is the exact location of the prophages within the shown region of the chromosome.

located at base pair 16 of *sicP* gene. This gene codes a chaperone required for the correct secretion and folding of SptP protein, a tyrosine phosphatase important in *Salmonella* virulence (Fu and Galán, 1998). The insertion produces a frameshift originating a premature stop codon and thus, SicP

could not be successfully translated. SptP is encoded by *sptP* gene whose coding sequence overlaps the one of *sicP,* thereby this mutation could also affect its expression (Table 4.3).

In addition, 125 SNPs were detected when comparing the UA1582 and UA1685 strains to the wild type LT2 strain. Of them, only two were found to be present only in the UA1685 strain (Table 4.3).

The first one is an adenine to guanine transition located at base pair 359 of *crp* gene. This mutation gives place to a glutamine to arginine change when the protein is translated. The second one is another adenine to guanine transition located at base pair 73 of *ysdA* gene. There is not a known gene product but, if it exists, the mutation gives place to a threonine to alanine change.

Table 4.3. Remarkable indels and SNPs found in UA1685 strain.

Type	Position	Affected gene	Change	Effect	Function
SNP	3616003	*crp* (STM3466)	A→G	Gln→Arg	c-AMP regulatory protein
SNP	3998405	*ysdA* (STM3797A)	A→G	Unknown	Putative SOS-regulated toxin
INS	3024066	*sicP* (STM2879)	C→CG	Frameshift	SptP secretion chaperone

To further determine the importance of these mutations we decided to construct knock out strains for the described genes and check for their ability to inherit the Δ*lexA11* allele from the LT2 Δ*sulA* Δ*lexA* strain

(UA1685) by P22 transduction. Mutants were constructed on the UA1922 strain background, an ATCC 14028 derivative that lacks both Gifsy-1 and Gifsy-2 and also the *sulA* gene as this mutations are known to affect the viability of a *lexA* null strain (Bunny *et al.*, 2002).

Deletion of *crp* was dismissed due to the potential pleiotropic effects caused by the lack of this gene as it is a global transcriptional regulator. In addition, *crp* is not considered as part of the SOS system thus this mutation is unlikely to affect cell viability through *lexA*-coupled lethality.

Deletion of *sicP* causes non detectable effects when transducing the *lexA* null allele but the strain is roughly able to grow at 42 °C whereas no grow defect is detected at 30 °C (not shown).

Finally, it was decided to delete the entire *ysdAB* locus. The resultant strain (UA1923) is significantly more proficient than the parental isogenic UA1922 strain to inherit the Δ*lexA11* allele and transductant colonies appear at high frequency. This indicates that the *ysdAB* locus is involved in the toxicity of the *lexA* knock out mutation by some mechanism that still remains unclear.

4.3.2 *S.* Typhimurium ATCC 14028 Δ*lexA* mutant strain construction

To evaluate the *S.* Typhimurium swarming behavior under SOS induced conditions it was decided to construct an *S.* Typhimurium ATCC 14028 Δ*lexA* mutant strain. This was necessary to maintain the strain consistency throughout this work.

Based on the sequencing results explained in section 4.3.1, a Δ*lexA* mutant strain was obtained by transducing the Δ*lexA11::Ω-Km* allele from the original LT2 Δ*sulA* Δ*lexA* (UA1685) strain to a controlled ATCC 14028

background. Transduction recipient used was the UA1923 strain, an ATCC 14028 derivative that lacks both Gifsy-1 and Gifsy-2 prophages, the *sulA* gene and also the entire *ysdAB* locus as it was previously found to be necessary to obtain a good transduction efficiency (Section 4.3.1) . Two types of transductant colony morphologies were obtained: few big and round-shaped colonies and a high number of small irregular-shaped ones.

After check by PCR the presence of the Δ*lexA* mutant allele, small irregular-shaped colonies proved to be true Δ*lexA* mutants whereas big and round colonies were kanamycin resistant but they lacked the mutant allele. Several Δ*lexA* transductant colonies were selected and phage clean-up steps were conducted as explained in materials and methods (Sections 3.5.2 and 3.5.4). Finally, one clone was selected and was PCR-checked for the *lexA*, *sulA* and *ysdAB* loci and Gifsy-1 and Gifsy-2 insertion sites to confirm their absence. The resultant Δ*lexA* mutant strain was coded as UA1925.

Figure 4.13 shows the result for the amplification of the five loci above mentioned. The *lexA* locus was checked using two distinct primer pairs (Fig. 4.13 *lexAext* and *lexA*). The image corresponding to *lexAext* locus shows the amplification using lexAextF and lexAextR primer pair. This allowed the amplification of the whole kanamycin resistance cassette and the *lexA* gene in the Δ*lexA* strain giving a band of 3200 bp whereas amplifications from either the parental UA1923 or wild type strains give a 1024 bp product. This confirms the presence of the mutant allele placed in the correct locus. To further confirm the correct location, a second PCR was conducted using lexAstmF1 and lexAstmR primer pair. The forward primer (lexAstmF1) includes three nucleotides of the HincIII site were kanamycin resistance was originally cloned (Clerch *et al.*, 1996) and therefore if the kanamycin cassette is correctly located this primer is unable to properly hybridize. As shown in Figure 4.13 in the image corresponding to *lexA* locus, no amplification

product was detected for the UA1925 strain. By contrast, a 615 bp product corresponding to *lexA* gene is detected in both UA1923 and wild type strains confirming the correct location of the kanamycin resistance gene within the *lexA* gene.

The remaining locations were checked to ensure that the expected background mutations were present in the final Δ*lexA* strain (UA1925). The UA1923 and the wild type ATCC 14028 strains were used as controls. Figure 4.13 shows the result for the *ysdAB* amplification. A 1524 bp product corresponding to chloramphenicol resistance inserted within *ysdAB* genes was detected as expected, thus confirming the presence of this mutation in the *lexA* strain. Figure 4.13 also shows the results for the *sulA* locus amplification. As expected, the amplification product obtained from both Δ*lexA* (UA1925) and UA1923 strains is 526 bp while the wild type strain product is 712 bp. This is due to the removal of the chloramphenicol resistance cassette and the partial deletion of the *sulA* gene.

Finally, Gifsy phages integration sites were checked by amplifying from flanking genes (Fig. 4.13). It should be noticed that two PCR products were amplified in this case. The 397 bp band corresponds to a partial amplification of the *oraA* gene, here used as PCR positive control. The second product presence is dependent on whether Gifsy phages are present or absent. If absent, an approximately 520 bp and 700 bp products are expected for Gifsy-1 and Gifsy-2 respectively. By contrast, if the phages are present, no band is expected as the length of this phages is over 45 kb in both cases. As shown, both phages were present in the wild type strain but absent in both the Δ*lexA* (UA1925) and UA1923 strains.

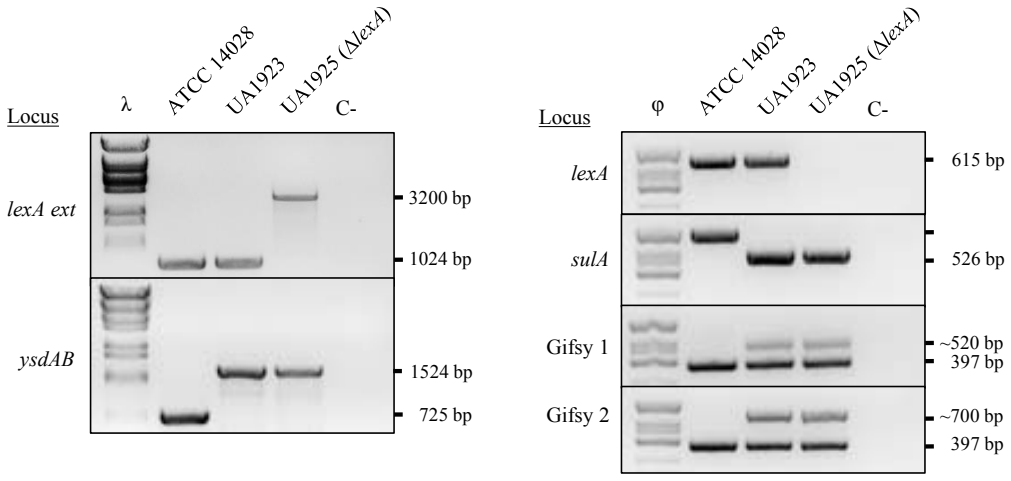

Figure 4.13. Amplification of the *lexA*, *ysdAB* and *sulA* loci and Gifsy prophages insertion sites from UA1923 and UA1925 strains. Amplification of several mutagenized loci and prophage integration sites for the UA1925 ($\Delta lexA$) strain and the parental strain UA1923. *S.* Typhimurium ATCC 14028 wild type is used as size control for the wild type alleles. Primer pairs used were: for *lexAext* locus, lexAstmexF and lexAstmexR; for *lexA* locus, lexAstmF1 and lexAstmR; for *ysdAB* locus, ysdABextF and ysdABextR; for *sulA* locus, sulAextF and sulAextR; for Gifsy-1 insertion site, STM2583 F and STM2637 R and for Gifsy-2, STM1004 F and STM1057 R. For the Gifsy prophages insertion sites PCRs, *oraA* gene amplification was used as positive control. Primer pair used was: oraAint dw and oraAint up. PCR products for the amplification of *lexAext* and *ysdAB* loci were loaded on an 1 % (w/v) agarose gel besides phage λ genome digested with BstEII enzyme used as molecular weight marker. PCR products for the amplification of *lexA* and *sulA* loci and Gifsy-1 and Gifsy-2 insertion sites were loaded on an 2 % (w/v) agarose gel besides phage ϕ X174 genome digested with HinfI enzyme used as molecular weight marker.

4.3.3 Swarming behavior of the Δ*lexA* mutant strain

Once the *S.* Typhimurium ATCC 14028 Δ*lexA* mutant strain was constructed, its behavior on a semisolid surface was tested. Several swarming assays were conducted under experimental conditions explained in materials and methods (Section 3.3.3).

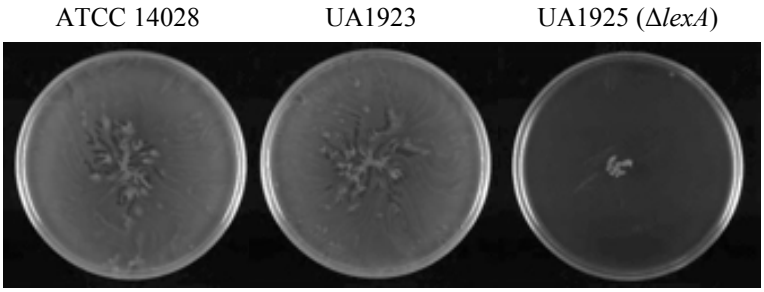

Figure 4.14. Swarming pattern of the Δ*lexA* strain (UA1925). *S.* Typhimurium Δ*lexA* strain swarming pattern on 0.5% semi-solid agar plates. Strains ATCC 14028 wild type and UA1923 are shown as positive controls. The UA1923 strain is the parental and isogenic to the UA1925 except for the Δ*lexA* mutation.

Figure 4.14 shows the swarming pattern of the ATCC 14028 Δ*lexA* strain (UA1925) compared to the profiles displayed by the parental UA1923 and ATCC 14028 wild type strains. As shown, no movement was achieved after a 9 hour incubation at 37 °C for ATCC 14028 Δ*lexA* strain whereas the UA1923 strain is able to do swarming like the wild type strain. This result confirmed that the induction of the SOS system prevent the swarming motility in *S.* Typhimurium. In addition, this result could be directly

attributed to $\Delta lexA$ mutation as the control isogenic strain UA1923 was still able to swarm. Also, it should be noticed that no damaging agent was added and cells were not subjected to any stress situation therefore, the depletion of the swarming ability is not due to external factors.

4.4 Visualization of chemotaxis receptor clusters

The definition of the molecular mechanism governing the relationship between the SOS system and the swarming motility in *S.* Typhimurium was one of the main objectives of the present work.

Previous work conducted by Cardozo *et al.* (2010) reported that an overexpression of CheW causes a decrease of the chemoreceptor clusters aggregation in *E. coli.* Also, work conducted by Gómez-Gómez *et al.* (2007) and Medina-Ruiz *et al.* (2010) showed that either the lack or the excess of *recA* impaired the swarming motility. Regarding the previous results that stated for a RecA/CheW interaction and the effects of stoichiometry variations, including the induction of the SOS system, on the swarming ability of *S.* Typhimurium, it was hypothesized that the overexpression of RecA may also cause some affectation in the integrity of the chemotaxis apparatus affecting in turn the swarming ability of this bacterium.

To test this hypothesis a translational fusion between the *eYFP* and *cheR* genes was constructed as reported by Kentner *et al.* (2006). This construction allowed the visualization of chemotaxis receptor clusters formed in living cells as CheR is part of the chemotaxis signaling complex. Moreover, this fusion was showed to fully complement a $\Delta cheR$ mutant and thus the three dimensional structure and the function of the eYFP fused variant of CheR are expected to have a minimum affectation over the clustering process (Kentner and Sourjik, 2009).

4.4.1 Construction of *S.* Typhimurium Δ*cheR* mutants and clustering patterns

As the naive CheR form is more efficient localizing to clusters than the eYFP fused variant, it was decided to use a Δ*cheR* background in the strains used to visualize cluster integrity to prevent this situation.

λ Red one-step inactivation procedure was used as described in materials and methods (Section 3.5.1) to construct a resistance free Δ*cheR* strain (UA1910). This strain was then used as transduction recipient for several alleles giving the Δ*recA* Δ*cheR* (UA1913), *recAo6869* Δ*cheR* (UA1914) and Δ*cheW* Δ*cheR* (UA1915) strains.

The *recAo6869* Δ*cheR* and Δ*recA* Δ*cheR* were the study strains while the Δ*cheR* and Δ*cheW* Δ*cheR* were used as controls to visualize the different types of known clustering patterns.

Several IPTG concentrations ranging from 1 to 1000 μM were tested on the Δ*cheR* strain (Fig. 4.15). Initially, 1000 μM IPTG was tested but the overexpression of the *eYFP::cheR* fusion at that level showed two major problems. First, the high expression level caused high background fluorescence of the entire cell body making it difficult to localize well shaped and diffraction limited spots at cell poles. Also, the overexpression of the fusion protein at that levels caused severe cell toxicity. This was observed through a significant decrease in growth rate under induction conditions (not shown) and the filamentation of cells as showed in Figure 4.15 A.

Regarding the toxicity and background issues, a decrease in the IPTG concentration used to induce the fluorescent fusion expression was required. Five concentrations ranging from 10 to 100 μM were tested (Fig. 4.15 B) using the growth conditions described in materials and methods (Section 3.7.2). If 10 μM IPTG was used, well shaped chemotaxis polar cluster

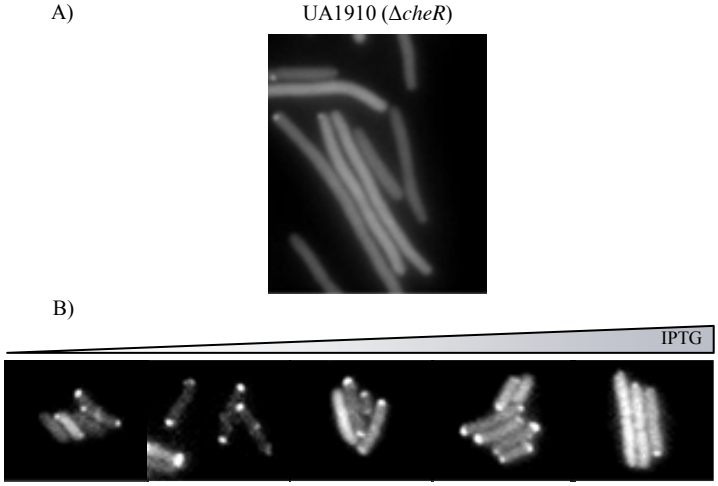

Figure 4.15. Optimization of chemotaxis clusters visualization in S. Typhimurium. A) Fluorescence microscope image at a total magnification of 1000X showing the filamentation and background fluorescence when inducing the *cheY-YFP*:*cheR* fusion expression at 1000 µM IPTG in the Δ*cheR* strain (UA1910). **B)** Induction kinetics in the Δ*cheR* strain harboring the *cheY-YFP*:*cheR* expression vector (UA1910 pUA1127) showing the evolution of structuring and background fluorescence at 10, 20, 30, 75 and 100 µM IPTG. Fluorescence images magnification was of 1000X. All the experiments were performed in duplicates. Images were selected to be representative of entire observation fields.

could be already observed but the fluorescence intensity was very low thus the image acquisition was difficult. At 20 µM IPTG a high amount of cells showed well-shaped polar structures, no filamentation was observed and the background fluorescence was low enough to allow a good differentiation of clusters from the cell body. At 30 µM IPTG polar fluorescent spots

could be observed but with an increased fluorescence intensity and a less rounded shape. Also, at that induction level, a higher background of the cell body was observed and cells tend to be bigger and more elongated. At 75 µM IPTG no significant differences regarding on cell dimensions, cell body fluorescence or polar aggregation was observed when compared to 50 µM IPTG images. Finally, at 100 µM IPTG cells size was clearly bigger than for the rest of concentrations tested indicating that some filamentation could occur. Also, polar structures could not be easily distinguished mainly due to two factors: an increase in the cell body background fluorescence and the decrease in the percentage of cells showing any polar mass.

From this results, it was decided to use 20 µM IPTG as the standard inductor concentration as it gave the best signal to noise ratio for the detection of polar structures in the $\Delta cheR$ strain.

Once the procedure was optimized, the four experimental strains were observed for their structuring profiles. Figure 4.16 shows the five identified clustering patterns found in *S.* Typhimurium. The structuring patters observed matched those previously described by Sourjik and Berg (2000) and Kentner *et al.* (2006) in *E. coli.* The nomenclature used in this study is maintained as in the previously commented works to give a ready comparison to the literature. From more compact to more diffuse, the clustering patterns were classified as follows: a cluster, either polar or lateral (Fig. 4.16 A and C), is defined as a limited diffraction area of well defined round/oval shape. Clusters may exist in single or multimeric forms, being double and triple the only ones observed during the present work (Fig. 4.16 B). A polar cap is defined as a diffused diffraction region located at cell poles mainly of lunar shape (Fig. 4.16 D). Diffused pattern is defined as a non-structured condition where fluorescence is spread across the entire cell body without any outstanding area (Fig. 4.16 E).

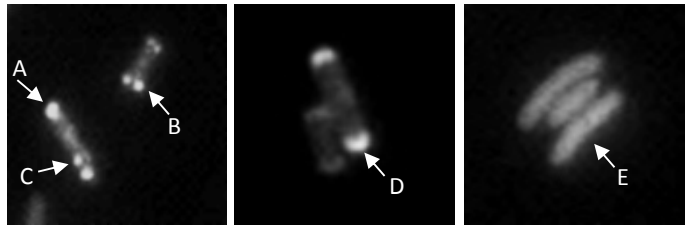

Figure 4.16. Different structuring patterns observed in *S.* Typhimurium. Images above show the different structuring patterns found in *S.* Typhimurium when expressing the *eYFP::cheR* fusion. Nomenclature: A, Single polar cluster; B, double polar cluster; C, lateral cluster; D, polar cap and D; diffused. Fluorescence images magnification was of 1000X. All the experiments were performed per triplicate. Images were selected to be representative of entire observation fields. Reference: Kentner *et al.* (2006).

Using the system optimized here, the amount of cells presenting either one of the previously shown structuring patterns were quantified in order to elucidate if some of the different study strains presented an altered aggregation of the chemoreceptor clusters.

4.4.2 Receptor clustering

Figure 4.17 shows the location of chemotaxis clusters in ATCC 14028 Δ*cheR* (UA1910), Δ*recA* Δ*cheR* (UA1913), *recAo6869* Δ*cheR* (UA1914) and Δ*cheW* Δ*cheR* (UA1915) strains all of them containing the plasmid borne and inducible *eYFP::cheR* fusion (pUA1127).

Strains Δ*cheR* and Δ*cheW* Δ*cheR* showed the expected structuring patterns thus validating the rest of results. The former one, shows clearly defined polar or lateral clusters whilst the latest showed a diffused polar

structuring patterns, arcaps, as previously described by Kentner *et al.* (2006) for an *E. coli* Δ*che* W strain.

Study strains *recAo6869* Δ*che R* and Δ*recA* Δ*che R* were analyzed in the same way. Both strains showed less aggregation than the wild type, specially the *recAo6869* Δ*che R* but both were different than the Δ*che* W Δ*che R* strain.

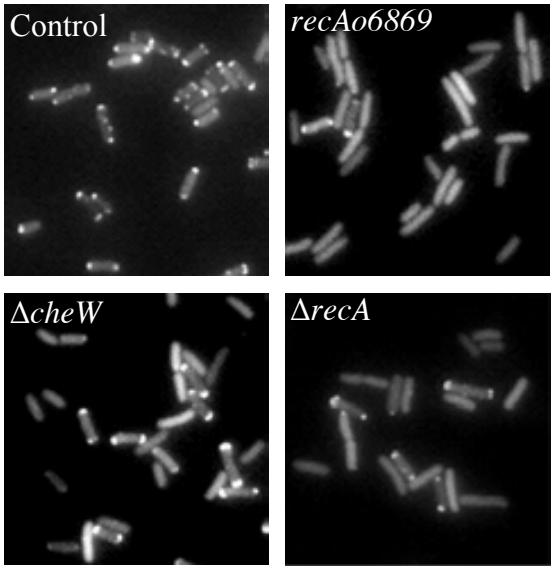

Figure 4.17. Chemotaxis clusters localization in *S.* Typhimurium. Fluorescence microscope images showing the structuring patters found in the *S.* Typhimurium ATCC 14028 strains Control, UA1510; Δ*recA*, UA1513, *recAo6869*, UA1514 and Δ*che* W, UA1512 all of them harboring the pUA1127 plasmid containing the inducible *YFP:che R* fusion. Fluorescence images magnification was of 100X. All the experiments were performed per triplicate. Images were selected to be representative of entire observation fields.

A quantification of the percent cells with clusters for every strain is showed in Figure 4.18. As shown, significant differences are found between the $\Delta cheR$ strain and the rest indicating that some clustering defects were present in study strains.

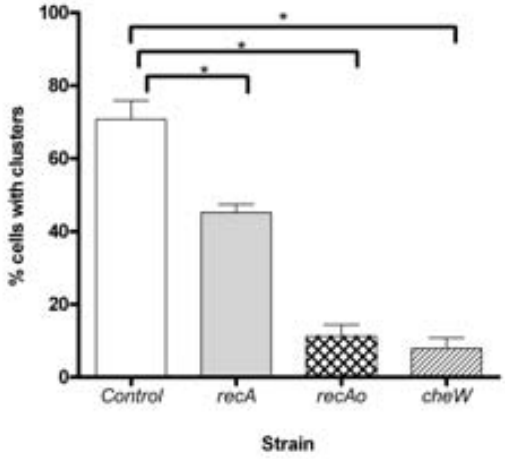

Figure 4.18. Fraction of cells showing well structured polar clusters. Number of cells showing polar round-shaped and diffraction limited spots previously defined as clusters were quantified in *S.* Typhimurium ATCC 14028 strains control (UA1910), $\Delta recA$ (UA1913), *recAo* (UA1914) and $\Delta cheW$ (UA1915). Results are the mean (SD) of three independent imaging experiments. Significant differences ($p<0.001$) amongst two conditions are denoted by the (*) symbol.

The fraction of population able to form clusters for the $\Delta cheR$ strain is 70 %, nearly the 5 % forms caps and approximately a 25 % does not structure at all.

For the $\Delta recA$ $\Delta cheR$, approximately the 45 % of the population is able to form clusters whereas the rest of cells show a diffuse pattern (38

%) or polar caps (17 %). In contrast, only an 11 % of *recAo6869* Δ*cheR* population is able to show structured clusters whereas the vast majority show a diffuse pattern (87 %). Percentage of clustering proficient population for the *recAo6869* Δ*cheR* strain is similar to the percentage obtained for Δ*cheW* Δ*cheR* strain where only 8 % of the population is able to form properly shaped clusters. The difference between them is that in the latter one, the fraction of population able to structure caps raises to 33 % and the diffusion pattern is observed in the 59 % of individuals whereas for the *recAo6869* Δ*cheR* strain, only a 2 % of the population is able to structure caps.

Clustering patterns were quantified, classified and basic statistics were performed for each strain. Results are summarized in Table 4.4.

The average clusters/caps per cell ratio accounts for the high amount of unstructured individuals present in the *recAo6869* Δ*cheR* population while in the Δ*cheR* and Δ*recA* Δ*cheR* strains every cell shows, on average, at least one cluster/cap. Strain Δ*cheW* Δ*cheR* is quite distinct and only 2 out of 3 cells have some observable structuring.

A more detailed analysis was conducted to account for differences in the kind of structures formed in every strain. Independently of the strain, the vast majority of clusters or caps counted were found to localize at cell poles. The Δ*cheR* strain cells showed all the reported structures but the 81 % of counted structures were polar clusters. The Δ*recA* Δ*cheR* strain also showed every structure but in contrast to what previously seen for the Δ*cheR* strain, only the 55 % of structures were found to be clusters while nearly a 30 % were the more unstructured caps. Even though little clustering is shown by the *recAo6869* Δ*cheR* strain when compared to the Δ*cheR* strain population, calculated percentages are quite similar. Approximately 77 % of counted structures were polar clusters while caps accounted only for

a 13.5 % of the overall structures quantified. The $\Delta cheW$ $\Delta cheR$ cells are clearly different from the rest. Approximately 86 % of structures quantified were found to be polar caps while single polar clusters abundance is of only 11.5 %.

Three out of every four cells of the reference $\Delta cheR$ (UA1910) strain of *S.* Typhimurium showed polar clustering. Of these structures, the vast majority were found to be well shaped polar clusters. On the other hand, cells overexpressing *recA* (*recAo6869* $\Delta cheR$) showed a dramatic decrease in the aggregation ability, not only to form well shaped polar clusters but also caps. This is supported by the fact that nearly 9 out of 10 cells quantified failed into show any cap or cluster. In cells lacking *recA* ($\Delta recA$ $\Delta cheR$), data obtained also pointed towards a depletion of the aggregation ability but the effects were less severe than in cells overexpressing *recA*.

When put together, this results indicate that either the overexpression or the lack of RecA have a negative effect on the chemoreceptor aggregation ability of *S.* Typhimurium. The excess of RecA have the more dramatic effects in the depletion of the ability to form polar chemotaxis clusters and, in fact, nearly no clusters or caps are formed in that conditions. The lack of RecA also have a depleting effect over cluster formation but in a milder way than the observed for RecA excess. In this case, aggregation is still possible in approximately the half of the population but the ability to form polar clusters is clearly depleted when compared to the $\Delta cheR$ control strain.

Table 4.4. Receptor clustering statistics.

Strain	**UA1910**	**UA1913**	**UA1914**	**UA1915**
Genetic background	$\Delta cheR$	$\Delta recA\ \Delta cheR$	$recAo6869\ \Delta cheR$	$\Delta cheW\ \Delta cheR$
Counted cells	1071	1192	1487	1183
Clusters/caps	1228	1151	232	779
Clusters/caps per cell	1.15	0.97	0.16	0.66
Cells without clusters/caps	261 (24.4%)	458 (38.4%)	1303 (87.6%)	718 (60.7%)
Cells with clusters/caps	810 (75.6%)	734 (61.6%)	184 (12.4%)	465 (39.3%)
Polar clusters/caps	1122 (91.4%)	1072 (93.1%)	224 (96.6%)	772 (99.1%)
Single	910 (81.1%)	630 (54.7%)	173 (77.2%)	89 (11.5%)
Double	138 (12.3%)	110 (9.6%)	21 (9.4%)	22 (2.8%)
Triple	7 (0.6%)	4 (0.3%)	0 (0%)	0 (0%)
Caps	67 (6%)	328 (28.5%)	30 (13.4%)	661 (85.6%)
Lateral clusters	106 (8.6%)	79 (6.9%)	8 (3.4%)	7 (0.9%)

4.5 Chemotactic behavior of *S.* Typhimurium *recA* mutants

Results presented above show that strains with variations in the *recA* gene expression presented swarming deficiencies and distinct degrees of affectation in the aggregation ability to properly form the chemotaxis clusters. If the correct aggregation of the chemotaxis clusters is affected, it might be expected some affectation of the chemotactic ability of these strains.

Following the capillary method initially described by Adler (1973), the present work focused on the capacity of *S.* Typhimurium to move towards a gradient of L-aspartate to evaluate the chemotactic response of several study strains.

Figure 4.19 shows the quantitative results obtained from the chemotaxis assays conducted for the wild type *S.* Typhimurium ATCC 14028 and the *recAo6869* (UA1876), Δ*cheW* (UA1908), Δ*recA* (UA1912) and Δ*cheY* (UA1926) mutant strains.

Surprisingly, at the usual conditions used for chemotaxis assays (1 hour at 30 °C) both the wild type and the *recAo6869* strains showed a positive chemotactic behavior towards aspartate. This result was unexpected as the *recAo6869* strain showed a very low degree of aggregation of the chemotaxis receptor clusters and thus was expected to have a reduced chemotactic ability. Due to this results, it was decided to evaluate if the affected parameter was the chemotactic response rate instead of the chemotactic ability itself. This is, the ability of a given strain to quickly respond to an attractant.

To put light into this fact, a shorter experiment using a 10 minutes at 30 °C incubation step instead of the commonly used 1 hour at 30 °C was performed. Results show that, whereas the wild type strain was significantly more attracted to the aspartate than to the buffer at shorter times, the

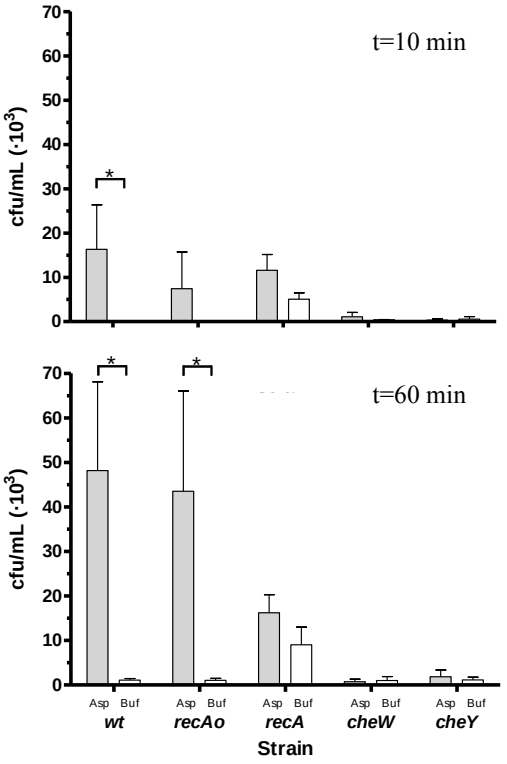

Figure 4.19. Chemotactic response of *S.* Typhimurium *recA* mutants. Chemotactic response of the *S.* Typhimurium ATCC 14028 wild type (wt); Δ*recA*, UA1912; *recAo*, UA1876; Δ*cheW*, UA1908 and Δ*cheY*, UA1926 strains expressed as the number of cfu/mL found inside a capillary tube containing either 10 mM aspartate or tethering buffer alone. Incubations were performed at 30 °C for 10 or 60 minutes. Results are the mean (SD) of two independent experiments of three capillaries each. Significant differences ($p<0.001$) amongst two conditions are denoted by the (*) symbol.

recAo6869 strain was not. This indicates that the *recAo6869* strain might have some deficiency in the chemotaxis ability but also that this impairment would not be phenotypically expressed through the absolute chemotactic ability but through the chemotactic response rate.

The $\Delta cheW$ and the $\Delta cheY$ strains were used as negative chemotaxis controls. As shown, neither one was attracted by the aspartate gradient and thus both have an impaired chemotactic ability.

The $\Delta recA$ strain have a more complex behavior as shown by the chemotaxis assays. The amount of bacteria attracted by the aspartate was not significantly different than the amount found in buffer-containing capillaries but the amount of bacteria found in the later ones was abnormally high when compared with the rest of the values obtained. This behavior was reproducible throughout several experiments and cultures.

Chapter 5

Discussion

5.1 Swarming motility is linked to the SOS system through the interaction between RecA and CheW proteins

Previous studies conducted by Medina-Ruiz (2012) using a two-hybrid assay system showed that CheW and RecA were able to interact *in vivo* when overexpressed in *E. coli,* however two-hybrid results alone are not conclusive enough to state a direct interaction between the two assayed proteins. Results obtained in this work demonstrate that a true interaction occurs between CheW and RecA proteins through two independent yet related procedures, a far-Western blot and a co-immunoprecipitation. Data acquired from the far-Western blot assay demonstrate that, *in vitro*, the purified RecA is able to interact with purified and immobilized CheW in controlled conditions (Figure 4.3). These results point towards a direct interaction rather than a complex contact involving other bridge proteins. Neverthe-

less a more complex protein structure formed after an initial CheW-RecA interaction could not be discarded as it may be required in order to stabilize the initial contact. Such complexes could be observed *in vivo* to stabilize weak protein-protein contacts (Fuentes *et al.*, 2005; Ozbabacan *et al.*, 2011).

To test for CheW-RecA interaction under approximately naive conditions, a co-immunoprecipitation using a whole-cell lysate form a *S.* Typhimurium mutant strain carrying the *cheW::FLAG* allele was performed. It should be noticed that, in such strain, both *cheW* and *recA* genes are expressed at their endogenous levels and surrounded by the common environment where the contact presumably occurs. Results obtained from this experiment unambiguously demonstrate the interaction of CheW and RecA under natural conditions in *S.* Typhimurium (Figure 4.4). In this case a complex contact involving not only RecA and CheW but also other proteins can not be discarded as a crude extract of *S.* Typhimurium was used.

Put together, all the results presented in this work unequivocally demonstrate the interaction between CheW and RecA proteins both *in vivo* and *in vitro.* However, the exact stoichiometry of the interaction and the overall number of proteins involved in remains unclear and should be further investigated.

A simple protein docking conducted *in silico* (Figure 4.5) reinforced this findings as apparently a stable contact between both proteins could be found using such a theoretic physicochemical approach. The putative contact region identified on the CheW structure falls with a high probability within a free and solvent-exposed domain that is not involved neither in CheA nor in MCPs contacts (Boukhvalova *et al.*, 2002a; Vu *et al.*, 2012; Li *et al.*, 2013). Further efforts should be done to better determine the RecA

and CheW regions and residues directly implicated in the contact and this results should be taken only as an orientation.

If a more systemic approach is used, the present work provides the confirmation of the link between two important cell systems: the SOS and the chemotaxis systems. It is known that the lack of *recA* causes a depletion of the swarming ability in *E. coli* (Gómez-Gómez *et al.*, 2007). Also, previous work conducted in our laboratory succeeded in demonstrate that the overexpression of *recA* also caused a depletion of the swarming ability in *S.* Typhimurium (Medina-Ruiz *et al.*, 2010). These two facts pointed towards an interaction between the SOS system and the chemotaxis apparatus via RecA. In this work, the RecA and CheW interaction has been demonstrated and, although not fully defined, it directly implies the confirmation of this new link between the SOS and the chemotaxis systems governing the cell motility in *S.* Typhimurium that was previously reported using phenotypic approaches.

5.2 *S.* Typhimurium swarming ability is modulated by the RecA/CheW stoichiometry in a strain-dependent fashion

As any protein-protein interaction, the amount each protein required to achieve a correct and stable contact might be limited and thus, the excess or lack of any of the constituents of the protein complex may lead to instability and lately to the interaction break down. The importance of the stoichiometry issue has been exemplified in the introduction of the present work (Section 1.2.2.2) for the chemoreceptor signaling arrays structuring. Regarding the importance that the absolute amount of each constituent

have in the formation of protein complexes, it may also have a key role in the RecA/CheW interaction although the molecular basis for this contact is already unknown.

In this work, efforts have been done to evaluate the cellular stoichiometry that exists between RecA and CheW when cells grow under swarming promoting conditions. As a result, the tolerance intervals for swarming motility of the *S.* Typhimurium strains *cheW::FLAG* (UA1916) and *recAo6869 cheW:FLAG* (UA1917) are reported (Section 4.2.2).

Quantifications have demonstrated that in the absence of inductor, the relative motility of the *cheW::FLAG* strain either carrying the *recA* (pUA1129) or *cheW::FLAG* (pUA1128) overexpression plasmid is approximately 1 and thus no difference is observed when compared to the same strain with the empty vector (pUA1108). From that point on, both strains showed distinct behaviors as the inductor levels rose.

When overexpressing *recA*, the *cheW::FLAG* strain showed a dramatic depletion of swarming ability at lowest levels of induction and the relative movement rapidly falls around a third of the motility shown by same strain but carrying the empty expression vector. No substantial variation in relative movement is observed as the inductor concentration increases indicating that a plateau state is quickly reached at very low IPTG concentrations (Section 4.2.2.1). This behavior matches well with the RecA quantification profile obtained from this strain (Section 4.2.2.2.2). This expression profile explains the observation of the non-progressive loss of swarming ability through the IPTG interval tested.

In contrast, when overexpressing *cheW::FLAG*, the *cheW::FLAG* strain showed a more progressive depletion of swarming ability being necessary to reach higher induction levels to completely abolish the swarming. At low IPTG concentrations, the relative motility of this strain nearly matched the

one observed for the same strain but with the empty expression vector, indicating a certain tolerance to CheW amount variation. Then, the relative movement decreased gradually as CheW concentration increased until the minimum movement value was reached. As observed before, this phenotypic behavior matches well with the *cheW::FLAG* expression profile. In contrast to what happened when overexpressing *recA*, in this case a progressive increase in the *cheW::FLAG* amount is detected and it correlates well with the depletion of swarming ability.

These findings show that the swarming behavior of the *cheW::FLAG* strain is closely linked to the RecA and CheW::FLAG amounts. It is observed that two distinct expression profiles (for *recA* and *cheW::FLAG*) gave two distinct phenotypic patterns confirming the link between protein expression and phenotypic behavior. Also, it is shown that the swarming motility is abolished as protein concentration increases and that if no variation in protein amount occurs, no substantial variation in the swarming capability is observed (as in the case of *recA* expression at high IPTG concentrations). This confirms the previously stated link between the SOS system and the chemotaxis apparatus via the modulation of the cell displacement capability by the RecA/CheW relationship.

Regarding the previously discussed arguments, swarming capability could be defined through the RecA/CheW ratio. For the *cheW::FLAG* strain harboring the empty expression vector, the amounts of RecA and CheW::FLAG were found to be approximately equal throughout the whole IPTG range tested and thus, a ratio of 1 is constantly observed in the assayed conditions. In this case, when the ratio is approximately 1, the swarming ability of the *cheW::FLAG* strain was found to be the same than the wild type strain. When the same strain harbored the *recA* overexpression vector, the ratio greatly increased towards RecA excess as expected. The last ratio

where the strain harboring the *recA* overexpression vector showed a positive swarming phenotype was of approximately 30. On the other hand, when the *cheW::FLAG* strain harbored the *cheW::FLAG* overexpression vector, the ratio rapidly decreased towards CheW excess, also as expected. Consistent with previously published results, the excess of *cheW::FLAG* caused the abolition of the swarming motility (Liu and Parkinson, 1989; Sanders *et al.*, 1989b; Cardozo *et al.*, 2010) and in this case, the last ratio where the strain was found to be swarming capable was of 0.01. Together, this data defines the interval [30-0.01] for the RecA/CheW ratio as the range where the *cheW::FLAG* strain shows a positive swarming phenotype whereas out of that specific interval the swarming movement is dramatically depleted. A possible model that explains the importance of the stoichiometric relationship between these two proteins is extensively discussed in section 5.5 but, in summary, RecA would participate in the structuring of the chemoreceptor signaling arrays by forming part of them through its ability to bind CheW.

A proof of concept is also presented in this work to confirm the link between CheW::FLAG and RecA. Results obtained from a complementation experiment have clearly demonstrated that the swarming phenotype could be restored by overexpressing the *cheW::FLAG* allele in a strain that constitutively expresses *recA* (*recAo6869 cheW::FLAG*) and therefore shows a swarming deficient phenotype.

The *recAo6869 cheW::FLAG* strain harboring the empty expression vector showed to be unable to swarm in the whole induction interval thus confirming that the overexpression of *recA* causes the depletion of the swarming ability. RecA and CheW quantifications in this strain showed constant levels of both proteins and thus, the ratio between them remains constant around 500 throughout the whole IPTG range tested. In contrast, the

same strain but harboring the *cheW::FLAG* overexpressing vector showed constant RecA concentration but the CheW::FLAG amount increased as the IPTG concentration does. Surprisingly, quantified ratios in this strain fall within the range [2-0.15]. As shown above, if the ratio between RecA and CheW falls within a range of [30-0.01], the strain is supposed to be swarming capable but the *recAo6869 cheW::FLAG* strain overexpressing the *cheW::FLAG* allele only recovers the swarming phenotype when the ratio is around 0.3. This fact points towards a strain dependency of the RecA/CheW ratio controlling the swarming motility.

Also, as briefly reviewed in the introduction of the present work (Section 1.4), the RecA protein has been related to several cellular processes, mainly the induction of the SOS system and recombination functions but also the modulation of the swarming motility. Thus, it could be hypothesized that the tightest tolerance interval found in the *recAo6869 cheW::FLAG* strain may be due to the constitutive expression of the *recA* gene itself that gives place to a cellular state only able to tolerate narrower stoichiometry variations than its wild type counterpart. Further work is needed to elucidate the effects that unbalanced genetic backgrounds potentially have over the tolerated RecA/CheW stoichiometries.

Results presented here, demonstrate that the swarming ability of *S.* Typhimurium is clearly influenced by the existing balance between RecA and CheW and therefore, the SOS system is responsible of a certain degree of modulation over the swarming ability. While the interaction between the SOS system and the chemotaxis apparatus (through RecA and CheW proteins respectively) have been unequivocally demonstrated in this work, it has also been reported that this link is influenced by the strain type itself. Thus, as demonstrated by the previously presented RecA/CheW ratios, a universal swarming tolerance interval for *S.* Typhimurium could not be de-

fined but particular tolerance intervals might be defined for each strain. To maintain the RecA/CheW equilibrium within the tolerance interval is a necessary condition to swarm as demonstrated by the phenotypic complementation experiments carried using the *recAo6869 cheW::FLAG* strain.

5.3 The locus *ysdAB* contributes to Δ*lexA* lethality in *S.* Typhimurium

The Δ*lexA* mutation in *S. enterica*, in contrast to what happens in *E. coli*, is known to give a lethal phenotype even in a Δ*sulA* background (Bunny *et al.*, 2002). It has been showed that the induction of a subset of genes contained within the Fels-2 prophage was the primarily responsible of the Δ*lexA* lethal phenotype displayed by an *S.* Typhimurium strain LT2. Moreover, both Gifsy-1 and Gifsy-2 phages showed to have a negative effect over a *S.* Typhimurium Δ*lexA* mutant strain growth as they are apparently destabilized in the absence of LexA (Bunny *et al.*, 2002).

The molecular mechanism by which the three prophages seem to impair *S.* Typhimurium growth in the absence of LexA was related to the presence of an homologous of the *tum* cI antirepressor of the coliphage 186 in all three of these phages. The *tum* homologous genes found in the three *Salmonella* phages include a putative LexA binding site in their promoter regions (Bunny *et al.*, 2002). For a coliphage 186 developing a lysogenic cycle, the LexA protein of the host cell is blocking the *tum* antirepressor expression. If LexA protein is absent or at sufficient low concentrations (for example by SOS induction), the *tum* expression raises and the Tum protein acts against the CI repressor releasing the expression of the genes related to the lytic cycle (Shearwin *et al.*, 1998). In *S.* Typhimurium LT2 the behavior

is homologous to the one explained for coliphage 186. When LexA is absent (due to a *lexA* null mutation), a partial induction of some subset of genes, mainly from the Fels-2 prophage and whose products might restrict the cell growth, is hypothesized to occur through a Tum antirepressor mediated pathway and thus the cell viability is dramatically affected. The behavior is considered to be the same for the Gifsy phages (Bunny *et al.*, 2002).

In this work, it was of interest to develop an *S.* Typhimurium strain ATCC 14028 Δ*lexA* mutant to evaluate the swarming behavior of *S.* Typhimurium under SOS induction conditions but avoiding the treatment with any damaging agent that could potentially develop a masking effect. By applying the previously explained knowledge, an ATCC 14028 strain carrying a Δ*sulA* background and lacking both Gifsy phages was used to generate a Δ*lexA* mutant by transduction. It should be noticed that, by contrast to LT2 strain, the ATCC 14028 strain naturally lacks the Fels-1 and Fels-2 prophages (Jarvik *et al.*, 2010). Surprisingly a very low efficiency of transduction of the Δ*lexA* mutant allele on this strain was obtained and thus it pointed towards other factors involved in the *lexA* null lethality apart from the prophages.

The sequencing of the LT2 Δ*lexA* mutant strain (UA1685) available in our laboratory that was conducted in this work allowed the identification of the *ysdAB* locus as a potential candidate to secondary lethality factor in *S.* Typhimurium Δ*lexA* mutants. Site directed mutagenesis and transduction assays have confirmed that the inactivation of this locus greatly increases the transduction efficiency of the Δ*lexA* mutant allele (unpublished results). Although further work is needed to precisely quantify and elucidate the implication of *ysdAB* in the lethal phenotype of the Δ*lexA* mutants of *S.* Typhimurium, this locus displays more than a 90 % identity with the *E. coli tisAB* locus whose toxic effects are already known (Vogel *et al.*, 2004;

Darfeuille *et al.*, 2007; Unoson and Wagner, 2008; Weel-Sneve *et al.*, 2008). In *E. coli*, the *tisAB* locus (*ysdAB* in *Salmonella*) encodes a SOS-controlled bicistronic operon formed by two overlapped open reading frames: *tisA* and *tisB* (Fig. 5.1).

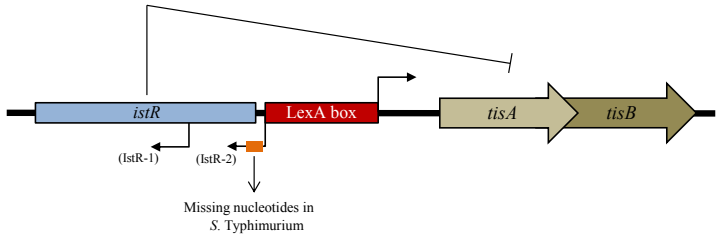

Figure 5.1. *E. coli tisAB/istR* locus chromosomic organization. Schematic representation of the *E. coli* chromosomic region showing the *tisAB* and *istR* loci arrangement. The IstR-1 small RNA is the responsible of targeting the *tisAB* mRNA for inactivation through an RNAse III-driven process. The small orange box in the *istR-2* small RNA transcription initiation site shows the schematic location of the missing nucleotides in *S.* Typhimurium that potentially affect the *istR* locus expression.

Of them, the translation of TisB but not TisA was proved to confer toxicity through cell growth arrest (Courcelle *et al.*, 2001; Vogel *et al.*, 2004; Darfeuille *et al.*, 2007). TisB is thought to localize at the inner membrane thus affecting the membrane integrity. In fact, the energy supply in form of ATP is severely impaired upon insertion of TisB into the membrane (Unoson and Wagner, 2008). Regulation of the *tisAB* locus is achieved through an small RNA system located upstream of the *tisAB* locus but on the opposite direction (Fig. 5.1). This small RNA locus is called *istR* and comprises the coding sequence for two RNA molecules. The first one,

istR-1, is not SOS controlled and its function is to target the *tisAB* mRNA for cleavage through an RNAse III coupled mechanism thus inhibiting the TisB translation (Vogel *et al.*, 2004; Darfeuille *et al.*, 2007). The second one, called *istR-2*, is under the control of the the SOS system through the same LexA box that exists for the *tisAB* operon and contains the entire *istR-1* coding sequence. Its role in *tisAB* expression regulation still remains unknown (Vogel *et al.*, 2004; Dörr *et al.*, 2010).

The biological significance of this toxin-antitoxin system remains controversial. In *E. coli*, it is known that the *tisAB* operon have several interferences in distinct SOS response processes. For example, the overexpression of the *tisAB* locus leads to a delay in the expression of some other genes of the system (e.g. *recA*), inhibits the classical cell filamentation observed upon SOS induction and interfere with some prophage life cycle (Weel-Sneve *et al.*, 2008). Furthermore, the TisB peptide has been linked to the formation of persisters (dormant cells highly tolerant to antibiotics and other damaging agents) in a SOS-regulated fashion to increase the population survival rate in a concomitant strategy with the active repair processes that occur during SOS induction (Dörr *et al.*, 2010).

Although the *tisAB* system is well defined in *E. coli*, little is known about the importance it could have in other bacteria. As aforementioned, the *S.* Typhimurium strain LT2 *ysdAB* locus show a great percent identity to its *E. coli* homologue and in both cases the genetic organization is also similar (Vogel *et al.*, 2004). The *ysdAB* locus in *S.* Typhimurium is also a bicistronic operon and apparently a SOS box could be identified between the -10 and -35 boxes of the promoter region. The locus corresponding to the *istR* small RNAs coding sequence could be also found but some nucleotides are missing in the *istR* transcription initiation site (Vogel *et al.*, 2004) thus

potentially affecting their expression. The same organization and features are found in the *S.* Typhimurium ATCC 14028 strain.

The differences mentioned above may indicate important differences in the regulation/expression of this locus between *E. coli* and *S.* Typhimurium and thus, its role in each specie may differ. A proof of this different role is obtained through the analysis of Δ*lexA* mutants of both species. As mentioned, while in *S.* Typhimurium a Δ*lexA* mutation causes a lethal phenotype only corrected by the lack of *sulA*, the Fels and Gifsy phages and the *ysdAB* locus as demonstrated in this work, the *E. coli* Δ*lexA* mutant strains are viable by only knocking-out the *sulA* gene (Bunny *et al.*, 2002; Vogel *et al.*, 2004).

Further work is needed to deeply understand the role of this toxin-antitoxin system in *S.* Typhimurium but it could be hypothesized that a miss-regulation of the *ysdAB* expression due to a putative lack of expression of the small *istR* RNAs might be at the core of the lethality phenotype produced in *S.* Typhimurium upon *ysdAB* induction.

5.4 The SOS system induction under non-stress conditions blocks the swarming motility

The induction of the SOS response with the DNA-damaging agent mitomycin C have been reported to inhibit the swarming motility in *S.* Typhimurium. Concretely, the overexpression of the *recA* gene, which is up-regulated during the SOS response, have been identified as the factor responsible of this inhibition (Medina-Ruiz *et al.*, 2010). As mentioned, one of the most concerning elements of these findings is the use of damaging agents such as mitomycin C that could mask the true effect of the induc-

tion of the SOS system over the swarming motility behind the potentially toxic effects derived of their use.

Results presented in this work clearly demonstrate that an *S.* Typhimurium ATCC 14028 Δ*lexA* (UA1925) strain, with a constitutively induced SOS response, is unable to swarm when compared to its parental and wild type counterparts. This indicates that the induction of the SOS response itself rather than the intrinsic toxicity produced by the damaging agents used to trigger it, is the responsible of the swarming inhibition in *S.* Typhimurium.

Previous works have clearly defined the excess/lack of the RecA protein as the key element abolishing the swarming motility either in *E. coli* or in *S.* Typhimurium (Gómez-Gómez *et al.*, 2007; Medina-Ruiz *et al.*, 2010). The *recA* gene is part of the SOS system and it is up-regulated during SOS response thus, the excess but not the lack of RecA is a condition naturally achievable under certain stress conditions (Courcelle *et al.*, 2001; Erill *et al.*, 2007). During a naturally occurring SOS response caused by the presence of ssDNA originated from any DNA damage, the activated (RecA*) and non-activated forms of the RecA protein are expected to coexist in the cell (Janion, 2008). In the *S.* Typhimurium Δ*lexA* strain, the presence of ssDNA originated from DNA damage is not expected as no DNA damaging agent is used to trigger the SOS response and thus it could be hypothesized that the non-activated RecA fraction could be also here the responsible of the inhibition of the swarming motility as previously reported by the work of Gómez-Gómez *et al.* (2007) in *E. coli.*

5.5 Chemotaxis receptor clustering is affected by RecA concentration

Aside from demonstrating that the RecA concentration and the RecA/CheW balance are essential for the swarming motility in *S.* Typhimurium, to elucidate the molecular mechanism by which variations in the RecA concentration severely impairs the swarming ability of this bacteria was one of the main objectives of the present work.

Up to date, it has been demonstrated in *E. coli* that having the correct structuring of the chemoreceptor arrays involves the creation of a stable complex between several proteins, among others, the MCPs (Methyl-accepting Chemotaxis Proteins), the histidine kinase CheA and the coupling protein CheW (Sourjik and Berg, 2000). Preferentially, new clusters appear to be formed laterally and, upon several cell division rounds, they become polar (Thiem *et al.*, 2007; Thiem and Sourjik, 2008).

It has been shown that variations in the stoichiometry of the proteins forming the chemoreceptor clusters lead to abnormal structuring patterns. For example, *E. coli* knock-out mutants for the CheW coupling protein were able to structure chemotaxis receptors arrays but in a less compact fashion when compared to a wild type strain (Maddock and Shapiro, 1993; Kentner *et al.*, 2006). On the other hand, high levels of CheW lead to the total disruption of chemotaxis clusters (Cardozo *et al.*, 2010). Similarly, the absence of CheA lead to reduced polar clustering but its presence greatly enhances the polarity and the clustering of the chemoreceptor arrays (Maddock and Shapiro, 1993; Skidmore *et al.*, 2000).

In this work, it has been demonstrated that both the overexpression or the lack of RecA had a dramatic effect over the chemotaxis clustering process. The results presented here indicate that the lack of RecA is not

equivalent to the excess of the same protein despite of having the same phenotypical effects, the inhibition of swarming behavior. The *recAo6869* mutants (excess of RecA) showed a significant difference in their ability to structure chemotaxis clusters when compared to the $\Delta recA$ mutants. The origin of this difference is not yet fully understood and several hypothesis could explain this behavior. The most plausible explanation to this difference may be obtained through a direct participation of RecA in the structuring of the chemotaxis clusters. The dynamics of cluster formation when RecA amount is modified is similar to the one observed upon CheW amount variations. If an excess of RecA is present, a complete disruption of the clusters occurs (as when overexpressing *cheW,* Cardozo *et al.* 2010) while if RecA is absent, a partial disruption also occurs but the more interesting fact is that the percent population showing less aggregated structures (caps) in that case greatly increases when compared to the wild type strain as happens in $\Delta cheW$ mutants (Kentner *et al.*, 2006). Put together this results indicate that RecA plays a central role in the structuring of the chemoreceptor clusters through its interaction with CheW. This hypothesis may be supported by some the experiments conducted up to date. Results published by Garvey *et al.* (1985) pointed towards a localization of RecA (activated or not) at the cell membrane of *E. coli.* Also, it was shown that RecA is able to interact with two of the major acidic phospholipids found in the *E. coli* membrane and that this situation leads to changes in its function (Krishna and van de Sande, 1990). More recently, fluorescence microscopy experiments showed that GFP fusion variants of the RecA protein were located at the cell poles in *E. coli* and in *B. subtilis* (Kidane and Graumann, 2005; Renzette *et al.*, 2005). Supporting this observation, recent work conducted by Rajendram (2013) reported the localization of RecA primarily at the cell poles in line with previous observations.

A molecular model to explain the role of RecA in the structuring of the chemoreceptors signaling arrays is proposed in this work (Figure 5.2).

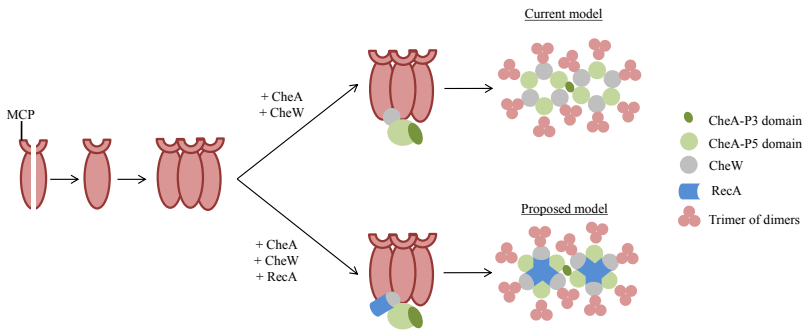

Figure 5.2. Molecular model for receptor clustering. Schematic representation of the current accepted model for the chemoreceptor arrays structuring and the proposed model involving the participation of the RecA protein, as derived from the observations showed in the present work.

The model showed below has been derived from the observations made in both the structuring (see above) and the stoichiometry (Section 5.2) fields. In this model, RecA would be a part of the signaling teams composed by the MCPs trimer of dimers, CheA and CheW through its interaction with the former one. These signaling teams are then packed in the hexagonal lattice as described in section 1.2.2.2. An excess of RecA (as in the *recAo6869* strains) would prevent the formation of the correct contacts between the proteins finally leading to the complete disruption of the chemoreceptor arrays. As reported for CheA and CheW (Skidmore *et al.*, 2000; Zhang *et al.*, 2004; Kentner *et al.*, 2006), the presence of RecA would not be essential for

the formation of the signaling arrays as a Δ*recA* mutant of *S.* Typhimurium is able to show a certain structuring degree. However, its presence would be required to obtain a full functionality of the arrays in terms of regulation of the swarming motility.

Apart from the structuring issues reported above, both of the *recA* mutant strains tested in this work were completely unable to swarm. A direct and clear link between the difficulty in structuring the chemoreceptor signaling arrays and inability to swarm can be established. As the swarming behavior is known to rely on several factors, including those related to the environment (Wang *et al.*, 2005; Partridge and Harshey, 2013a,b) that usually tend to generate complex situations, the swarming phenotype displayed by the *recA* mutant strains may require a more complex explanation involving several factors but within them, the clustering deficiency shown here undoubtedly play a central role.

5.6 Chemotactic response of the *recAo6869* mutant strain is affected

It has been reported that mutants for the *che* genes, such as the Δ*cheW* and Δ*cheA*, display defects in cluster structuring leading to a less compact or unstructured chemoreceptor arrays (Maddock and Shapiro, 1993; Kentner *et al.*, 2006). Furthermore, *che* mutants of *E. coli* and *S.* Typhimurium have been widely characterized and usually display a non-swarmer and non-chemotactic phenotype (Aswad and Koshland, 1975; Parkinson, 1976, 1978; Liu and Parkinson, 1989; Sanders *et al.*, 1989b; Harshey and Matsuyama, 1994; Boukhvalova *et al.*, 2002b) thus a clear link might be established between the cluster structuring and the chemotactic ability of these species.

Hence, the disruption of the chemoreceptor clusters observed in the *recA* mutants, and concretely in the *recAo6869* mutant strain, could also lead to defects in their chemotactic ability.

When assessing the 1-hour chemotactic response of the *recAo6869* (excess RecA) and the Δ*recA* mutant strains, only the second one failed to show any chemotactic ability. In a short-time chemotaxis experiment conducted with the same strains, the wild type strain demonstrated a significant chemotactic response whereas the test with the Δ*recA* mutant strain failed to show any difference again thus indicating that differences observed for long experiments could also be reproduced at short times but in a less reliable fashion. Nevertheless, the *recAo6869* strain showed no significant chemotactic response at short times in contrast to what was found for the 1 hour experiment. This data might indicate that the *recAo6869* strain is more likely to have a defect in the response rate instead of in its chemotactic ability.

Altogether this data also indicates that the chemoreceptor clustering is not essential for the chemotaxis as the *recAo6869* display a non-structured clustering pattern but a positive chemotactic profile. To explain this, it could be hypothesized that the excess of RecA in the *recAo6869* strain abolishes the formation of the chemoreceptor cluster arrays by associating to the cell membrane (Discussed in section 5.5) but that the delocalized chemoreceptor clusters still retain their activity, at least partially, thus allowing the detection of chemical gradients. This would represent a novel idea apparently challenging the currently established knowledge.

Another non-contemptible hypothesis might be that the response observed in the *recA* mutant strains was an artifact produced by the fraction of the population that showed well-structured chemotaxis clusters. As described by Adler (1973) when reporting the data for the capillary method

he developed, the chemotactic response measured using the capillary assay is sensitive to the initial inoculum of cells in an hyperbolic fashion. As shown in the results (Section 4.4.2, Table 4.4) the population of either *recAo6869* or Δ*recA* strains are non-homogeneous for the clustering pattern and thus the capillary assay is likely to fail when assessing for differences in the chemotactic ability of non-axenic cultures (or strains) like in this case.

Further work is needed to elucidate the role of *recA* and the implication of the clustering state over the chemotaxis ability as the results presented here are not conclusive enough. Also, complementary methods should be explored to clearly elucidate the chemotactic pattern displayed by the *recA* mutant strains, specially the Δ*recA* knock-out mutant which displays abnormal high rates of cells inside the capillary in the absence of aspartate. This abnormal chemotaxis pattern is not due to the CW bias observed in this strain (unpublished results) as the CW-biased mutant Δ*cheB* shows the same chemotaxis pattern that the one displayed by the CCW-biased Δ*cheY* or Δ*cheW* mutants (Mariconda *et al.*, 2006; Martínez *et al.*, 2013, and our unpublished results).

Chapter 6

Conclusions

1. The far-western blot and co-immunoprecipitation assays demonstrate that RecA and CheW proteins of *S.* Typhimurium interact both *in vivo* and *in vitro*.

2. The molecular ratio between RecA and CheW in *S.* Typhimurium wild type cells growing over semi-solid agar plates is of 1. The swarming motility is supported in this strain when the molecular ratio RecA/CheW falls within the interval [30-0.01].

3. The lack of swarming motility in a *recAo6869* strain, that constitutively expresses *recA* and thus it is swarming deficient, is phenotypically complemented by the overexpression of *cheW*. The swarming motility is reestablished when the RecA/CheW molecular ratio is of [2-0.15].

4. The whole genome sequencing of the *S.* Typhimurium LT2 Δ*lexA* mutant lead to the identification of three loci potentially involved in the *lexA* knock-out lethality: *ysdAB*, *sicP* and *crp*. Of them, only

the *ysdAB* locus has a direct implication in the lethality of the *S.* Typhimurium Δ*lexA* mutants. A knock out strain for this locus is far more proficient inheriting a Δ*lexA* allele than its isogenic counterpart.

5. The whole genome sequencing of the *S.* Typhimurium LT2 Δ*lexA* mutant strain and posterior experiments conducted on phage free cell backgrounds have confirmed that the absence of the Gifsy prophages, especially the Gifsy-2, and the Fels prophages, especially the Fels-2 is an essential condition to obtain a *lexA* knock-out strain.

6. The deregulation of the SOS system through a *lexA* knock out mutation inhibits the swarming motility of *S.* Typhimurium.

7. The absence and the variation of the RecA protein concentration cause a dramatic disruption of the chemoreceptor clusters. For the *S.* Typhimurium *recAo6869* Δ*cheR* strain, that constitutively expresses *recA*, only an 11 % of the population is able of structuring clusters whereas in the Δ*recA* Δ*cheR* strain, a 45 % of the population show well-structured clusters.

8. The inactivation of the *recA* gene causes a severe depletion of the chemotactic response of *S.* Typhimurium.

9. Despite the depletion of the chemoreceptor cluster structuring in the *S.* Typhimurium *recAo6869* strain, its absolute chemotactic ability remains at the same levels than those displayed by the wild type strain.

10. The RecA protein is proposed as a component of the chemoreceptor signaling arrays alongside with the MCPs, CheA and CheW proteins. The role of RecA in this structure would be related to the achievement

of the optimal physical structure and the full regulatory-competent state of the clusters.

11. The inhibition of the swarming motility caused by variations of the RecA protein concentration is due to the inability of *S.* Typhimurium cells to proficiently structure the chemoreceptor signaling arrays.

Bibliography

Abcam, 2012. Protocols book. Tech. rep.

Adler, J., 1973. A method for measuring chemotaxis and use of the method to determine optimum conditions for chemotaxis by *Escherichia coli*. *J Gen Microbiol* 74(1):77–91.

Alberti, L., Harshey, R.M., 1990. Differentiation of *Serratia marcescens* 274 into swimmer and swarmer cells. *J Bacteriol* 172(8):4322–4328.

Allison, C., Emödy, L., Coleman, N., Hughes, C., 1994. The role of swarm cell differentiation and multicellular migration in the uropathogenicity of *Proteus mirabilis*. *J Infect Dis* 169(5):1155–1158.

Allison, C., Lai, H.C., Hughes, C., 1992. Co-ordinate expression of virulence genes during swarm-cell differentiation and population migration of *Proteus mirabilis*. *Mol Microbiol* 6(12):1583–1591.

Alvarez-Ordóñez, A., Begley, M., Prieto, M., Messens, W., López, M., Bernardo, A., Hill, C., 2011. *Salmonella* spp. survival strategies within the host gastrointestinal tract. *Microbiology* 157(Pt 12):3268–3281.

Arifuzzaman, M., Maeda, M., Itoh, A., Nishikata, K., Takita, C., Saito, R., Ara, T., Nakahigashi, K., Huang, H.C., Hirai, A., Tsuzuki, K., Nakamura, S., Altaf-Ul-Amin, M., Oshima, T., Baba, T., Yamamoto, N., Kawamura, T., Ioka-Nakamichi, T., Kitagawa, M., Tomita, M., Kanaya, S., Wada, C., Mori, H., 2006. Large-scale identification of protein-protein interaction of *Escherichia coli* K-12. *Genome Res* 16(5):686–691.

Armitage, J.P., Macnab, R.M., 1987. Unidirectional, intermittent rotation of the flagellum of *Rhodobacter sphaeroides*. *J Bacteriol* 169(2):514–518.

Aswad, D., Koshland, Jr, D., 1975. Isolation, characterization and complementation of *Salmonella typhimurium* chemotaxis mutants. *J Mol Biol* 97(2):225–235.

Attmannspacher, U., Scharf, B., Schmitt, R., 2005. Control of speed modulation (chemokinesis) in the unidirectional rotary motor of *Sinorhizobium meliloti*. *Mol Microbiol* 56(3):708–718.

Attmannspacher, U., Scharf, B.E., Harshey, R.M., 2008. FliL is essential for swarming: motor rotation in absence of FliL fractures the flagellar rod in swarmer cells of *Salmonella enterica*. *Mol Microbiol* 68(2):328–341.

Baker, M.D., Wolanin, P.M., Stock, J.B., 2006a. Signal transduction in bacterial chemotaxis. *Bioessays* 28(1):9–22.

Baker, M.D., Wolanin, P.M., Stock, J.B., 2006b. Systems biology of bacterial chemotaxis. *Curr Opin Microbiol* 9(2):187–192.

Banno, S., Shiomi, D., Homma, M., Kawagishi, I., 2004. Targeting of the chemotaxis methylesterase/deamidase CheB to the polar receptor-kinase cluster in an *Escherichia coli* cell. *Mol Microbiol* 53(4):1051–1063.

Be'er, A., Harshey, R.M., 2011. Collective motion of surfactant-producing bacteria imparts superdiffusivity to their upper surface. *Biophys J* 101(5):1017–1024.

Belas, R., Erskine, D., Flaherty, D., 1991. *Proteus mirabilis* mutants defective in swarmer cell differentiation and multicellular behavior. *J Bacteriol* 173(19):6279–6288.

Belas, R., Goldman, M., Ashliman, K., 1995. Genetic analysis of *Proteus mirabilis* mutants defective in swarmer cell elongation. *J Bacteriol* 177(3):823–828.

Belas, R., Manos, J., Suvanasuthi, R., 2004. *Proteus mirabilis* ZapA metalloprotease degrades a broad spectrum of substrates, including antimicrobial peptides. *Infect Immun* 72(9):5159–5167.

Berg, H.C., 2003. The rotary motor of bacterial flagella. *Annu Rev Biochem* 72:19–54.

Besschetnova, T.Y., Montefusco, D.J., Asinas, A.E., Shrout, A.L., Antommattei, F.M., Weis, R.M., 2008. Receptor density balances signal stimulation and attenuation in membrane-assembled complexes of bacterial chemotaxis signaling proteins. *Proc Natl Acad Sci U S A* 105(34):12289–12294.

Birnboim, H.C., Doly, J., 1979. A rapid alkaline extraction procedure for screening recombinant plasmid DNA. *Nucleic Acids Res* 7(6):1513–1523.

Blat, Y., Gillespie, B., Bren, A., Dahlquist, F.W., Eisenbach, M., 1998. Regulation of phosphatase activity in bacterial chemotaxis. *J Mol Biol* 284(4):1191–1199.

Block, S.M., Segall, J.E., Berg, H.C., 1983. Adaptation kinetics in bacterial chemotaxis. *J Bacteriol* 154(1):312–323.

Blázquez, J., Couce, A., Rodríguez-Beltrán, J., Rodríguez-Rojas, A., 2012. Antimicrobials as promoters of genetic variation. *Curr Opin Microbiol* 15(5):561–569.

Boehm, A., Kaiser, M., Li, H., Spangler, C., Kasper, C.A., Ackermann, M., Kaever, V., Sourjik, V., Roth, V., Jenal, U., 2010. Second messenger-mediated adjustment of bacterial swimming velocity. *Cell* 141(1):107–116.

Boukhvalova, M., VanBruggen, R., Stewart, R.C., 2002a. CheA kinase and chemoreceptor interaction surfaces on CheW. *J Biol Chem* 277(26):23596–23603.

Boukhvalova, M.S., Dahlquist, F.W., Stewart, R.C., 2002b. CheW binding interactions with CheA and Tar. Importance for chemotaxis signaling in *Escherichia coli*. *J Biol Chem* 277(25):22251–22259.

Boyd, E.F., Wang, F.S., Beltran, P., Plock, S.A., Nelson, K., Selander, R.K., 1993. *Salmonella* reference collection B (SARB): strains of 37 serovars of subspecies I. *J Gen Microbiol* 139 Pt 6:1125–1132.

Boyd, E.F., Wang, F.S., Whittam, T.S., Selander, R.K., 1996. Molecular genetic relationships of the *Salmonellae*. *Appl Environ Microbiol* 62(3):804–808.

Bradford, M.M., 1976. A rapid and sensitive method for the quantitation of microgram quantities of protein utilizing the principle of protein-dye binding. *Anal Biochem* 72:248–254.

Braun, T.F., Blair, D.F., 2001. Targeted disulfide cross-linking of the MotB protein of *Escherichia coli*: evidence for two H(+) channels in the stator complex. *Biochemistry* 40(43):13051–13059.

Bray, D., Levin, M.D., Morton-Firth, C.J., 1998. Receptor clustering as a cellular mechanism to control sensitivity. *Nature* 393(6680):85–88.

Briegel, A., Li, X., Bilwes, A.M., Hughes, K.T., Jensen, G.J., Crane, B.R., 2012. Bacterial chemoreceptor arrays are hexagonally packed trimers of receptor dimers networked by rings of kinase and coupling proteins. *Proc Natl Acad Sci U S A* 109(10):3766–3771.

Bunny, K., Liu, J., Roth, J., 2002. Phenotypes of *lexA* mutations in *Salmonella enterica*: evidence for a lethal *lexA* null phenotype due to the Fels-2 prophage. *J Bacteriol* 184(22):6235–6249.

Burkart, M., Toguchi, A., Harshey, R.M., 1998. The chemotaxis system, but not chemotaxis, is essential for swarming motility in *Escherichia coli*. *Proc Natl Acad Sci U S A* 95(5):2568–2573.

Calvio, C., Celandroni, F., Ghelardi, E., Amati, G., Salvetti, S., Ceciliani, F., Galizzi, A., Senesi, S., 2005. Swarming differentiation and swimming motility in *Bacillus subtilis* are controlled by *swrA*, a newly identified dicistronic operon. *J Bacteriol* 187(15):5356–5366.

Cambray, G., Guerout, A.M., Mazel, D., 2010. Integrons. *Annu Rev Genet* 44:141–166.

Campoy, S., Hervàs, A., Busquets, N., Erill, I., Teixidó, L., Barbé, J., 2006. Induction of the SOS response by bacteriophage lytic development in *Salmonella enterica*. *Virology* 351(2):360–367.

Cantwell, B.J., Draheim, R.R., Weart, R.B., Nguyen, C., Stewart, R.C., Manson, M.D., 2003. CheZ phosphatase localizes to chemoreceptor patches via CheA-short. *J Bacteriol* 185(7):2354–2361.

Cardozo, M.J., Massazza, D.A., Parkinson, J.S., Studdert, C.A., 2010. Disruption of chemoreceptor signalling arrays by high levels of CheW, the receptor-kinase coupling protein. *Mol Microbiol* 75(5):1171–1181.

Castelli, M.E., Véscovi, E.G., 2011. The Rcs signal transduction pathway is triggered by enterobacterial common antigen structure alterations in *Serratia marcescens*. *J Bacteriol* 193(1):63–74.

Chaveroche, M.K., Ghigo, J.M., d'Enfert, C., 2000. A rapid method for efficient gene replacement in the filamentous fungus *Aspergillus nidulans*. *Nucleic Acids Res* 28(22):E97.

Chen, B.G., Turner, L., Berg, H.C., 2007. The wetting agent required for swarming in *Salmonella enterica* serovar typhimurium is not a surfactant. *J Bacteriol* 189(23):8750–8753.

Cheng, F., Hou, J., Chen, Y.Y., Zhou, Y., Zhang, H.T., Bi, L.J., Zhang, X.E., 2010. Functional interaction between MutL and 3'-5' exonuclease X in *Escherichia coli*. *Arch Biochem Biophys* 502(1):39–43.

Chilcott, G.S., Hughes, K.T., 2000. Coupling of flagellar gene expression to flagellar assembly in *Salmonella enterica* serovar Typhimurium and *Escherichia coli*. *Microbiol Mol Biol Rev* 64(4):694–708.

Clerch, B., Garriga, X., Torrents, E., Rosales, C.M., Llagostera, M., 1996. Construction and characterization of two *lexA* mutants of *Salmonella* Typhimurium with different UV sensitivities and UV mutabilities. *J Bacteriol* 178(10):2890–2896.

Comeau, S.R., Gatchell, D.W., Vajda, S., Camacho, C.J., 2004a. ClusPro: a fully automated algorithm for protein-protein docking. *Nucleic Acids Res* 32(Web Server issue):W96–W99.

Comeau, S.R., Gatchell, D.W., Vajda, S., Camacho, C.J., 2004b. ClusPro: an automated docking and discrimination method for the prediction of protein complexes. *Bioinformatics* 20(1):45–50.

Costa, C.S., Pettinari, M.J., Méndez, B.S., Antón, D.N., 2003. Null mutations in the essential gene *yrfF* (*mucM*) are not lethal in *rcsB*, *yojN* or *rcsC* strains of *Salmonella enterica* serovar Typhimurium. *FEMS Microbiol Lett* 222(1):25–32.

Courcelle, J., Khodursky, A., Peter, B., Brown, P.O., Hanawalt, P.C., 2001. Comparative gene expression profiles following UV exposure in wild-type and SOS-deficient *Escherichia coli*. *Genetics* 158(1):41–64.

Daniels, R., Vanderleyden, J., Michiels, J., 2004. Quorum sensing and swarming migration in bacteria. *FEMS Microbiol Rev* 28(3):261–289.

Darfeuille, F., Unoson, C., Vogel, J., Wagner, E.G.H., 2007. An antisense RNA inhibits translation by competing with standby ribosomes. *Mol Cell* 26(3):381–392.

Datsenko, K.A., Wanner, B.L., 2000. One-step inactivation of chromosomal genes in *Escherichia coli* K-12 using PCR products. *Proc Natl Acad Sci U S A* 97(12):6640–6645.

Davis, R., Botstein, D., Roth, J., *Advanced bacterial genetics*. Manual for genetic engineering (Cold Spring Harbor Laboratory, 1980).

Dower, W.J., Miller, J.F., Ragsdale, C.W., 1988. High efficiency transformation of *E. coli* by high voltage electroporation. *Nucleic Acids Res* 16(13):6127–6145.

Doyle, T.B., Hawkins, A.C., McCarter, L.L., 2004. The complex flagellar torque generator of *Pseudomonas aeruginosa*. *J Bacteriol* 186(19):6341–6350.

Dörr, T., Vuli, M., Lewis, K., 2010. Ciprofloxacin causes persister formation by inducing the TisB toxin in *Escherichia coli*. *PLoS Biol* 8(2):e1000317.

Dufour, A., Furness, R.B., Hughes, C., 1998. Novel genes that upregulate the *Proteus mirabilis flhDC* master operon controlling flagellar biogenesis and swarming. *Mol Microbiol* 29(3):741–751.

Duke, T.A., Bray, D., 1999. Heightened sensitivity of a lattice of membrane receptors. *Proc Natl Acad Sci U S A* 96(18):10104–10108.

D'Ulisse, V., Fagioli, M., Ghelardini, P., Paolozzi, L., 2007. Three functional subdomains of the *Escherichia coli* FtsQ protein are involved in its interaction with the other division proteins. *Microbiology* 153(Pt 1):124–138.

EFSA., 2013. The European Union Summary Report on Trends and Sources of Zoonoses, Zoonotic Agents and Food-borne Outbreaks in 2011. EFSA Journal 11(4):3129, European Food Safety Authority.

Erill, I., Campoy, S., Barbé, J., 2007. Aeons of distress: an evolutionary perspective on the bacterial SOS response. *FEMS Microbiol Rev* 31(6):637–656.

Fàbrega, A., Vila, J., 2013. *Salmonella enterica* serovar Typhimurium skills to succeed in the host: virulence and regulation. *Clin Microbiol Rev* 26(2):308–341.

Ferreira, R.B.R., Antunes, L.C.M., Greenberg, E.P., McCarter, L.L., 2008. *Vibrio parahaemolyticus* ScrC modulates cyclic dimeric GMP regulation of gene expression relevant to growth on surfaces. *J Bacteriol* 190(3):851–860.

Figueroa-Bossi, N., Bossi, L., 1999. Inducible prophages contribute to *Salmonella* virulence in mice. *Mol Microbiol* 33(1):167–176.

Finlay, B.B., Falkow, S., 1988. Virulence factors associated with *Salmonella* species. *Microbiol Sci* 5(11):324–328.

Fraser, G.M., Claret, L., Furness, R., Gupta, S., Hughes, C., 2002. Swarming-coupled expression of the *Proteus mirabilis hpmBA* haemolysin operon. *Microbiology* 148(Pt 7):2191–2201.

Fraser, G.M., Hughes, C., 1999. Swarming motility. *Curr Opin Microbiol* 2(6):630–635.

Frye, J., Karlinsey, J.E., Felise, H.R., Marzolf, B., Dowidar, N., McClelland, M., Hughes, K.T., 2006. Identification of new flagellar genes of *Salmonella enterica* serovar Typhimurium. *J Bacteriol* 188(6):2233–2243.

Fu, Y., Galán, J.E., Jul 1998. Identification of a specific chaperone for SptP, a substrate of the centisome 63 type III secretion system of *Salmonella* Typhimurium. *J Bacteriol* 180(13):3393–3399.

Fuentes, M., Mateo, C., Pessela, B.C.C., Guisán, J.M., Fernandez-Lafuente, R., 2005. Purification, stabilization, and concentration of very weak

protein-protein complexes: Shifting the association equilibrium via complex selective adsorption on lowly activated supports. *Proteomics* 5(16):4062–4069.

Gabel, C.V., Berg, H.C., 2003. The speed of the flagellar rotary motor of *Escherichia coli* varies linearly with protonmotive force. *Proc Natl Acad Sci U S A* 100(15):8748–8751.

Gallagher, S., Winston, S.E., Fuller, S.A., Hurrell, J.G.R., 2008. Immunoblotting and immunodetection. *Curr Protoc Mol Biol* Chapter 10:Unit 10.8.

Garvey, N., St John, A.C., Witkin, E.M., 1985. Evidence for RecA protein association with the cell membrane and for changes in the levels of major outer membrane proteins in SOS-induced *Escherichia coli* cells. *J Bacteriol* 163(3):870–876.

Garza, A.G., Biran, R., Wohlschlegel, J.A., Manson, M.D., 1996. Mutations in *motB* suppressible by changes in stator or rotor components of the bacterial flagellar motor. *J Mol Biol* 258(2):270–285.

Gillen, K.L., Hughes, K.T., 1991. Negative regulatory loci coupling flagellin synthesis to flagellar assembly in *Salmonella* Typhimurium. *J Bacteriol* 173(7):2301–2310.

Gillen, K.L., Hughes, K.T., 1993. Transcription from two promoters and autoregulation contribute to the control of expression of the *Salmonella* Typhimurium flagellar regulatory gene *flgM*. *J Bacteriol* 175(21):7006–7015.

Gómez-Gómez, J.M., Manfredi, C., Alonso, J.C., Blázquez, J., 2007. A novel role for RecA under non-stress: promotion of swarming motility in *Escherichia coli* K-12. *BMC Biol* 5:14.

Green, M., Sambrook, J., *Molecular Cloning: Laboratory Manual, Fourth Edition* (Cold Spring Harbor Laboratory Press, 2012).

Greenfield, D., McEvoy, A.L., Shroff, H., Crooks, G.E., Wingreen, N.S., Betzig, E., Liphardt, J., 2009. Self-organization of the *Escherichia coli* chemotaxis network imaged with super-resolution light microscopy. *PLoS Biol* 7(6):e1000137.

Griswold, I.J., Zhou, H., Matison, M., Swanson, R.V., McIntosh, L.P., Simon, M.I., Dahlquist, F.W., 2002. The solution structure and interactions of CheW from *Thermotoga maritima*. *Nat Struct Biol* 9(2):121–125.

Guerin, E., Cambray, G., Sanchez-Alberola, N., Campoy, S., Erill, I., Da Re, S., Gonzalez-Zorn, B., Barbé, J., Ploy, M.C., Mazel, D., 2009. The SOS response controls integron recombination. *Science* 324(5930):1034.

Gygi, D., Rahman, M.M., Lai, H.C., Carlson, R., Guard-Petter, J., Hughes, C., 1995. A cell-surface polysaccharide that facilitates rapid population migration by differentiated swarm cells of *Proteus mirabilis*. *Mol Microbiol* 17(6):1167–1175.

Harshey, R.M., 2003. Bacterial motility on a surface: many ways to a common goal. *Annu Rev Microbiol* 57:249–273.

Harshey, R.M., Matsuyama, T., 1994. Dimorphic transition in *Escherichia coli* and *Salmonella* Typhimurium: surface-induced differentiation into hyperflagellate swarmer cells. *Proc Natl Acad Sci U S A* 91(18):8631–8635.

Hengge, R., 2009. Principles of c-di-GMP signalling in bacteria. *Nat Rev Microbiol* 7(4):263–273.

Hiramatsu, F., Wakita, J.i., Kobayashi, N., Yamazaki, Y., Matsushita, M., Matsuyama, T., 2005. Patterns of expansion produced by a structured cell population of *Serratia marcescens* in response to different media. *Microbes and environments* 20(2):120–125.

Hughes, K.T., Gillen, K.L., Semon, M.J., Karlinsey, J.E., 1993. Sensing structural intermediates in bacterial flagellar assembly by export of a negative regulator. *Science* 262(5137):1277–1280.

Inoue, T., Shingaki, R., Hirose, S., Waki, K., Mori, H., Fukui, K., 2007. Genome-wide screening of genes required for swarming motility in *Escherichia coli* K-12. *J Bacteriol* 189(3):950–957.

Janion, C., 2008. Inducible SOS response system of DNA repair and mutagenesis in *Escherichia coli*. *Int J Biol Sci* 4(6):338–344.

Jarvik, T., Smillie, C., Groisman, E.A., Ochman, H., 2010. Short-term signatures of evolutionary change in the *Salmonella enterica* serovar Typhimurium 14028 genome. *J Bacteriol* 192(2):560–567.

Kaiser, D., 2007. Bacterial swarming: a re-examination of cell-movement patterns. *Curr Biol* 17(14):R561–R570.

Karlin, S., Brocchieri, L., 1996. Evolutionary conservation of RecA genes in relation to protein structure and function. *J Bacteriol* 178(7):1881–1894.

Karlinsey, J.E., Lonner, J., Brown, K.L., Hughes, K.T., 2000. Translation/secretion coupling by type III secretion systems. *Cell* 102(4):487–497.

Karu, A.E., Belk, E.D., 1982. Induction of *E. coli* RecA protein via *recBC* and alternate pathways: quantitation by enzyme-linked immunosorbent assay (ELISA). *Mol Gen Genet* 185(2):275–282.

Kawagishi, I., Imagawa, M., Imae, Y., McCarter, L., Homma, M., 1996. The sodium-driven polar flagellar motor of marine *Vibrio* as the mechanosensor that regulates lateral flagellar expression. *Mol Microbiol* 20(4):693–699.

Kearns, D.B., 2010. A field guide to bacterial swarming motility. *Nat Rev Microbiol* 8(9):634–644.

Kearns, D.B., Losick, R., 2003. Swarming motility in undomesticated *Bacillus subtilis*. *Mol Microbiol* 49(3):581–590.

Kentner, D., Sourjik, V., 2009. Dynamic map of protein interactions in the *Escherichia coli* chemotaxis pathway. *Mol Syst Biol* 5:238.

Kentner, D., Thiem, S., Hildenbeutel, M., Sourjik, V., 2006. Determinants of chemoreceptor cluster formation in *Escherichia coli*. *Mol Microbiol* 61(2):407–417.

Kidane, D., Graumann, P.L., 2005. Intracellular protein and DNA dynamics in competent *Bacillus subtilis* cells. *Cell* 122(1):73–84.

Kim, K.K., Yokota, H., Kim, S.H., 1999. Four-helical-bundle structure of the cytoplasmic domain of a serine chemotaxis receptor. *Nature* 400(6746):787–792.

Kim, S.H., Joo, C., Ha, T., Kim, D., 2013. Molecular mechanism of sequence-dependent stability of RecA filament. *Nucleic Acids Res* .

Kim, W., Killam, T., Sood, V., Surette, M.G., 2003. Swarm-cell differentiation in *Salmonella enterica* serovar. Typhimurium results in elevated resistance to multiple antibiotics. *J Bacteriol* 185(10):3111–3117.

Kim, W., Surette, M.G., 2004. Metabolic differentiation in actively swarming *Salmonella*. *Mol Microbiol* 54(3):702–714.

Kim, W., Surette, M.G., 2005. Prevalence of surface swarming behavior in *Salmonella*. *J Bacteriol* 187(18):6580–6583.

Kim, W., Surette, M.G., 2006. Coordinated regulation of two independent cell-cell signaling systems and swarmer differentiation in *Salmonella enterica* serovar. Typhimurium. *J Bacteriol* 188(2):431–440.

Kinsinger, R.F., Kearns, D.B., Hale, M., Fall, R., 2005. Genetic requirements for potassium ion-dependent colony spreading in *Bacillus subtilis*. *J Bacteriol* 187(24):8462–8469.

Kojima, S., Blair, D.F., 2001. Conformational change in the stator of the bacterial flagellar motor. *Biochemistry* 40(43):13041–13050.

Kowalczykowski, S.C., Dixon, D.A., Eggleston, A.K., Lauder, S.D., Rehrauer, W.M., 1994. Biochemistry of homologous recombination in *Escherichia coli*. *Microbiol Rev* 58(3):401–465.

Kozakov, D., Brenke, R., Comeau, S.R., Vajda, S., 2006. PIPER: an FFT-based protein docking program with pairwise potentials. *Proteins* 65(2):392–406.

Kozakov, D., Hall, D.R., Beglov, D., Brenke, R., Comeau, S.R., Shen, Y., Li, K., Zheng, J., Vakili, P., Paschalidis, I.C., Vajda, S., 2010. Achieving reliability and high accuracy in automated protein docking: ClusPro,

PIPER, SDU, and stability analysis in CAPRI rounds 13-19. *Proteins* 78(15):3124–3130.

Krasteva, P.V., Giglio, K.M., Sondermann, H., 2012. Sensing the messenger: the diverse ways that bacteria signal through c-di-GMP. *Protein Sci* 21(7):929–948.

Krell, T., Lacal, J., Muñoz-Martínez, F., Reyes-Darias, J.A., Cadirci, B.H., García-Fontana, C., Ramos, J.L., 2011. Diversity at its best: bacterial taxis. *Environ Microbiol* 13(5):1115–1124.

Krishna, P., van de Sande, J.H., 1990. Interaction of RecA protein with acidic phospholipids inhibits DNA-binding activity of RecA. *J Bacteriol* 172(11):6452–6458.

Kutsukake, K., 1994. Excretion of the anti-sigma factor through a flagellar substructure couples flagellar gene expression with flagellar assembly in *Salmonella* Typhimurium. *Mol Gen Genet* 243(6):605–612.

Kutsukake, K., 1997. Autogenous and global control of the flagellar master operon, *flhD*, in *Salmonella* Typhimurium. *Mol Gen Genet* 254(4):440–448.

Kutsukake, K., Iino, T., 1994. Role of the FliA-FlgM regulatory system on the transcriptional control of the flagellar regulon and flagellar formation in *Salmonella* Typhimurium. *J Bacteriol* 176(12):3598–3605.

Lacal, J., García-Fontana, C., Muñoz-Martínez, F., Ramos, J.L., Krell, T., 2010. Sensing of environmental signals: classification of chemoreceptors according to the size of their ligand binding regions. *Environ Microbiol* 12(11):2873–2884.

Latasa, C., García, B., Echeverz, M., Toledo-Arana, A., Valle, J., Campoy, S., García-del Portillo, F., Solano, C., Lasa, I., 2012. *Salmonella* biofilm development depends on the phosphorylation status of RcsB. *J Bacteriol* 194(14):3708–3722.

Lazova, M.D., Butler, M.T., Shimizu, T.S., Harshey, R.M., 2012. *Salmonella* chemoreceptors McpB and McpC mediate a repellent response to L-cystine: a potential mechanism to avoid oxidative conditions. *Mol Microbiol* 84(4):697–711.

Lee, S.D., Alani, E., 2006. Analysis of interactions between mismatch repair initiation factors and the replication processivity factor PCNA. *J Mol Biol* 355(2):175–184.

Levit, M.N., Stock, J.B., 2002. Receptor methylation controls the magnitude of stimulus-response coupling in bacterial chemotaxis. *J Biol Chem* 277(39):36760–36765.

Li, F., Liu, Q., Chen, Y.Y., Yu, Z.N., Zhang, Z.P., Zhou, Y.F., Deng, J.Y., Bi, L.J., Zhang, X.E., 2008. *Escherichia coli* mismatch repair protein MutL interacts with the clamp loader subunits of DNA polymerase III. *Mutat Res* 637(1-2):101–110.

Li, G., Weis, R.M., 2000. Covalent modification regulates ligand binding to receptor complexes in the chemosensory system of *Escherichia coli*. *Cell* 100(3):357–365.

Li, M., Hazelbauer, G.L., 2004. Cellular stoichiometry of the components of the chemotaxis signaling complex. *J Bacteriol* 186(12):3687–3694.

Li, M., Hazelbauer, G.L., 2011. Core unit of chemotaxis signaling complexes. *Proc Natl Acad Sci U S A* 108(23):9390–9395.

Li, X., Fleetwood, A.D., Bayas, C., Bilwes, A.M., Ortega, D.R., Falke, J.J., Zhulin, I.B., Crane, B.R., 2013. The 3.2 Å resolution structure of a Receptor:CheA:CheW signaling complex defines overlapping binding sites and key residue interactions within bacterial chemosensory arrays. *Biochemistry* 52(22):3852–3865.

Link, A.J., Phillips, D., Church, G.M., 1997. Methods for generating precise deletions and insertions in the genome of wild-type *Escherichia coli*: application to open reading frame characterization. *J Bacteriol* 179(20):6228–6237.

Liu, J.D., Parkinson, J.S., 1989. Role of CheW protein in coupling membrane receptors to the intracellular signaling system of bacterial chemotaxis. *Proc Natl Acad Sci U S A* 86(22):8703–8707.

Liu, Y., Levit, M., Lurz, R., Surette, M.G., Stock, J.B., 1997. Receptor-mediated protein kinase activation and the mechanism of transmembrane signaling in bacterial chemotaxis. *EMBO J* 16(24):7231–7240.

Lusetti, S.L., Cox, M.M., 2002. The bacterial RecA protein and the recombinational DNA repair of stalled replication forks. *Annu Rev Biochem* 71:71–100.

Macnab, R.M., 1977. Bacterial flagella rotating in bundles: a study in helical geometry. *Proc Natl Acad Sci U S A* 74(1):221–225.

Macnab, R.M., Ornston, M.K., 1977. Normal-to-curly flagellar transitions and their role in bacterial tumbling. Stabilization of an alternative quaternary structure by mechanical force. *J Mol Biol* 112(1):1–30.

Maddock, J.R., Shapiro, L., 1993. Polar location of the chemoreceptor complex in the *Escherichia coli* cell. *Science* 259(5102):1717–1723.

Maiques, E., Ubeda, C., Campoy, S., Salvador, N., Lasa, I., Novick, R.P., Barbé, J., Penadés, J.R., 2006. Beta-lactam antibiotics induce the SOS response and horizontal transfer of virulence factors in *Staphylococcus aureus*. *J Bacteriol* 188(7):2726–2729.

Mariconda, S., Wang, Q., Harshey, R.M., 2006. A mechanical role for the chemotaxis system in swarming motility. *Mol Microbiol* 60(6):1590–1602.

Martínez, I.A., Campoy, S., Tort, M., Llagostera, M., Petrov, D., 2013. A simple technique based on a single optical trap for the determination of bacterial swimming pattern. *PLoS One* 8(4):e61630.

Matsuyama, T., Bhasin, A., Harshey, R.M., 1995. Mutational analysis of flagellum-independent surface spreading of *Serratia marcescens* 274 on a low-agar medium. *J Bacteriol* 177(4):987–991.

Matsuyama, T., Sogawa, M., Nakagawa, Y., 1989. Fractal spreading growth of *Serratia marcescens* which produces surface active exolipids. *FEMS Microbiol Lett* 52(3):243–246.

Mattick, J.S., 2002. Type IV pili and twitching motility. *Annu Rev Microbiol* 56:289–314.

McCarter, L., 1999. The multiple identities of *Vibrio parahaemolyticus*. *J Mol Microbiol Biotechnol* 1(1):51–57.

McCarter, L.L., 2004. Dual flagellar systems enable motility under different circumstances. *J Mol Microbiol Biotechnol* 7(1-2):18–29.

McQuiston, J.R., Waters, R.J., Dinsmore, B.A., Mikoleit, M.L., Fields, P.I., 2011. Molecular determination of H antigens of *Salmonella* by use of a microsphere-based liquid array. *J Clin Microbiol* 49(2):565–573.

Medina-Ruiz, L., 2012. *Implicación del sistema SOS y de la proteína RecA en el proceso infectivo de* Salmonella enterica *sv. Typhimurium.* Ph.D. thesis, Facultad de Biociencias, Universitat Autònoma de Barcelona.

Medina-Ruiz, L., Campoy, S., Latasa, C., Cardenas, P., Alonso, J.C., Barbé, J., 2010. Overexpression of the *recA* gene decreases oral but not intraperitoneal fitness of *Salmonella enterica*. *Infect Immun* 78(7):3217–3225.

Melton, T., Hartman, P.E., Stratis, J.P., Lee, T.L., Davis, A.T., 1978. Chemotaxis of *Salmonella* Typhimurium to amino acids and some sugars. *J Bacteriol* 133(2):708–716.

Mignot, T., 2007. The elusive engine in *Myxococcus xanthus* gliding motility. *Cell Mol Life Sci* 64(21):2733–2745.

Monack, D.M., 2012. *Salmonella* persistence and transmission strategies. *Curr Opin Microbiol* 15(1):100–107.

Murray, T.S., Kazmierczak, B.I., 2008. *Pseudomonas aeruginosa* exhibits sliding motility in the absence of type IV pili and flagella. *J Bacteriol* 190(8):2700–2708.

O'Callaghan, D., Charbit, A., 1990. High efficiency transformation of *Salmonella* Typhimurium and *Salmonella* Typhi by electroporation. *Mol Gen Genet* 223(1):156–158.

Ohnishi, K., Kutsukake, K., Suzuki, H., Iino, T., 1990. Gene *fliA* encodes an alternative sigma factor specific for flagellar operons in *Salmonella* Typhimurium. *Mol Gen Genet* 221(2):139–147.

Ottemann, K.M., Miller, J.F., 1997. Roles for motility in bacterial-host interactions. *Mol Microbiol* 24(6):1109–1117.

Overhage, J., Bains, M., Brazas, M.D., Hancock, R.E.W., 2008. Swarming of *Pseudomonas aeruginosa* is a complex adaptation leading to increased production of virulence factors and antibiotic resistance. *J Bacteriol* 190(8):2671–2679.

Ozbabacan, S.E.A., Engin, H.B., Gursoy, A., Keskin, O., 2011. Transient protein-protein interactions. *Protein Eng Des Sel* 24(9):635–648.

Parkinson, J.S., 1976. *cheA, cheB*, and *cheC* genes of *Escherichia coli* and their role in chemotaxis. *J Bacteriol* 126(2):758–770.

Parkinson, J.S., 1978. Complementation analysis and deletion mapping of *Escherichia coli* mutants defective in chemotaxis. *J Bacteriol* 135(1):45–53.

Parry, C.M., Hien, T.T., Dougan, G., White, N.J., Farrar, J.J., 2002. Typhoid fever. *N Engl J Med* 347(22):1770–1782.

Partridge, J.D., Harshey, R.M., 2013a. More than motility: *Salmonella* flagella contribute to overriding friction and facilitating colony hydration during swarming. *J Bacteriol* 195(5):919–929.

Partridge, J.D., Harshey, R.M., 2013b. Swarming: flexible roaming plans. *J Bacteriol* 195(5):909–918.

Patrick, J.E., Kearns, D.B., 2012. Swarming motility and the control of master regulators of flagellar biosynthesis. *Mol Microbiol* 83(1):14–23.

Paul, K., Nieto, V., Carlquist, W.C., Blair, D.F., Harshey, R.M., 2010. The c-di-GMP binding protein YcgR controls flagellar motor direction and speed to affect chemotaxis by a "backstop brake" mechanism. *Mol Cell* 38(1):128–139.

Rahman, M.M., Guard-Petter, J., Asokan, K., Hughes, C., Carlson, R.W., 1999. The structure of the colony migration factor from pathogenic *Proteus mirabilis*. A capsular polysaccharide that facilitates swarming. *J Biol Chem* 274(33):22993–22998.

Rajendram, M., The *Escherichia coli* membrane regulates the RecA protein's DNA repair activity. In *American Society for Microbiology, general meeting* (2013).

Rehrauer, W.M., Kowalczykowski, S.C., 1996. The DNA binding site(s) of the *Escherichia coli* RecA protein. *J Biol Chem* 271(20):11996–12002.

Renzette, N., Gumlaw, N., Nordman, J.T., Krieger, M., Yeh, S.P., Long, E., Centore, R., Boonsombat, R., Sandler, S.J., 2005. Localization of RecA in *Escherichia coli* K-12 using RecA-GFP. *Mol Microbiol* 57(4):1074–1085.

Rescigno, M., Urbano, M., Valzasina, B., Francolini, M., Rotta, G., Bonasio, R., Granucci, F., Kraehenbuhl, J.P., Ricciardi-Castagnoli, P., 2001. Dendritic cells express tight junction proteins and penetrate gut epithelial monolayers to sample bacteria. *Nat Immunol* 2(4):361–367.

Salvetti, S., Faegri, K., Ghelardi, E., Kolstø, A.B., Senesi, S., 2011. Global gene expression profile for swarming *Bacillus cereus* bacteria. *Appl Environ Microbiol* 77(15):5149–5156.

Samatey, F.A., Matsunami, H., Imada, K., Nagashima, S., Shaikh, T.R., Thomas, D.R., Chen, J.Z., Derosier, D.J., Kitao, A., Namba, K., 2004. Structure of the bacterial flagellar hook and implication for the molecular universal joint mechanism. *Nature* 431(7012):1062–1068.

Sanders, D.A., Gillece-Castro, B.L., Stock, A.M., Burlingame, A.L., Koshland, Jr, D., 1989a. Identification of the site of phosphoryla-

tion of the chemotaxis response regulator protein, CheY. *J Biol Chem* 264(36):21770–21778.

Sanders, D.A., Mendez, B., Koshland, Jr, D., 1989b. Role of the CheW protein in bacterial chemotaxis: overexpression is equivalent to absence. *J Bacteriol* 171(11):6271–6278.

Sar, N., McCarter, L., Simon, M., Silverman, M., 1990. Chemotactic control of the two flagellar systems of *Vibrio parahaemolyticus*. *J Bacteriol* 172(1):334–341.

Sauer, R.T., Ross, M.J., Ptashne, M., 1982. Cleavage of the lambda and P22 repressors by RecA protein. *J Biol Chem* 257(8):4458–4462.

Schaubach, O.L., Dombroski, A.J., 1999. Transcription initiation at the flagellin promoter by RNA polymerase carrying sigma 28 from *Salmonella* Typhimurium. *J Biol Chem* 274(13):8757–8763.

Schleker, S., Sun, J., Raghavan, B., Srnec, M., Müller, N., Koepfinger, M., Murthy, L., Zhao, Z., Klein-Seetharaman, J., 2012. The current *Salmonella*-host interactome. *Proteomics Clin Appl* 6(1-2):117–133.

Schrödinger, LLC, 2010. The PyMOL Molecular Graphics System, Version 1.3r1.

Sharp, L.L., Zhou, J., Blair, D.F., 1995. Features of MotA proton channel structure revealed by tryptophan-scanning mutagenesis. *Proc Natl Acad Sci U S A* 92(17):7946–7950.

Shearwin, K.E., Brumby, A.M., Egan, J.B., 1998. The Tum protein of coliphage 186 is an antirepressor. *J Biol Chem* 273(10):5708–5715.

Shimada, H., Ikeda, T., Wakita, J.i., Itoh, H., Kurosu, S., Hiramatsu, F., Nakatsuchi, M., Yamazaki, Y., Matsuyama, T., Matsushita, M., 2004. Dependence of local cell density on concentric ring colony formation by bacterial species *Bacillus subtilis*. *Journal of the Physical Society of Japan* 73:1082.

Shiomi, D., Zhulin, I.B., Homma, M., Kawagishi, I., 2002. Dual recognition of the bacterial chemoreceptor by chemotaxis-specific domains of the CheR methyltransferase. *J Biol Chem* 277(44):42325–42333.

Skidmore, J.M., Ellefson, D.D., McNamara, B.P., Couto, M.M., Wolfe, A.J., Maddock, J.R., 2000. Polar clustering of the chemoreceptor complex in *Escherichia coli* occurs in the absence of complete CheA function. *J Bacteriol* 182(4):967–973.

Sourjik, V., Berg, H.C., 2000. Localization of components of the chemotaxis machinery of *Escherichia coli* using fluorescent protein fusions. *Mol Microbiol* 37(4):740–751.

Sourjik, V., Berg, H.C., 2002. Receptor sensitivity in bacterial chemotaxis. *Proc Natl Acad Sci U S A* 99(1):123–127.

Sourjik, V., Berg, H.C., 2004. Functional interactions between receptors in bacterial chemotaxis. *Nature* 428(6981):437–441.

Soutourina, O.A., Bertin, P.N., 2003. Regulation cascade of flagellar expression in Gram-negative bacteria. *FEMS Microbiol Rev* 27(4):505–523.

Sowa, Y., Berry, R.M., 2008. Bacterial flagellar motor. *Q Rev Biophys* 41(2):103–132.

Sperandio, V., Torres, A.G., Kaper, J.B., 2002. Quorum sensing *Escherichia coli* regulators B and C (QseBC): a novel two-component regulatory system involved in the regulation of flagella and motility by quorum sensing in *E. coli*. *Mol Microbiol* 43(3):809–821.

Stafford, G.P., Hughes, C., 2007. *Salmonella* Typhimurium *flhE*, a conserved flagellar regulon gene required for swarming. *Microbiology* 153(Pt 2):541–547.

Story, R.M., Weber, I.T., Steitz, T.A., 1992. The structure of the *E. coli* RecA protein monomer and polymer. *Nature* 355(6358):318–325.

Stoscheck, C.M., 1990. Quantitation of protein. *Methods Enzymol* 182:50–68.

Studdert, C.A., Parkinson, J.S., 2004. Crosslinking snapshots of bacterial chemoreceptor squads. *Proc Natl Acad Sci U S A* 101(7):2117–2122.

Studdert, C.A., Parkinson, J.S., 2005. Insights into the organization and dynamics of bacterial chemoreceptor clusters through in vivo crosslinking studies. *Proc Natl Acad Sci U S A* 102(43):15623–15628.

Surette, M.G., Stock, J.B., 1996. Role of alpha-helical coiled-coil interactions in receptor dimerization, signaling, and adaptation during bacterial chemotaxis. *J Biol Chem* 271(30):17966–17973.

Swanson, R.V., Sanna, M.G., Simon, M.I., 1996. Thermostable chemotaxis proteins from the hyperthermophilic bacterium *Thermotoga maritima*. *J Bacteriol* 178(2):484–489.

Teixidó, L., Carrasco, B., Alonso, J.C., Barbé, J., Campoy, S., 2011. Fur activates the expression of *Salmonella enterica* pathogenicity island 1 by

directly interacting with the *hilD* operator in vivo and in vitro. *PLoS One* 6(5):e19711.

Terashima, H., Kojima, S., Homma, M., 2008. Flagellar motility in bacteria structure and function of flagellar motor. *Int Rev Cell Mol Biol* 270:39–85.

Terpe, K., 2003. Overview of tag protein fusions: from molecular and biochemical fundamentals to commercial systems. *Appl Microbiol Biotechnol* 60(5):523–533.

Thermo, 2008. Co-immunoprecipitation (co-IP) Troubleshooting Guide. Tech. rep., Thermo Fisher Scientific.

Thiem, S., Kentner, D., Sourjik, V., 2007. Positioning of chemosensory clusters in *E. coli* and its relation to cell division. *EMBO J* 26(6):1615–1623.

Thiem, S., Sourjik, V., 2008. Stochastic assembly of chemoreceptor clusters in *Escherichia coli*. *Mol Microbiol* 68(5):1228–1236.

Thiennimitr, P., Winter, S.E., Bäumler, A.J., 2012. *Salmonella*, the host and its microbiota. *Curr Opin Microbiol* 15(1):108–114.

Toguchi, A., Siano, M., Burkart, M., Harshey, R.M., 2000. Genetics of swarming motility in *Salmonella enterica* serovar Typhimurium: critical role for lipopolysaccharide. *J Bacteriol* 182(22):6308–6321.

Toutain, C.M., Zegans, M.E., O'Toole, G.A., 2005. Evidence for two flagellar stators and their role in the motility of *Pseudomonas aeruginosa*. *J Bacteriol* 187(2):771–777.

Tremblay, J., Déziel, E., 2010. Gene expression in *Pseudomonas aeruginosa* swarming motility. *BMC Genomics* 11:587.

Turner, L., Ryu, W.S., Berg, H.C., 2000. Real-time imaging of fluorescent flagellar filaments. *J Bacteriol* 182(10):2793–2801.

Ubeda, C., Maiques, E., Knecht, E., Lasa, I., Novick, R.P., Penadés, J.R., 2005. Antibiotic-induced SOS response promotes horizontal dissemination of pathogenicity island-encoded virulence factors in *staphylococci*. *Mol Microbiol* 56(3):836–844.

Unoson, C., Wagner, E.G.H., 2008. A small SOS-induced toxin is targeted against the inner membrane in *Escherichia coli*. *Mol Microbiol* 70(1):258–270.

Velge, P., Wiedemann, A., Rosselin, M., Abed, N., Boumart, Z., Chaussé, A.M., Grépinet, O., Namdari, F., Roche, S.M., Rossignol, A., Virlogeux-Payant, I., 2012. Multiplicity of *Salmonella* entry mechanisms, a new paradigm for *Salmonella* pathogenesis. *Microbiologyopen* 1(3):243–258.

Verstraeten, N., Braeken, K., Debkumari, B., Fauvart, M., Fransaer, J., Vermant, J., Michiels, J., 2008. Living on a surface: swarming and biofilm formation. *Trends Microbiol* 16(10):496–506.

Vogel, J., Argaman, L., Wagner, E.G.H., Altuvia, S., 2004. The small RNA IstR inhibits synthesis of an SOS-induced toxic peptide. *Curr Biol* 14(24):2271–2276.

Vu, A., Wang, X., Zhou, H., Dahlquist, F.W., 2012. The receptor-CheW binding interface in bacterial chemotaxis. *J Mol Biol* 415(4):759–767.

Walker, K.E., Moghaddame-Jafari, S., Lockatell, C.V., Johnson, D., Belas, R., 1999. ZapA, the IgA-degrading metalloprotease of *Proteus mirabilis*, is a virulence factor expressed specifically in swarmer cells. *Mol Microbiol* 32(4):825–836.

Wang, Q., Frye, J.G., McClelland, M., Harshey, R.M., 2004. Gene expression patterns during swarming in *Salmonella* Typhimurium: genes specific to surface growth and putative new motility and pathogenicity genes. *Mol Microbiol* 52(1):169–187.

Wang, Q., Mariconda, S., Suzuki, A., McClelland, M., Harshey, R.M., 2006a. Uncovering a large set of genes that affect surface motility in *Salmonella enterica* serovar Typhimurium. *J Bacteriol* 188(22):7981–7984.

Wang, Q., Suzuki, A., Mariconda, S., Porwollik, S., Harshey, R.M., 2005. Sensing wetness: a new role for the bacterial flagellum. *EMBO J* 24(11):2034–2042.

Wang, S., Fleming, R.T., Westbrook, E.M., Matsumura, P., McKay, D.B., 2006b. Structure of the *Escherichia coli* FlhDC complex, a prokaryotic heteromeric regulator of transcription. *J Mol Biol* 355(4):798–808.

Waters, C.M., Bassler, B.L., 2005. Quorum sensing: cell-to-cell communication in bacteria. *Annu Rev Cell Dev Biol* 21:319–346.

Weel-Sneve, R., Bjørås, M., Kristiansen, K.I., 2008. Overexpression of the LexA-regulated *tisAB* RNA in *E. coli* inhibits SOS functions; implications for regulation of the SOS response. *Nucleic Acids Res* 36(19):6249–6259.

Whitfield, C., Roberts, I.S., 1999. Structure, assembly and regulation of expression of capsules in *Escherichia coli*. *Mol Microbiol* 31(5):1307–1319.

WHO, 2007. Antigenic Formulae of the *Salmonella* Serovars.

Worley, M.J., Nieman, G.S., Geddes, K., Heffron, F., 2006. *Salmonella* Typhimurium disseminates within its host by manipulating the motility of infected cells. *Proc Natl Acad Sci U S A* 103(47):17915–17920.

Wozniak, C.E., Chevance, F.F.V., Hughes, K.T., 2010. Multiple promoters contribute to swarming and the coordination of transcription with flagellar assembly in *Salmonella*. *J Bacteriol* 192(18):4752–4762.

Yorimitsu, T., Homma, M., 2001. Na(+)-driven flagellar motor of *Vibrio*. *Biochim Biophys Acta* 1505(1):82–93.

Zhang, P., Bos, E., Heymann, J., Gnaegi, H., Kessel, M., Peters, P.J., Subramaniam, S., 2004. Direct visualization of receptor arrays in frozen-hydrated sections and plunge-frozen specimens of *E. coli* engineered to overproduce the chemotaxis receptor Tsr. *J Microsc* 216(Pt 1):76–83.

Zhang, X., McDaniel, A.D., Wolf, L.E., Keusch, G.T., Waldor, M.K., Acheson, D.W., 2000. Quinolone antibiotics induce Shiga toxin-encoding bacteriophages, toxin production, and death in mice. *J Infect Dis* 181(2):664–670.

Zhao, R., Collins, E.J., Bourret, R.B., Silversmith, R.E., 2002. Structure and catalytic mechanism of the *E. coli* chemotaxis phosphatase CheZ. *Nat Struct Biol* 9(8):570–575.

Zhulin, I.B., 2001. The superfamily of chemotaxis transducers: from physiology to genomics and back. *Adv Microb Physiol* 45:157–198.

Appendix A

Mediums, Solutions and Buffers

A.1 Mediums

A.1.1 Brain heart infusion (BHI)

Table A.1. Brain heart infusion broth composition.

Component	Supplier	Concentration (w/v)
BHI Mix	Oxoid	3.7 %
MQ-water		to desired volume

A.1.2 Green plates

Table A.2. Green plates composition.

Component	Supplier	Concentration (w/v)
Tryptone	Difco	0.8 %
Yeast extract	Difco	0.1 %
NaCl	Panreac	0.5 %
Agar	Difco	1.5 %
Alizarin Yellow	Panreac	0.083 %
Aniline Blue	Panreac	0.013 %
D-(+)-glucose	Merck	1.3 %
MQ-water		to desired volume

D-(+)-glucose should be prepared 40% concentrated and sterilized apart. Once the medium has been sterilized and has cooled down to around 50 °C, glucose should be added to the specified final concentration using sterile conditions.

A.1.3 LB-Lennox broth

Table A.3. LB-Lennox broth composition.

Component	Supplier	Concentration (w/v)
Tryptone	Difco	1 %
Yeast extract	Difco	0.5 %
NaCl	Panreac	0.5 %
MQ-water		to desired volume

A.1.4 LB-Miller

Table A.4. LB-Miller composition.

Component	Supplier	Concentration (w/v)
Tryptone	Pronadisa	1 %
Yeast extract	Pronadisa	0.5 %
NaCl	Panreac	1 %
Agar (if required)	Pronadisa	1.7 %
MQ-water		to desired volume

A.1.5 LB-swarming

Table A.5. LB-swarming composition.

Component	Supplier	Concentration (w/v)
Tryptone	Difco	1 %
Yeast extract	Difco	0.5 %
NaCl	Panreac	0.5 %
D-(+)-glucose	Merck	0.5 %
Agar	Difco	0.5 %
MQ-water		to desired volume

(Medina-Ruiz *et al.*, 2010)

A.1.6 One-step inactivation mediums

A.1.6.1 Super optimal broth (SOB)

Table A.6. Super optimal broth composition.

Component	Supplier	Concentration
Tryptone	Difco	2 % (w/v)
Yeast extract	Difco	0.5 % (w/v)
NaCl	Panreac	0.05 % (w/v)
KCl (A.2.20)	Panreac	1.25 mM
DL-arabinose (A.2.9)	Sigma	20 mM
MQ-water		to desired volume

(Datsenko and Wanner, 2000)

DL-arabinose should be prepared at 0.5 M and filter sterilized. The rest of the constituents should be mixed and autoclaved as usual. Once the medium has been cooled down to around 50 °C the required volume of DL-arabinose could be added.

A.1.6.2 Super optimal broth with catabolite (SOC)

Table A.7. Super optimal broth with catabolite composition.

Component	Supplier	Concentration (mM)
DL-arabinose (A.2.9)	Sigma	20
D-(+)-glucose (A.2.14)	Merck	20
$MgSO_4$ (A.2.17)	Panreac	10
SOB w/o DL-arabinose		to desired volume

(Datsenko and Wanner, 2000)

DL-arabinose should be prepared at 0.5 M and D-(+)-glucose at 1 M. Both must be filter sterilized. Once the SOB medium has been prepared, D-(+)-glucose and DL-arabinose must be added to the specified final concentration.

A.1.7 Terrific broth (TB)

Table A.8. Terrific broth composition.

Component	Supplier	Concentration
Tryptone	Difco	1.2 % (w/v)
Yeast extract	Difco	2.4 % (w/v)
Glicerol	Panreac	0.4 % (v/v)
MQ-water		to desired volume

A.1.8 Tryptone broth (TBr)

Table A.9. Tryptone broth composition.

Component	Supplier	Concentration (w/v)
Tryptone	Difco	1 %
NaCl	Panreac	0.5 %
MQ-water		to desired volume

A.2 Solutions

A.2.1 Acetic acid 10 %

Table A.10. Acetic acid 10 % solution composition.

Component	Supplier	Amount
Acetic acid 96 %	Panreac	104 mL
MQ-water		to 1 L

A.2.2 Alkaline phosphatase substrate solution

Table A.11. Alkaline phosphatase substrate solution composition.

Component	Supplier	Amount
BCIP stock solution (A.2.5)		35 µL
NBT stock solution (A.2.18)		45 µL
Alkaline buffer (A.3.1)		to 10 mL

A.2.3 Ammonium persulfate 10 %

Table A.12. Ammonium persulfate 10 % solution composition.

Component	Supplier	Amount
Ammonium persulfate	Amresco	100 mg
MQ-water		to 10 mL

A.2.4 Aspartate 10 mM

Table A.13. Aspartate 10 mM solution composition.

Component	Supplier	Amount
L-aspartic acid 99 %	Panreac	66.5 mg
Tethering buffer (A.3.19)		to 50 mL

Adjust to pH 7 using NaOH or, better, KOH. Should be sterilized by filtration.

A.2.5 BCIP stock solution

Table A.14. BCIP stock solution composition.

Component	Supplier	Amount
BCIP	Roche	50 mg
N,N-Dimethylformamide	Panreac	1 mL

A.2.6 BSA 10 mg/mL

Table A.15. BSA 10 mg/mL solution composition.

Component	Supplier	Amount
BSA fraction V	Roche	0.1 g
MQ-water		to 10 mL

Once prepared, adjust to pH 8. EDTA solution should be autoclaved 15 minutes at 121 °C for a better preservation.

A.2.7 Coomassie gel staining solution

Table A.16. Coomassie gel staining solution composition.

Component	Supplier	Amount
Coomassie Brilliant Blue R-250	Bio-Rad	0.5 g
Acetic acid 96%	Panreac	50 mL
Methanol	Panreac	200 mL
MQ-water		to 500 mL

A.2.8 Diatomaceous earth

Diatomaceous earth must be washed before its final dilution in guanidine hydrochloride 5 M.
Weigh 3.5 g of diatomaceous earth powder and mix with 50 mL of MQ-water. Allow the diatomaceous earth to settle for a minimum of 3 hours. After that, remove the supernatant, containing impurities, and add the guanidine hydrochloride 5 M directly to the washed powder.

Table A.17. Diatomaceous earth solution composition.

Component	Supplier	Amount
Diatomaceous earth powder	Sigma	3.5 g
Guanidine hydrochloride 5 M (A.2.15)		200 mL

A.2.9 DL-arabinose 0.5 M

Table A.18. DL-arabinose 0.5 M solution composition.

Component	Supplier	Amount
DL-arabinose	Sigma	0.75 g
MQ-water		to 10 mL

Filter sterilized and preserved at 4 °C.

A.2.10 EDTA 0.5 M

Table A.19. EDTA 0.5 M solution composition.

Component	Supplier	Amount
EDTA	Sigma	186.12 g
MQ-water		to 1 L

Once prepared adjust to pH 8. EDTA solution should be autoclaved 15 minutes at 121 °C for a better preservation.

A.2.11 Ethanol 70 %

Table A.20. Ethanol 70 % solution composition.

Component	Supplier	Amount
Ethanol absolute	Panreac	70 mL
MQ-water		to 100 mL

A.2.12 Glicerol 10 %

Table A.21. Glicerol 10 % solution composition.

Component	Supplier	Amount
Glicerol	Panreac	5 mL
MQ-water		to 50 mL

Autoclaved 15 minutes at 121 °C and preserved at 4 °C.

A.2.13 Glucose 40 %

Table A.22. Glucose 40 % solution composition.

Component	Supplier	Amount
D-(+)-glucose	Merck	40 g
MQ-water		to 100 mL

Autoclaved 15 minutes at 121 °C and preserved at 4 °C.

A.2.14 Glucose 1 M

Table A.23. Glucose 1 M solution composition.

Component	Supplier	Amount
D-(+)-glucose	Merck	1.8 g
MQ-water		to 10 mL

Filter sterilized and preserved at 4 °C.

A.2.15 Guanidine hydrochloride 5 M

Table A.24. Guanidine hydrochloride 5 M solution composition.

Component	Supplier	Amount
Guanidine hydrochloride	Sigma	100 g
Tris-HCl 1 M pH 8	AppliChem	8.75 mL
EDTA 0.5 M pH 8 (A.2.10)		14 mL
MQ-water		to 200 mL

A slow dilution procedure must be used to ensure a correct dilution of guanidine hydrochloride. Add 50 mL of MQ-water and wait until the solution becomes transparent, then adjust the volume to 200 mL.

Table A.25. IPTG 1 M solution composition.

Component	Supplier	Amount
IPTG	AppliChem	1.19 g
MQ-water		to 5 mL

Filter sterilized and preserved at 4 °C.

A.2.16 IPTG 1 M

A.2.17 Magnesium sulfate 1 M

Table A.26. Magnesium sulfate 1 M solution composition.

Component	Supplier	Amount
$MgSO_4$	Panreac	1.56 g
MQ-water		to 10 mL

Filter sterilized and preserved at 4 °C. When required, magnesium sulfate 10 mM is prepared by dilution, autoclaved 15 minutes at 121 °C and preserved at 4 °C until needed.

A.2.18 NBT stock solution

Table A.27. NBT stock solution composition.

Component	Supplier	Amount
NBT	Roche	75 mg
N,N-Dimethylformamide	Panreac	0.3 mL
MQ-water		1 mL

A.2.19 Potassium acetate 5 M

Table A.28. Potassium acetate 5 M solution composition.

Component	Supplier	Amount
Potassium acetate	Panreac	49 g
MQ-water		to 100 mL

A.2.20 Potassium chloride 2.5 M

Table A.29. Potassium chloride 2.5 M solution composition.

Component	Supplier	Amount
Potassium chloride	Panreac	1.86 g
MQ-water		to 10 mL

A.2.21 SDS 10 %

Table A.30. SDS 10 % solution composition.

Component	Supplier	Amount
SDS	Merck	100 g
MQ-water		to 1 L

A.2.22 Sodium chloride 0.9 %

Table A.31. Sodium chloride 0.9 % solution composition.

Component	Supplier	Amount
NaCl	Panreac	9 g
MQ-water		to 1 L

Autoclave 15 minutes at 121 °C to ensure sterility.

A.2.23 Sodium hydroxide 10 M

Table A.32. Sodium hydroxide 10 M solution composition.

Component	Supplier	Amount
NaOH	Panreac	4 g
MQ-water		to 100 mL

A.2.24 Solution I

Table A.33. Solution I composition.

Component	Supplier	Amount
Tris HCl 1 M pH 8	AppliChem	50 mL
EDTA 0.5 M pH 8 (A.2.10)		40 mL
MQ-water		to 1 L

Store at 4 °C.

A.2.25 Solution II

Table A.34. Solution II composition.

Component	Supplier	Amount
SDS 10% (A.2.21)		5 mL
NaOH 10 M (A.2.23)		1 mL
MQ-water		to 50 mL

Solution II must be freshly prepared for best results. Store at room temperature.

A.2.26 Solution III

Table A.35. Solution III composition.

Component	Supplier	Amount
Potassium acetate 5 M (A.2.19)		600 mL
Acetic acid, glacial	Panreac	115 mL
MQ-water		to 1 L

Once prepared adjust pH to 4.8 using HCl and store at 4 °C.

A.2.27 Polyacrylamide gel electrophoresis (PAGE)

A.2.27.1 Stacking Gel

Table A.36. Stacking gel preparation recipe.

Component	Supplier	Amount
Stacking buffer 4X (A.3.15)		0.75 mL
30 % (w/v) acrylamide : 0.8 % (w/v) bis-acrylamide stock solution	National Diagnostics	0.3 mL
APS 10 % (A.2.3)		15 µL
TEMED	Amresco	3 µL
MQ-water		1.95 mL

A.2.27.2 Separating Gel

Table A.37. Separating gel preparation recipe.

Component	Supplier	Amount
Separating buffer 4X (A.3.12)		1.875 mL
30 % (w/v) acrylamide : 0.8 % (w/v) bis-acrylamide stock solution	National Diagnostics	x mL[a]
APS 10 % (A.2.3)		50 µL
TEMED	Amresco	10 µL
MQ-water		to 7.5 mL

[a] Depending on the desired final acrylamide (v/v) composition.

A.3 Buffers

A.3.1 Alkaline buffer 1X

Table A.38. Alkaline buffer 1X composition.

Component	Supplier	Concentration (mM)
$MgCl_2 \cdot 6\ H_2O$	Merck	50
Tris-HCl	Sigma	6.6
Trizma Base	Sigma	100
NaCl	Panreac	10
MQ-water		to desired volume

Once prepared adjust to pH 9.5 with NaOH.

A.3.2 Carbonate buffer 0.1 M

Table A.39. Carbonate buffer 0.1 M composition.

Component	Supplier	Amount
Na_2CO_3	Panreac	3.03 g
$NaHCO_3$	Panreac	6 g
MQ-water		to 1 L

Once prepared adjust to pH 9.6 with HCl and store at 4 °C.

A.3.3 DNA loading solution 5X

Table A.40. DNA loading solution 5X composition.

Component	Supplier	Concentration
Xilene-Cyanol	Clontech	0.25 % (w/v)
Bromophenol Blue	Panreac	0.25 % (w/v)
Glicerol	Panreac	30 % (v/v)
EDTA 0.5 M (pH 8) (A.2.10)		2 % (v/v)
MQ-water		to desired volume

A.3.4 ELISA blocking buffer 1X

Table A.41. ELISA blocking buffer 1X.

Component	Supplier	Concentration
PBS 10X (A.3.10)		1X
Tween 20	Panreac	0.05 % (v/v)
BSA Fraction V	Roche	3 % (w/v)
MQ-water		to desired volume

A.3.5 Far-Western blocking buffer 1X

Table A.42. Far-western blocking buffer 1X.

Component	Supplier	Concentration
TBS 10X (A.3.20)		1X
Tween 20	Panreac	0.05 % (v/v)
Powder skimmed-milk	Nestlé	5 % (w/v)
MQ-water		to desired volume

A.3.6 Immunoprecipitation blocking buffer 1X

Table A.43. Immunoprecipitation lysis buffer 1X.

Component	Supplier	Concentration
TBS 10X (A.3.20)		1X
Glycerol	Panreac	15 % (v/v)
Triton X-100	Roche	1 % (v/v)
BSA Fraction V	Roche	3 % (w/v)
MQ-water		to desired volume

A.3.7 Immunoprecipitation lysis buffer 1X

Table A.44. Immunoprecipitation wash buffer 1X.

Component	Supplier	Concentration
TBS 10X (A.3.20)		1X
Glycerol	Panreac	10 % (v/v)
Triton X-100	Roche	1 % (v/v)
EDTA 0.5 M (pH 8) (A.2.10)		1 mM
Lysozyme	Roche	1 mg/mL
cOmplete mini EDTA-free tablets	Roche	1 tablet
MQ-water		to desired volume

Store at 4 °C up to 6 months.

A.3.8 Immunoprecipitation wash buffer 1X

Table A.45. Immunoprecipitation lysis buffer 1X.

Component	Supplier	Concentration
TBS 10X (A.3.20)		1X
Glycerol	Panreac	15 % (v/v)
Triton X-100	Roche	1 % (v/v)
MQ-water		to desired volume

Store at 4 °C up to 6 months.

A.3.9 Laemmli buffer 4X

Table A.46. Laemmli buffer 4X composition.

Component	Supplier	Concentration
SDS	Merck	8 % (w/v)
Bromophenol Blue	Panreac	0.4 % (w/v)
Glicerol	Panreac	40 % (v/v)
Stacking buffer 4X (A.3.15)		50 % (v/v)
MQ-water		to 100 mL

A.3.10 Phosphate-buffered saline (PBS) 10X

Table A.47. Phosphate-buffered saline 10X composition.

Component	Supplier	Concentration (mM)
NaCl	Panreac	1370
KCl	Panreac	27
$Na_2HPO_4 \cdot 7\ H_2O$	Panreac	10
KH_2PO_4	Panreac	18
MQ-water		to desired volume

Once prepared adjust to pH 7.3 using HCl. For other uses, pH could be slightly modified. PBS could be autoclaved 15 minutes at 121 °C if required.

A.3.11 Potassium phosphate buffer 0.1 M

Table A.48. Potassium phosphate buffer 0.1 M composition.

Component	Supplier	Concentration (mM)
Monobasic solution		
KH_2PO_4	Panreac	1000
MQ-water		to 1 L
Dibasic solution		
K_2HPO_4	Merck	1000
MQ-water		to 1 L

By using the Henderson-Hasselbach equation, the amount of each solution required to obtain the final desired buffer pH could be calculated. In the present work, a pH 7 solution was required and thus, 38.5 mL of monobasic solution and 61.5 mL of dibasic solution were mixed and the final volume adjusted to 1 L. Final pH should be checked and adjusted. Potassium phosphate buffer could be autoclaved 15 minutes at 121 °C if required.

A.3.12 Separating buffer 4X (PAGE)

Table A.49. Separating buffer 4X composition.

Component	Supplier	Concentration (mM)
Trizma Base	Sigma	370
SDS	Merck	3.5
MQ-water		to 250 mL

Once prepared adjust to pH 8.8 with HCl previously to SDS addition. If conducting native-PAGE, avoid the addition of SDS.

A.3.13 Sodium phosphate buffer 0.1 M

Table A.50. Sodium phosphate buffer 0.1 M composition.

Component	Supplier	Concentration (mM)
Monobasic solution		
$NaH_2PO_4 \cdot H_2O$	Merck	1000
MQ-water		to 1 L
Dibasic solution		
Na_2HPO_4	Merck	1000
MQ-water		to 1 L

By using the Henderson-Hasselbach equation, the amount of each solution required to obtain the final desired buffer pH could be calculated. In the present work, a pH 7 solution was required and thus 42.3 mL of monobasic solution and 57.7 mL of dibasic solution were mixed and the final volume adjusted to 1 L. Final pH should be checked and adjusted. Potassium phosphate buffer could be autoclaved 15 minutes at 121 °C if required.

A.3.14 Sonication buffer

Table A.51. Sonication buffer composition.

Component	Supplier	Concentration
PBS 10 X (A.3.10)		1 X
cOmplete mini EDTA-free tablets	Roche	1 tablet
MQ-water		to 10 mL

Final pH will depend on protein stability and the selected type of purification. Generally, proteins are stable between pH 7 and 8 thus, the kind of purification chosen is a critical factor to decide the final pH used. In this work, pH 7 was used for TALON resin purification procedure and pH 7.3 for Sepharose 4B resin purification procedure. For whole-cell lysates intended for either ELISA or co-immunoprecipitation, pH 7.3 was used.

A.3.15 Stacking buffer 4X (PAGE)

Table A.52. Stacking buffer 4X composition.

Component	Supplier	Concentration (mM)
Trizma Base	Sigma	125
SDS	Merck	3.5
MQ-water		to 250 mL

Adjust to pH 6.8 with HCl previously to SDS addition. If conducting native-PAGE, avoid the addition of SDS.

A.3.16 TAE 50X

Table A.53. TAE 50X composition.

Component	Supplier	Concentration
Trizma Base	Sigma	2000 mM
EDTA 0.5 M pH 8 (A.2.10)		10 % (v/v)
Acetic acid, glacial	Panreac	5.7 % (v/v)
MQ-water		to desired volume

A.3.17 TALON elution buffer

Table A.54. TALON elution buffer composition.

Component	Supplier	Concentration
PBS 10X pH 7 (A.3.10)		1 X
Imidazole	Sigma	150 mM
MQ-water		to desired volume

A.3.18 TALON wash buffer

Table A.55. TALON wash buffer composition.

Component	Supplier	Concentration (mM)
Sodium phosphate buffer pH 7 (A.3.13)		50
NaCl	Panreac	300
MQ-water		to desired volume

A.3.19 Tethering buffer

Table A.56. Tethering buffer composition.

Component	Supplier	Concentration (mM)
Potassium phosphate buffer pH 7 (A.3.11)		10
NaCl	Panreac	67
Sodium lactate	Fluka	10
EDTA	Sigma	0.1
L-methionine	Merck	0.001

(Block *et al.*, 1983)

A.3.20 Tris-buffered saline (TBS) 10X

Table A.57. Tris-buffered saline buffer 10X composition.

Component	Supplier	Concentration (mM)
NaCl	Panreac	1500
Trizma Base	Sigma	250
MQ-water		to desired volume

Once prepared adjust to pH 7.3 with concentrated HCl. TBS could be autoclaved 15 minutes at 121 °C if required.

A.3.21 Wash buffer 1X

Table A.58. Wash buffer 1X composition.

Component	Supplier	Concentration (v/v)
PBS or TBS 10X (A.3.10 or A.3.20)		10 %
Tween 20	Panreac	0.05 %
MQ-water		to desired volume

A.3.22 Western blot transfer buffer 1X

Table A.59. Western blot transfer buffer 1X composition.

Component	Supplier	Concentration
Tris-base	Bio-Rad	25 mM
Glicine	Roche	190 mM
Methanol	Panreac	20 % (v/v)
MQ-water		to desired volume

A.3.23 Western blot blocking buffer 1X

Table A.60. Western blot blocking buffer 1X composition.

Component	Supplier	Concentration
TBS 10X (A.3.20)		1 X
Tween 20	Panreac	0.05 % (v/v)
BSA Fraction V	Roche	3 % (w/v)
MQ-water		to desired volume